A photoluminescence and electroluminescence study of the properties of polyfluorene copolymers for display applications

Jin, Yu

A photoluminescence and electroluminescence study of the properties of polyfluorene copolymers for display applications

By

Yu Jin

A thesis submitted to the Faculty of Science, The University of Durham,

for the degree of Master of Science

Organic Electroactive Materials Group

Department of Physics

University of Durham

September 2006

Abstract.

Optical and electrical characterizations of 2 series of polyfluorene copolymers which are p(F8-co-27DBTO)s and p(F8-36DBT)s including 5 different units' percentages each are reported. The optical properties of them in solution, film are characterized principally by using the techniques of absorption and emission spectra. The effects of changing the concentration of the new unit in the polyfluorene copolymers are investigated by comparing the absorption and PL emission spectra of them in solution and solid state.

The preparation of electroluminescent device using these copolymers as the active layer is reported. The external quantum efficiency and other characteristics such as brightness and turn-on voltage using the LEDs test system are presented. The effects of extending the width of spectrum, shifting the EL wavelength and enhancing quantum yield by the new units are presented.

The variations in external quantum efficiency and EL spectrum of devices with different thicknesses of the light-emitting layer are reported and analysed.

Acknowledgements.

During the past year there are many people who have helped me a lot in my studies. Without you I would never get to this stage.

Firstly I would like to thank my supervisors, Prof. Andy Monkman and Dr. Lars-Olof Palsson for their help and support throughout my one year's time in Durham. Also I would like to be grateful to all the staffs in OEM group, especially Simon who has provided me with many papers and suggestions during the whole year, and Hammeed and Carsten who have given me many help on making organic devices.

Finally, I should also thank my friends and parents for their support, I am very grateful to my parents who have paid my study and living fees during the whole year that made it possible for me to get the Msc degree in Durham University. And I would thank my girlfriend very much who is in China and has given me necessary support in spirit in the last year.

Declaration.

The material in this thesis has not been submitted for examination for any other degree or part thereof at the University of Durham or any other institution. The material in this thesis is the work of the author except where formally acknowledged by reference.

Table of Contents.

Table of Figures.

Chapter 1 Introduction.

1.1 Introduction.

Since the first display based upon conjugated polymers (poly(p-phenylenevinylene), PPV) (show structure) as the light-emitting layer was reported by Burroughes et al in 1990[1], research on conjugated polymer for display applications has become a active and advanced research area.

Conjugated polymers have a wide range of applications, for example, flat panel display, polymer lasers, solar cells etc [2,3,4,5]. But perhaps the most important direction of research with conjugated polymers is their application in electroluminescent devices.

Polymer LEDs have many advantages compared with conventional inorganic LEDs. Polymers are easy to fabricate in the solution state and hence devices can be easily made by deposition of layers of polymers on a substrate using spin coating, inkjet printing and roll-to-roll processing techniques[6]. Polymers can be used to cover large areas, hence flat and large area displays with large viewing angles is a real possibility. The mechanical properties of polymers make it possible to fabricate flexible and portable displays. Polymer materials are normally not expensive which makes it possible to produce devices for various applications at a low cost.

Other very important and attractive feature is related to the optical properties of the system, polymers are tunable, which means the physical properties and emission wavelength can be modified by simple chemistry, such as changing the structure of the polymer chain, adding dopants into the polymer system, making co-polymers and so on.

However, there are still many unresolved questions with this technology today, such as full-color stability and the low quantum efficiency in polymer LEDs. This can be solved partially by using techniques including addition of phosphorescent dyes[7], white emitting polymer blends with color filters, hole transport layers and electron

injection from metals with low work functions. Another very important and promising approach is to use co-polymers in combination with the main light-emitting polymer units. The added units can have an impact on the PL and EL spectral positions and enhance the efficiencies through energy transfer from the main polymer and direct carrier trapping in devices.

Of the numerous polymers been used so far, polyfluorenes are a particularly promising electroluminescent polymer for light-emitting diodes because of the thermal and chemical stability, good solubility in common organic solvents and high fluorescent quantum yields in the solid state[8]. But a stable blue-emitting polyfluorene is still a challenge for polymer synthesis. Rigid-rod polyfluorene has a tendency toward a liquid crystalline nematic type of packing arrangement in the bulk and thus is inherently prone to chain aggregation that leads to a red-shifted emission[9] and to a reduction of quantum efficiency[10]. This is referred to as the β -phase. Many efforts have been made to depress the formation of the ordered segments (β -conformation). Different kinds of disorder units have been introduced into the polyfluorene conjugated system, such as carbazole[11], end-capping[12], polyphenylene dendrimer substituents[13], distyrylbenzene[14], 5,7-dihydrodibenzoxepine and dibenzothiepine[15]. The co-polymers exhibit better spectral properties than the polyfluorene homopolymer.

During recent years, Dibenzothiophene (DBTO) has been reported to be the most abundant compound in petroleum. Because the sulfur in dibenzothiophene can be easily converted to sulfoxide[16], sulfone[17], and sulfonium derivatives[18], polymers containing dibenzothiophene moieties should be interesting in that they may similarly be converted to various functional polymers.

To explore if the DBTO unit can effectively improve the PL and EL properties of pure PF, Professor Martyn Bryce and co-workers at the chemistry department in Durham has developed two new series of PF co-polymers. The motivation of this work is to see whether these two series of PF co-polymers can enhance the quantum yield and luminance of PF LEDs. Another important aim is to investigate if the PL and EL color can be tuned towards white by adding the DBTO and DBT unit into the

PF backbone randomly.

LEDs currently dominate the exit sign market and many cities have adopted them as a replacement for incandescent lamps in traffic signals. In the architectural market, the development of a visible/white light LED has alerted lighting designers to new possibilities with this light source. White light LEDs, however, currently do not produce enough lumen output to make them competitive with many general light sources. Thus a lot of work should be done on them. More and more attractive materials have been invented, and more and more fabricating methods have been created as well. These two series of PFO co-polymers are also prospective in the field of white light LEDs.

These 2 series of polyfluorene co-polymers are p(F8-co-28DBTO)s and p(F8-co-37DBT)s. In the 28 series, dibenzothiophene (DBTO) unit is introduced through the 2,8 position into the poly(2,7-(9,9-dioctyl)fluorene backbone, and in the 37 series, DBT unit is introduced through the 3,7 position into the PFO backbone. Different DBTO and DBT unit ratios in the polymer composition are incorporated to study the trend of properties. The results show that the EL spectra range can be expanded very well in devices and the external quantum efficiency and luminance of device can be improved by adding these units to form a new charge transfer state. In addition, the EL color can be shifted from dark blue to light blue and green-blue obviously, but not white. However, the result is still encouraging. And also there is potential to motivate and defend the future work on these co-polymers.

This thesis is divided into 6 chapters. Chapter 1 provides the necessary background theories. Chapter 2 described the basic knowledge of conjugated polymers, co-polymers, polyfluorene and the two series of PFO co-polymers investigated in this thesis as well. Chapter 3 gives a summary of the experimental methods and apparatus required for investigating the photoluminescence (PL) and electroluminescence (EL) properties of these two series of co-polymers. Chapter 4 presents the optical characters of the two series of polyfluorene co-polymers in solution and solid state. Chapter 5 presents the measurements and analyses of the electrical characters of these polyfluorene co-polymer light-emitting devices. Chapter

6 gives a conclusion of the PL and EL characters of these polyfluorene co-polymers with different concentrations of new units and with different light-emitting layer (LEL) thicknesses.

1.2 References.

1. J. H. Burroughes, D. D. C. Bradley, A. R. Brown, et al., Nature 347, 539 (1990).
2. F. L. Zhang, M. Johansson, M. R. Andersson, et al., Synthetic Metals 137, 1401 (2003).
3. S. V. Frolov, M. Shkunov, A. Fujii, et al., Ieee Journal of Quantum Electronics 36, 2 (2000).
4. A. J. Heeger, Solid State Communications 107, 673(1998).
5. R. J. Visser, Philips Journal of Research 51, 467 (1998).
6. B. J. de Gans, P. C. Duineveld, and U. S. Schubert, Advanced Materials 16, 203 (2004).
7. M. S. Jang, S. Y. Song, H. K. Shim, et al., Synthetic Metals 91, 317 (1997).
8. G. Klarner, J. I Lee, M. H. Davey and R. D. Miller, Adv. Mater., 11, 115 (1999).
9. V. N. Bliznyuk, S. A. Carter, J. C. Scott, G. Klarner, R. D. Miller and D. C. Miller, Macromolecules, 32, 361 (1999).
10. D. D. C. Bradley, M. Grell, A. Grice, A. Tajbakhsh, D. O'Brien and A. Bleyer, Opt. Mater., 9, 1 (1998).
11. C. Xia and C. A. Rigoberto, Macromolecules, 34, 5854 (2001).
12. T. Miteva, A. Meisel, W. Knoll, H. G. Nothofer, U. Scherf, D. C. Muller, K. Meerholz, A. Yasuda and D. Neher, Adv. Mater., 13(8), 565 (2001).
13. S. Setayesh, A. C. Grimsdale, T. Weil, V. Enkelmann, K. Mullen, F. Meghdadi, E. J. W. List and G. Leising, J. Am. Chem. Soc., 123, 946 (2001).
14. A. B. Holmes, T. Sano, C. Fischmeister, J. Frey, U. Hennecke, C. Tuan, B. S. Chuah, Y. Ma, R. Martin, I. D. Rees, J. Li, A. D. Bond, F. Cacialli and R. H. Friend, Proc. SPIE, 4464, 42 (2002).

15. S. F. Lim, I. D. Rees, F. Cacialli, A. B. Holmes and R. H. Friend, Book of Abstracts, International Conference of Science and Technology of Synthetic Metals, Shanghai, p. 239 (June 29–July 5 2002).
16. H. Gilman and D. L. Esmay, J. Am. Chem. Soc., 74, 271 (1952).
17. J. Bundt, W. Herbel and H. Steinhart, J. High Resolut. Chromatogr., 15, 682 (1992).
18. T. Umemoto and S. Ishihara, J. Am. Chem. Soc., 1993, 115, 2156.

Chapter 2 Theory.

2.1 Molecular orbital theory and Electronic structure of organic mateials.

A valence-bond theory used to be involved because the arguments about atomic orbital focus on the bonds formed between valence electrons on an atom. But the valence-bond model can not explain the molecular formation very well. The best it can do is to suggest that these molecules are mixtures, or hybrids.

However, by using a more sophisticated model of bonding based on molecular orbitals, this problem and many others can be overcome. Molecular orbital theory[1] is more useful than valence-bond theory because the orbitals reflect the geometry of the molecule to which they are applied. But this carries a significant cost in terms of the ease with which the model can be visualized.

As a start, we can simulate the single atomic orbitals using quantum. The first five solutions of the wave equation for an electron associated with a proton can be shown in the figure below:

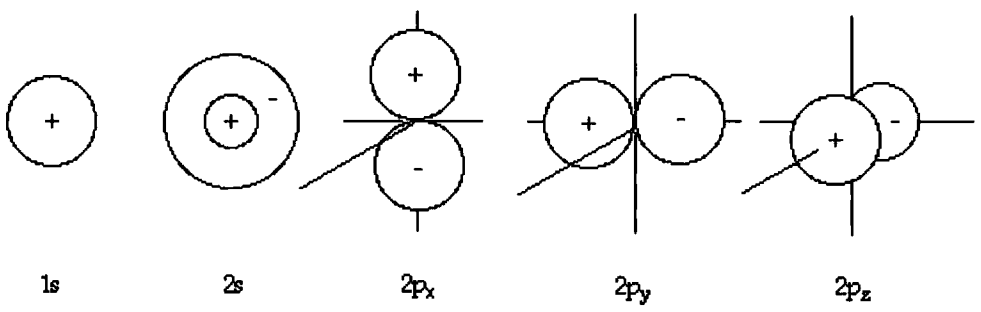

Figure 2-1 The first five shapes for an electron associated with a proton[2].

In a bonded system these orbits will be mixed together to form a hybrid orbital. Take the most common used model carbon system for example, the hybrid orbital is called sp^3 hybrid orbital. As shown in Figure 2-2, the sp^3 orbital is a mixture of the *2s*

and $2p_x$, $2p_y$, $2p_z$ orbitals on a carbon atom.

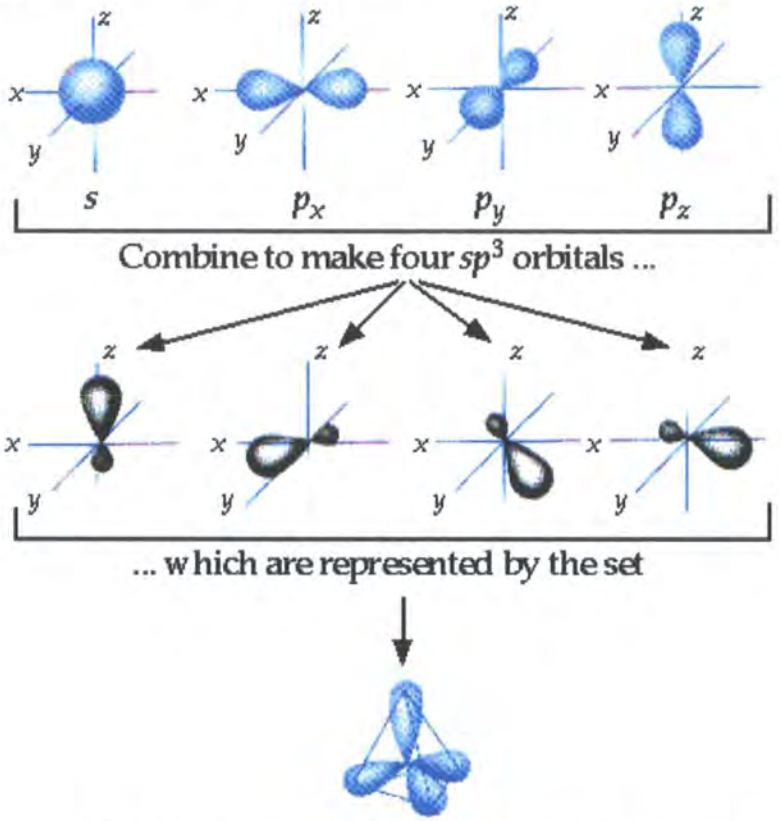

Figure 2-2 The formation of sp^3 hybrid orbital in a carbon atom[3].

And if any one of these four lobes is bonded with another *s* or *p* orbital, a bond which is called the σ-bond is formed, as shown in Figure 2-3.

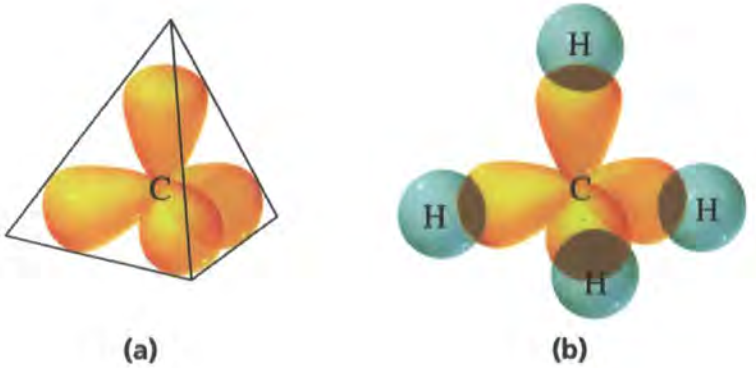

Figure 2-3 The formation of the σ -bond between sp3 and s orbitals[4].

But if the p_z orbital is left with no combination with the *s* orbital, another hybrid orbital called sp^2 is formed together with the left p_z orbital, as shown in Figure 2-4.

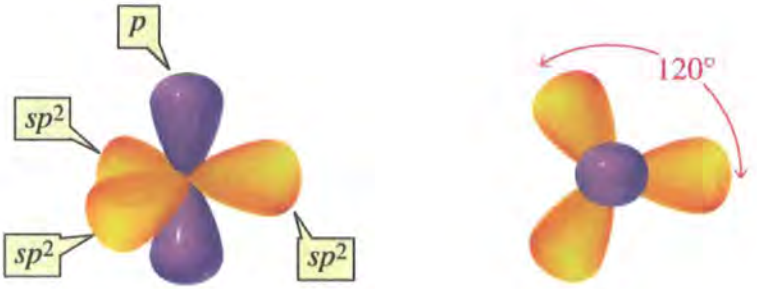

side view top view

Figure 2-4 The sp^2 orbital with the left p_z orbital unmixed with s[5].

In this hybrid orbital, three σ-bonds can form, and thus one valence electron is left in the p_z orbital. This electron can form another kind of bond that is called the π-bond. Obviously the π-bond is a double bond because of the two-direction structure of the p_z orbital. This is shown in Figure 2-5 below.

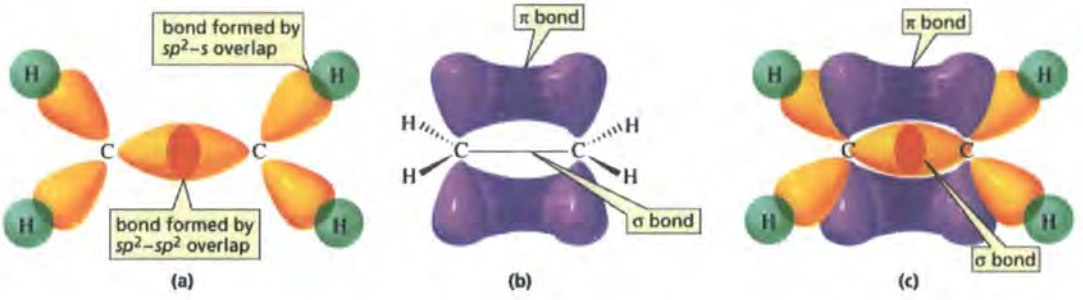

Figure 2-5 The formation of the π-bond between two $sp2$ orbitals[6].

Similarly, if there are 2 p orbitals not combined with the s orbital, the third formation is formed, which is called sp hybrid orbital as shown in Figure 2-6.

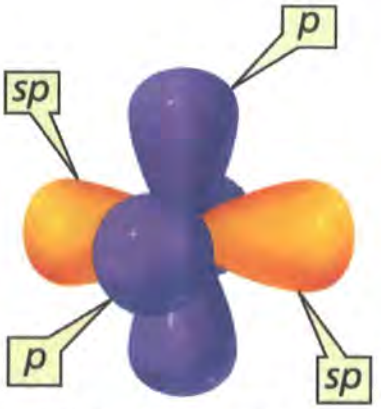

Figure 2-6 The *sp* orbital with p_y and p_z unmixed with s[7].

And also similarly, this hybrid orbital can form a triple bond which is the formation of two π-bonds, as shown in Figure 2-7.

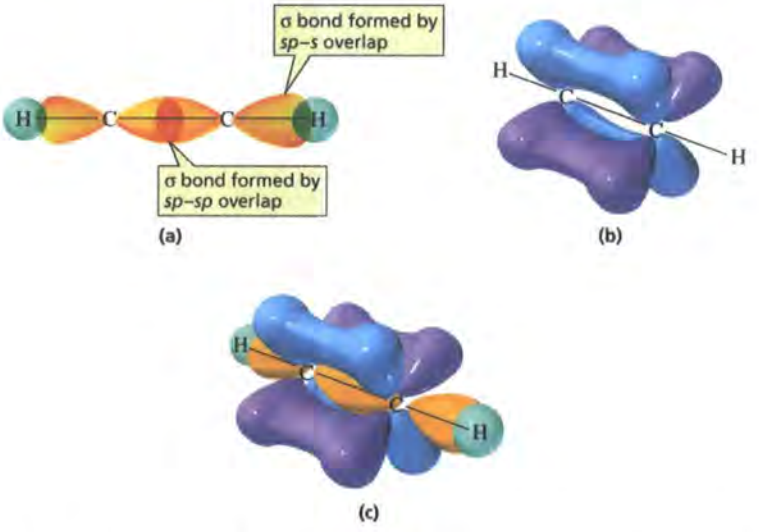

Figure 2-7 The formation of two π-bonds between two *sp* orbitals[8].

Normally in a molecule whose electron orbitals are not completely filled, there is a level called HOMO (highest occupied molecular orbital), which means the electrons will fill this lowest energy level first. And correspondingly there is a LUMO (lowest unoccupied molecular orbital) exiting.

Of these different bonds, the π-bond is the most important one in polymer systems. Many element atoms can form π-bonds besides carbon, for example nitrogen, oxygen and sulphur. In an even longer molecular chain which is connected through the σ-bonds, we can see that the remaining p_z orbitals can overlap to form π-bonds through the system. And in addition, the π-bonds can produce a bond order of

1.5 for carbon atoms along the chain. This is called the conjugated polymer. A chain segment for example is shown in Figure 2-8 below.

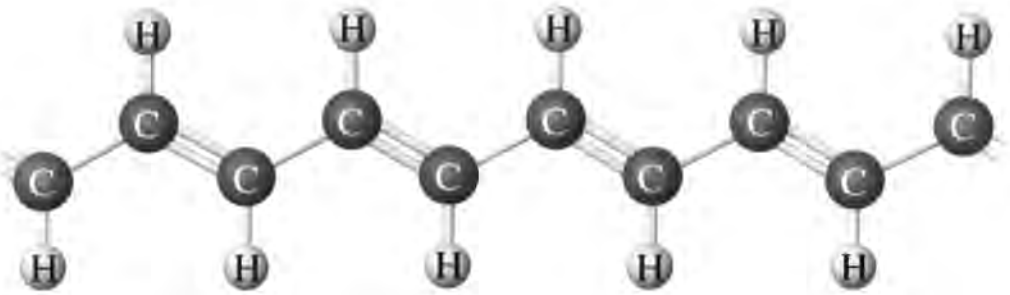

Figure 2-8 The polymer chain of poly(acetylene)[9].

It is important to see that the π-bonding states are completely filled, and the π-antibonding states are completely empty, so an energy gap now exists between the states as a result of the effect called Peierls distortion[10]. This phenomena leads to a result that the whole polymer becomes a semiconductor itself, and the HOMO and LUMO levels form again. Because of the overlap and interaction of the π-bonds, the electrons are allowed to move freely along the polymer backbone. So the polymer becomes electrically conductor.

Conjugated polymers behave like wide gap semiconductors due to the Peierls distortion. π-bonding, which due to their occupation, are designated highest occupied molecular orbitals (HOMOs), can interact to produce the lower energy band. This low energy band is called the valence band as in inorganic systems. The π -antibonding orbitals, known as lowest unoccupied molecular orbitals (LUMOs), can interact to form the higher energy band, which is called the conduction band.

Thus, as a conclusion, by the π-bonds' overlap and interact over the whole polymer chain, and as result an organic semiconducting conjugated polymer is obtained.

2.2 Absorption and emission of radiation.

2.2.1 Absorption.

Absorption is a general process that can occur in atomic as well as molecular systems, and can occur either in gas phase, liquid or solid state. Generally, when light of the correct energy is incident on the sample, photons will be absorbed by the sample, and cause an excitation to a higher excited state. The process results in a transition from a ground state to a higher energy state.

2.2.1.1 Fermi's golden rule.

From quantum mechanics, Fermi's golden rule[11] gives the transition rate between two eigenstates of a quantum system using time-dependent perturbation theory, which means it's an approximation.

We consider the system to begin in an eigenstate $|i\rangle$ of a given Hamiltonian H_0. We consider the effect of a time-independent perturbing Hamiltonian H'.

The one-to-many transition probability per unit of time from the state $|i\rangle$ to a set of states $|f\rangle$ is given, to first order in the perturbation, by:

$$T_{i\to f} = \frac{2\pi}{\hbar}\left|\langle f|H'|i\rangle\right|^2 \rho \qquad \textbf{(Equation 2-1)}$$

Where ρ is the density of final states, and $\langle f|H'|i\rangle$ is the matrix element of the perturbation, *H'*, between the final and initial states.

Fermi's golden rule is valid when H' is time-independent, $|i\rangle$ is an eigenstate of the unperturbed Hamiltonian, the states $|f\rangle$ form a continuum, and the initial state has not been significantly depleted (eg, by scattering into the final states).

The most common way to derive the equation is to start with time-dependent perturbation theory and to take the limit for absorption under the assumption that the time of the measurement is much larger than the time needed for the transition.

Here we also use the electric dipole approximation. In the electric field

$\vec{E}(\vec{r},t) = E_0 \sin \omega t \cdot e^{i\vec{k}\cdot\vec{r}}$ we consider the exponential term and the following approximation can be made:

$$e^{i\vec{k}\cdot\vec{r}} = 1 + (i\vec{k}\cdot\vec{r}) + \frac{(i\vec{k}\cdot\vec{r})^2}{2!} + \ldots$$

We notice that the term $(\vec{k}\cdot\vec{r})$ is only non-zero over the extent of the interacting atom, roughly 1 Å. In contrast, $k = \frac{2\pi}{\lambda} \sim 10^{-3}$ Å^{-1} for optical or near UV radiation. Hence $(\vec{k}\cdot\vec{r}) \sim 10^{-3}$, and so we replace $e^{i\vec{k}\cdot\vec{r}}$ by 1. This is known as the electric dipole approximation.

As $H' = -e\cdot\vec{E}(\vec{r},t)\cdot\vec{r} \approx -e\cdot\vec{r} = \vec{\mu}_{12} \bullet \vec{E}_0$ we reformulate Fermi's Golden rule to the following time independent property

$T_{i\to f} = E_0^2 \frac{2\pi}{\hbar} \left|\langle f|\mu_{12}|i\rangle\right|^2 \rho$ where μ_{12} is the transition dipole moment..

2.2.1.2 Oscillator strength.

The intensity of a UV-Visible absorption band is a function of the oscillator strength and of the energy of the absorption band.

The strength of the optical absorption is called the oscillator strength[12]. It is a measure of the strength of an electric dipole transition compared to that of a free electron oscillating in three dimensions. It is given by

$$f = \left[\frac{4\varepsilon_0 \cdot m_e \cdot c \cdot \ln(10)}{N_A \cdot e^2}\right] \cdot A \qquad \textbf{(Equation 2-2)}$$

Where ε_0 is the permittivity of free space, m_e is the electron mass, c is the speed of light, e is the charge of an electron, and A is the integrated area of the

absorption peak.

Theory also provides a connection between the oscillator strength f_{nm} and the transition dipole moment, μ_{nm}:

$$f_{nm} = \left[\frac{8\pi^2 m_e c}{3e^2 h}\right] \cdot \tilde{\nu}_{nm} \cdot |\mu_{nm}|^2 \qquad \textbf{(Equation 2-3)}$$

Here ν_{nm} is the transition in wavenumbers [cm^{-1}]. This is a very important change from a microscopic property to a macroscopic property.

To define the transition dipole moment μ_{nm}, we first need to factorize it according to the contributions to the molecular wavefunctions from the electrons and the nuclei. The molecular wavefunction ψ is given below.

$$\psi = N\varepsilon = N\varphi\phi \qquad \textbf{(Equation 2-4)}$$

Where φ is the electronic spatial wavefunction, ϕ is the electronic spin wavefunction, and N is the nuclear wavefunction. The electronic dipole moment vector $\vec{\mu}$ operates only on the electronic spatial wavefunctions, and so the electronic spin and nuclear wavefunctions can be taken out of the transition dipole moment integral. This is shown in the equation below.

$$\mu_{nm} = \langle \psi_n | \vec{\mu} | \psi_m \rangle = \langle \varphi_n | \vec{\mu} | \varphi_m \rangle \langle \phi_n | \phi_m \rangle \langle N_n | N_m \rangle \qquad \textbf{(Equation 2-5)}$$

From this equation we can see that the transition dipole moment can be regarded as the product of the electronic transition moment $\langle \varphi_n | \vec{\mu} | \varphi_m \rangle$, the electron spin overlap integral $\langle \phi_n | \phi_m \rangle$ and the nuclear wavefunctions overlap integral $\langle N_n | N_m \rangle$.

2.2.1.3 Absorption in organic molecular systems.

In the molecular system, photons will cause an electronic excitation of the molecule when light of the energy corresponding to the transition energy is incident on the sample. In an organic molecule, this energy is required to promote an electron from the HOMO to the LUMO or higher antibonding orbital.

Another consideration that should be taken into account is the effect of coupling of molecular vibrations on the electronic transition. These vibrations can couple with the electronic transition producing a series of additional energy levels in the ground state and excited states. The following figure shows how light can be absorbed by molecules in any of the vibrational levels of the ground state (n = 0) and be excited to any vibrational level of both the ground state and the excited state.

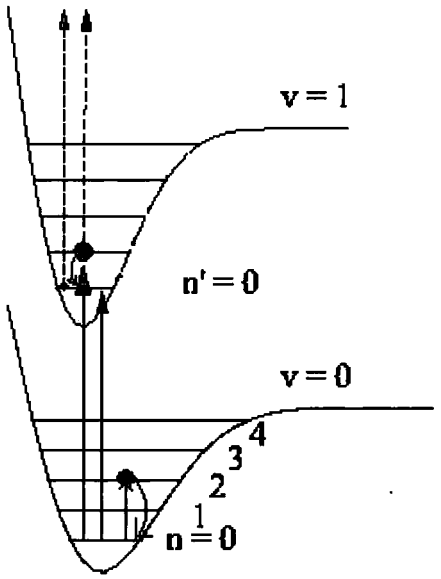

Figure 2-9 Diagram of optical absorption.

From this figure we see that the excitation takes place from the n = 0 vibrational level of the ground state, and is most likely to occur from the most probable conformation of the molecule. This point is at the equilibrium nuclear co-ordinate position. The vertical transitions take place to the excited state vibrational levels with

the relative strength of the transition depending on the overlap of the vibrational wavefunctions that is presented as $\langle \psi_1 | \psi_2 \rangle$.

2.2.2 Photoluminescence.

Photoluminescence is the radiative decay of an excitation caused by absorption of a photon which results in the emission of a photon. In the molecular systems, absorption and photoluminescence spectra can be very similar in shape. The photoluminescence is usually a red shifted and mirror image of the absorption spectrum. This is shown in Figure 2-10 below.

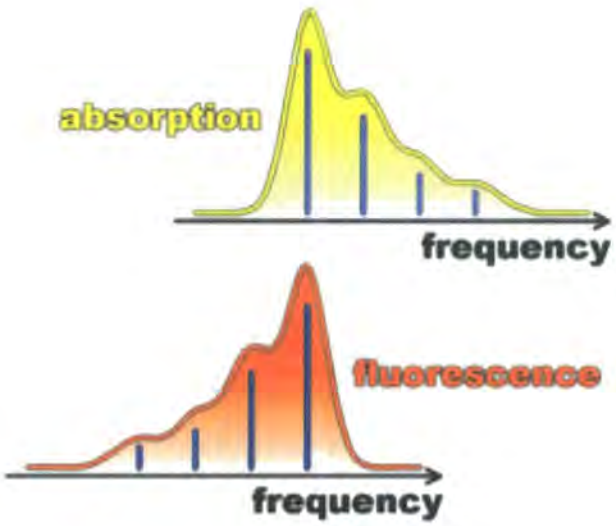

Figure 2-10 Diagram of the mirror image relationship of absorption and photoluminescence[13].

2.2.2.1 The Franck-Condon principle.

In the figure above, we notice that both the absorption and fluorescence spectra have progression of peaks. This is called the *Franck-Condon* progression of the vibronic progression.

The *Franck-Condon* principle[12] is a rule in spectroscopy and quantum chemistry that explains the intensity of vibronic transitions. Vibronic transitions are the simultaneous change in electronic and vibrational energy levels of a molecule due to the absorption or emission of a photon of the appropriate energy. The principle states that during an electronic transition, a change from one vibrational energy level to another will be more likely to happen if the two vibrational wave functions overlap that is defined as $\langle \psi_1 | \psi_2 \rangle$ more significantly.

2.2.2.2 Stoke's losses and Stoke's shift.

The general mechanism underlying luminescence is the absorption of photons of certain energy by a luminescent material, which is then excited from the ground state to an unstable high-energy state. Then it will undergo another process called vibrational relaxation[14] (or *Stoke*'s losses). It means a loss of vibrational excitation energy by the molecular entity through energy transfer to the environment. The molecular entity relaxes into a vibrational equilibrium with its environment.

As the compound falls back to its lower energy level, it luminescences by emitting a photon of lower energy than the photon that excited the compound due to the loss of energy through relaxation as intraband transition. Being lower in energy, the emitted light has a longer wavelength than the exciting light; the difference between these two wavelengths is known as the *Stoke*'s shift[15]. Anti-stoke shift: the emission of photons having shorter wavelengths than absorbed photons due to incorporation of thermal energy such as phonons.

2.2.3 Non-radiative decays.

2.2.3.1 Internal conversion.

Internal conversion (IC) [16] is an excited state process. It is the isoenenergetic radiationless transition between two electronic states of the same multiplicity. When

the transition results in a vibrationally excited molecular entity in the lower electronic state, this usually undergoes deactivation to its lowest vibrational level, provided the final state is not unstable to dissociation.

2.2.3.2 Vibrational relaxation.

Vibrational relaxation[17] means the loss of vibrational excitation energy by a molecular entity through energy transfer to the environment caused by collisions. The molecular entity relaxes into vibrational equilibrium with its environment.

2.2.3.3 Conformational relaxation.

Nowadays, fluorescent conjugated polymers have become more and more widely researched for their applications in light-emitting diodes[18]. However, they are a complex class of materials with a high degree of energetic disorder. Either breaks in the molecular structure or wormlike fast fluctuations[19, 20] cause this. Energy in the excited state will undergo a non-radiative decay back to the ground state. This non-radiative process is called the conformational relaxation.

In the fluorescent conjugated polymer systems, after vibrational relaxation the polymer's structural and energetic disorder drives further relaxation mechanism[21, 22, 23]. This will cause additional Stoke's shift as well as breaks in the mirror symmetry between the absorption and photoluminescence spectra. And because of this additional non-radiative decay process, more energy will be lost.

2.2.3.4 Quenching.

The radiative processes in polymers are not always so efficient. Sometimes both the singlet fluorescence and triplet phosphorescence may become quenched through some external influence. Normally quenching will cause a result of energy lost. For example energy transfer to a non-radiatively decaying state[24, 25].

In addition, there are a lot of particles cause quenching. These particles are called quenchers or scavengers. One of the most important quenchers for example for triplets is oxygen.

2.2.4 Photoluminescence quantum yield.

Photoluminescence quantum yield (PLQY) is a very important measurement for investigating the sample's optical properties. It is defined as the ratio of the number of photons emitted by the sample to the number of photons absorbed by the sample. It is presented by the following equation.

$$\phi_{pl} = \frac{n_{emi}}{n_{abs}} \qquad \textbf{(Equation 2-6)}$$

n_{emi} is the number of the photons emitted from the sample, and n_{abs} is the number of the photons absorbed by the sample.

Another important definition of the PLQY is

$$\phi_{pl} = \frac{k_f^0}{k_f^0 + \sum k_i} = \frac{\tau_f}{\tau_f^0} \qquad \textbf{(Equation 2-7)}$$

k_f^0 is the natural fluorescence rate coefficient, $\sum k_i = k_f = k_f^0 + k_{ISC} + k_{IC}$, k_{ISC} is the rate coefficient for intersystem crossing and k_{IC} is the rate coefficient for internal conversion, $\tau_f = \frac{1}{\sum k_i}$ and $\tau_f^0 = \frac{1}{k_f^0}$.

2.2.5 Homogenous and inhomogenous broadening.

In polymer systems, absorption and photoluminescence are more complex than a single molecule spectrum. In general, the bands of an absorption spectrum never are infinitely narrow or vibrational, i.e. they are always broadened. This band broadening

can be divided into two types: the homogenous and the inhomogenous broadening. The homogenous broadening is determined by the lifetime of the states that take part in the transition, while the inhomogenous is caused by the motion of the particle (Gaussian broadening), differing intermolecular and other mechanisms.

As the inhomogenous broadening is a result of the local environment, this broadening is not observed in the gas phase. The homogenous broadening is independent of the matrix of the molecule, and is therefore the same for all (chemically identical) molecules.

2.2.6 Electronic state and fluorescence.

2.2.6.1 singlet and triplet electronic state.

First we need to define the total spin vectors and total quantum number S of an electronic state shown as the equations below.

$$\vec{S} = \sum_i \vec{s}_i = \vec{s}_1 + \vec{s}_2 + \vec{s}_3 + \ldots \qquad \textbf{(Equation 2-8)}$$

The magnitude of $\vec{S} = \left[S(S+1)\right]^{\frac{1}{2}}\hbar$ **(Equation 2-9)**

And $S = s_1 + s_2, s_1 + s_2 - 1, \ldots, |s_1 - s_2|$ **(Equation 2-10)**

If $\vec{S} = 0$, so $S = 0$, and this state is called the singlet state. If $\vec{S} = 1$, then $S = \pm 1, 0$, the total spin quantum of this state has three values, thus this state is called the triplet state.

2.2.6.2 Fluorescence.

The photoluminescence usually contains two parts, which is fluorescence and phosphorescence. Fluorescence occurs due to the radiative decay from a singlet excited. Since there is no change of spin multiplicity, the transition is strongly allowed

with the result that it occurs on relatively fast timescales. The emission process is shown in Figure 2-11.

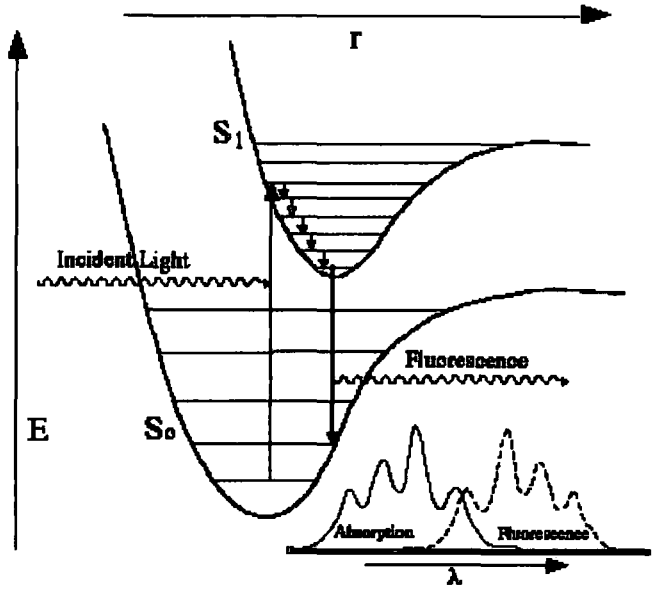

Figure 2-11 Diagram of fluorescence[26].

2.2.7 Inter-system crossing and phosphorescence.

2.2.7.1 Inter-system crossing.

Intersystem crossing (ISC)[27] is an excited state process. It is the isoenergetic radiationless transition between two electronic states having different multiplicities. It often results in a vibrationally excited molecular entity in the lower electronic state, which then usually deactivates to its lowest vibrational level.

2.2.7.2 Phosphorescence.

Phosphorescence occurs due to the radiative decay from a singlet excited from triplet state. Since the spin multiplicity is changed, the transition is much less intense

than fluorescence and occurs less rapidly than fluorescence. The emission process is shown in Figure 2-12.

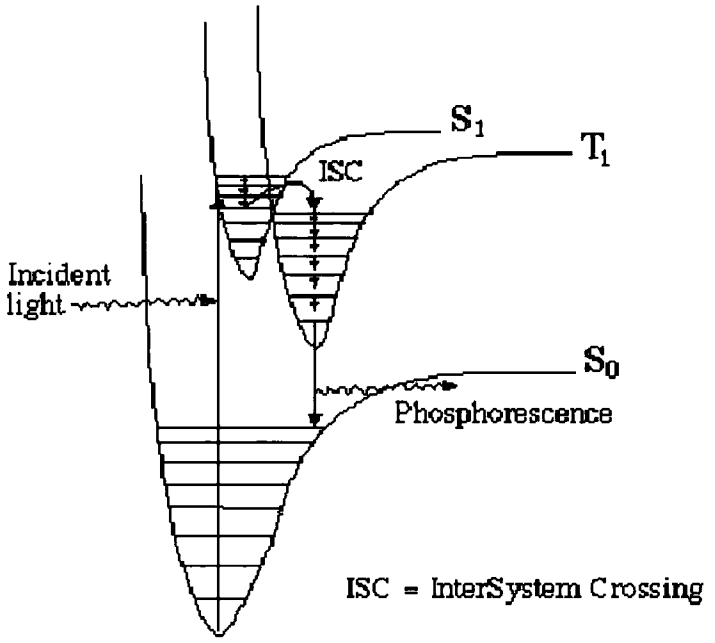

Figure 2-12 Diagram of phosphorescence[28].

2.2.8 The Jablonski diagram.

The process discussed so far can be summarized in a so called Jablonski diagram shown below in figure 2-13.

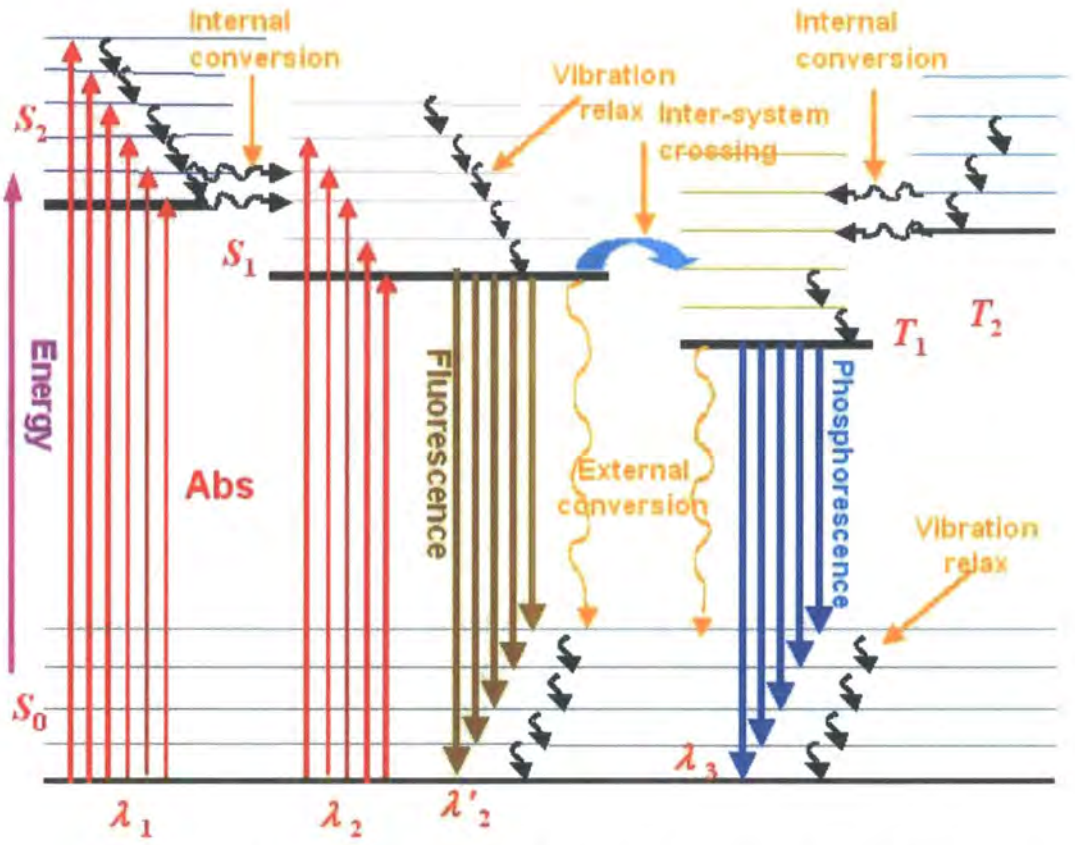

Figure 2-13 Jablonski diagram of a typical semiconductive molecule energy level system.

This figure has summarises very well all the processes discussed previously, such as fluorescence, phosphorescence, inter-system crossing, internal conversion, vibration relax and so on. It also gives an indication of the relative positions of the energy levels of organic electronic systems.

2.3 Important quasi particles in conjugated polymers.

2.3.1 Molecular interactions.

The Su, Schrieffer and Heeger (SSH) theory[29-32] provides a theoretical framework for conjugated polymers. The energy states in polymer systems are due to molecular interactions, such as the electron-electron, electron-dipole, and

dipole-dipole interactions. As a result of these interactions, new energy states can be formed between different polymer chains, and this will have an impact on the electronic transitions.

2.3.1.1 Electron-electron interaction.

An entirely classical model for electron-electron interaction is based on the electrostatic capacitive charging energy. It is the intermolecular or intramolecular interaction between two or more electrons on the same or different polymer chains. The strength of the interaction depends on the distance of the electrons in a r^{-1} dependence. It is shown in the equation below.

$$E = \frac{q_1 q_2}{4\pi\varepsilon_0 r} \qquad \textbf{(Equation 2-11)}$$

2.3.1.2 Electron-dipole interaction.

Dipole-dipole interaction is the intermolecular or intramolecular interaction between electron and molecules or groups having a permanent electric dipole moment. The strength of the interaction depends on the distance between the electron and dipole in a r^{-2} dependence, and relative orientation of the dipole.

$$E = \frac{q_1 \mu}{4\pi\varepsilon_0 r^2} \qquad \textbf{(Equation 2-12)}$$

2.3.1.3 Dipole-dipole interaction.

Dipole-dipole interaction is the intermolecular or intramolecular interaction between molecules or groups having a permanent electric dipole moment. The

strength of the interaction depends on the distance in a r^{-3} dependence, and relative orientation of the dipoles. The term applies also to intramolecular interactions between bonds having permanent dipole moments. For molecular systems this is also the most important interaction.

$$E = \frac{\mu_1 \mu_2}{4\pi\varepsilon_0 r^3} \qquad \textbf{(Equation 2-13)}$$

2.3.2 Aggregates.

2.3.2.1 Physical aggregates.

In densely packed polymer systems, it is possible to form energy states between different polymer chains caused by interchain affections. These are termed interchain aggregates and can affect the absorption and emission properties of polymer systems.

A physical aggregate is a physical dimer composed by two molecules spatially close enough to allow overlap of their wavefunctions. It will form new states in the polymer system.

The formation of a physical aggregate result in a dramatic change of the absorption spectra. The peak of the absorption spectrum is usually red-shifted and the spectrum is broadened.

2.3.2.2 Excited state aggregates or excimers.

Excimers are dimers that only exist in the excited state, because the ground state is dissociative. So unlike the case of aggregates, there is no direct optical excitation of the excimer from ground state and accordingly no change in the absorption spectrum. But because the excimers form a lower energy state without vibronic states, the emission of the excimer is red-shifted, broadened and featureless.

2.3.3 Solitons.

Su, Schreiffer and *Heeger et al* [29-32] have described the presence of several pseudo particles with properties similar with those in inorganic semiconductors. These particles are known as solitons, polarons and bipolarons travelling freely in the conduction bands.

Solitons are only found in degenerate ground state polymers. There are two kinds of solitons, which are neutral soliton and charged solitons. And it has been shown that the degenerate ground state polymer's conduction occurs due to charged solitons.

Solitons are mid-gap states and can form new energy levels between the HUMO and LUMO levels of the polymer where they form.

2.3.4 Polarons.

In non-degenerate ground state polymers, solitons can not be energetically stable, and they will be accompanied by an anti-soliton. This bound soliton anti-soliton pair is called a polaron. If there is a charge on the polymer chain, it will induce a structural relaxation of the chain, and hence form a particle known as a polaron.

Polarons are not mid-gap states, and they will form two energy levels near the HOMO and LUMO levels of the polymer chain.

2.3.5 Bipolarons.

If there is further charge input to the polymer, two polarons with opposite charges may meet and become bound by the coulomb interaction. This process gives the formation of a bipolaron.

Bipolarons will form two energy levels closer to the centre of the band gap of the polymer chain than the two states formed by polarons.

Most luminescent polymers have a non-degenerate ground state, and charge injection into polymer diodes has been said to occur on polaron levels, so in these three particles, polarons and bipolarons play a very important role in the field of PLEDs. When bipolarons with opposite charge are formed, they will decay to excitons[33, 34] and the excitons will undergo a radiative decay to emit light.

2.3.6 Excitons.

Bassler and co-workers suggested that in the polymer chain, the excitation is localised to a short length of the polymer chain, and the excitation is considered to be the formation of an exciton from a bound electron hole pair[35]. Once exciton is formed, it will undergo a radiative process and release a photon.

There are three different kinds of excitons, which are called *Frenkel* excitons, charge transfer excitons and *Wannier* excitons[36]. *Frenkel* excitons are the ones that the electron and hole are on the same molecular. To charge transfer excitons, the electron and hole are separated on two different molecules, so the exciton is transferred from one molecule to another one. The *Wannier* exciton has a electron and hole separated by a large distance, so the intrachain exciton may even form if the electron and hole are not on the same polymer chain.

And another important feature is the two types of spin states of the excitons, singlet state and triplet state. The singlet and triplet states have a ratio of 1:3, which means the singlet only takes a small portion of 25% while the triplet takes 75%. The two kinds of spin states are shown in Figure 2-14 below.

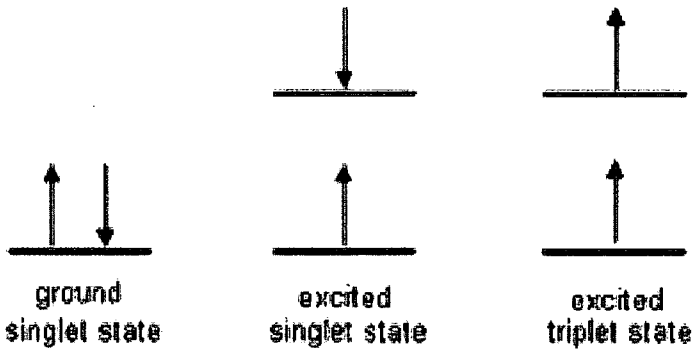

Figure 2-14 Two spin states in excitons.

The ratio calculation is given as:

Singlet state:

$$s=0, s_z=0 \qquad \frac{1}{\sqrt{2}}\left(|\downarrow\uparrow\rangle+|\downarrow\uparrow\rangle\right)$$

Triplet state:

(Equation 2-14)

$$s=1\begin{cases} s_z=-1 \\ s_z=0 \\ s_z=1 \end{cases} \qquad \frac{1}{\sqrt{2}}\left(|\uparrow\downarrow\rangle+|\downarrow\uparrow\rangle\right) \quad \begin{matrix} |\downarrow\downarrow\rangle \\ \\ |\uparrow\uparrow\rangle \end{matrix}$$

This ratio is pessimistic, because due to the spin conservation rule, triplets nearly can't decay radiatively to the ground state, and thus a big part of 75% efficiency will be lost, although it can be solved partially by adding a heavy metal atom which provides perturbation leading to the spin-orbit coupling effect thus the so-called phosphorescence will be produced from the triplet states.

2.4 Electronic energy transfer and charge transfer.

2.4.1 Förster energy transfer.

The most important non-radiative energy transfer process is the *Förster* energy

transfer (dipole–dipole energy transfer)[37] which will be described here.

The *Förster* energy transfer is a mechanism of excitation transfer that can occur between molecular entities separated by distances considerably exceeding the extent of their *van der Waals* radii. The donor dipole transfers its energy to the acceptor dipole, which has a similar resonance frequency. This process occurs in the weak-coupling limit. The typical process is shown in Figure 2-15 below.

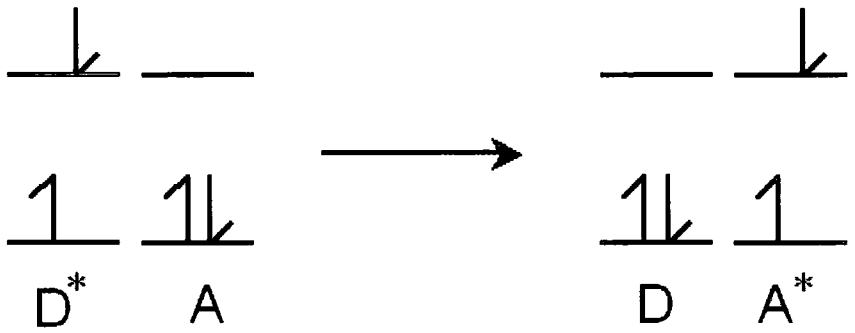

Figure 2-15 Förster energy transfer between the donor and acceptor.

One of the necessary conditions for this energy transfer is that the emission spectrum of the donor should overlap with the absorption spectrum of the acceptor. And another necessary condition is that the distance between the two dipoles moments fall within the *Förster* radius. The *Förster* radius is the distance at which energy transfer is 50% efficient. Efficiency of energy transfer is shown below.

$$E = \frac{k_{ET}}{k_{ET} + k_f + k'} \qquad \textbf{(Equation 2-15)}$$

Where k_{ET} means the rate of excitation energy, k_f means the rate of fluorescence, k' means the sum of all other deexcitation processes.

The overlap integral $J_{(\lambda)}$ of the absorption spectrum of the acceptor and the emission is shown in the figure below.

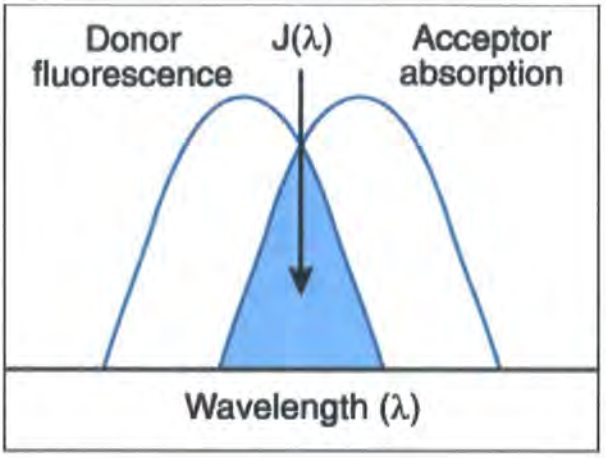

Figure 2-16 Overlap integral of donor and acceptor[38].

Consider a donor in the absence of any acceptor. Electromagnetic radiation incident on the molecule causes absorption when the energy of the radiation matches that for the transition from the ground to the excited state, and the electric vector of the electromagnetic field interacts with the transition dipole moment of the molecule.

In the presence of an acceptor, a new excited state pathway, *Förster* energy transfer, exists for depopulating the excited state of the donor. The yield of fluorescence of the donor will be diminished by the extent of energy transfer that occurs. The yield of energy transfer also depends on the magnitude of the competing processed for depopulating the excited state. The weak coupling treatment assumes that bringing an acceptor in the presence of the donor will not alter the rates of the intrinsic processes of the donor.

The *Förster* description of energy transfer involves weak coupling between the excited state donor and the ground state acceptor. A semi-classical treatment provides a suitable description of this process. The oscillating transition dipole moment of the excited state donor emanates an electromagnetic field that interacts with the transition dipole moment of the ground state acceptor. A resonant interaction can lead to transfer of the excited state from donor to acceptor. The rate of transfer depends on a variety of factors. The most important factors are described as follows.

(1). The through-space interaction of the donor and acceptor falls off as R^{-3} for both donor and acceptor, yielding a distance dependency that falls off as R^{-6} where R

is the distance between the centers of the respective of *Förster* energy transfer[39].

(2). The rate is proportional to the strength of the oscillators of the donor and acceptor. The rate constant (k_f) of fluorescence of the donor effectively provides a measure of the strength of the donor oscillator. The strength of the acceptor oscillator is provided by the molar absorption coefficient of the acceptor transition that matches the energy of the donor excited state.

(3). The rate depends on the orientation of the transition dipole moments of the donor and acceptor. This is presented by a constant κ^2. A collinear geometry provides the largest a value of 4; a parallel but not collinear geometry provides a value of 1, and orthogonal orientations give a value of 0.

(4). The rate depends on the energy matching of the oscillators. The extent of energy matching can be assessed by the overlap of the emission spectrum of the donor with the absorption spectrum of the acceptor.

The transfer rate constant k_{ET} is given in Equation 2-16.

$$k_{ET}(r) = \frac{Q_D \kappa^2}{\tau_D r^6}\left(\frac{9000\ln(10)}{128\pi^4 N n^4}\right)J(\lambda) \qquad \textbf{(Equation 2-16)}$$

Where Q_D is the luminescence quantum yield of the donor molecule, n is the refractive index of the medium, N is the Avogadro's number, κ^2 is the relative orientation of the donor and acceptor transition dipole moments, τ_D is the radiative lifetime of the donor, r is the distance (cm) between donor and acceptor, and $J(\lambda)$ is the spectral overlap (in coherent units $cm^6 mol^{-1}$) between the absorption spectrum of the acceptor and the fluorescence spectrum of the donor.

2.4.2 Dexter transfer.

For a shorter-range process requiring donor-acceptor separation of less than 1 nm,

another type of transfer may occur, which is known as the *Dexter* electron exchange transfer[40]. It requires quantum mechanical tunneling of electrons between the donor and acceptor. The process is given in Figure 2-17 below.

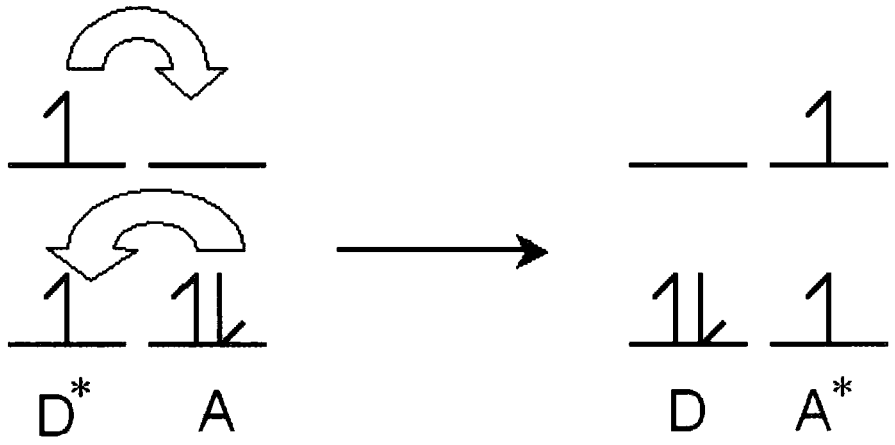

Figure 2-17 Dexter transfer between the donor and acceptor.

It is the dominant mechanism in triplet-triplet energy transfer. The transfer rate constant k_{ET}, is given by:

$$k_{ET}(r) = \frac{h}{(2\pi)^2} P^2 J e^{\frac{-2r}{L}} \qquad \textbf{(Equation 2-17)}$$

Where r is the distance between donor and acceptor, L and P are constants not easily related to experimentally determinable quantities, and J is the spectral overlap integral. For this mechanism the spin conservation rules are obeyed.

It will preserves the total spin of the system, buy change the spin state of donor and acceptor, so it allows triplet-triplet energy transfer from donor to acceptor. This process is called the triplet-triplet singlet-singlet annihilation shown in Equation 2-18 below.

$$T_1 + T_1 \rightarrow (T_1 + T_1)_{1,3,5} \rightarrow (S_0 + T_n), (S_0 + S_n) \qquad \textbf{(Equation 2-18)}$$

From this equation we can see that after the exchange of the electron between the two triplet states, the result state can form in three different ways due to the total 4 spin states of the two original triplets, which is singlet, triplet and quintuplet states. Thus the final states may also be two kinds as shown above.

2.4.3 Charge transfer (CT) state.

A charge transfer complex (CT complex) is defined as a pair of molecular groups, where one is electron-donating (donor) and the other is electron-accepting (acceptor) and where there is a partial transfer of electronic charge from the donor to the acceptor in an excited molecular state. This is often realized in conjugated copolymers, which consist of two or more different repetitive units.

CT complexes have a transition between the excited molecular state and a ground state and almost all CT complexes have unique absorption bands in the ultraviolet-visible (UV-Vis) region. The interaction between donor and acceptor is not only a charge transfer interaction but also electrostatic force and sometimes interaction. The interaction between donor and acceptor is usually much weaker than interactions of the hydrogen bond and the covalent bond, but it is useful for constructing crystal structures.

In some polymers where the charge transfer complexes exits, a new energy state called the charge transfer (CT) state will form[41]. For example, strong CT state can form in some benzene structures with one or more C atoms replaced by an electron-acceptor or electron-donor unit. The distribution of electrons on this new type of electron state can be approximately presented like D+-Ph-A- (D: electron donor, Ph: benzene ring, A: electron acceptor).

Normally this new electron state is lower than the old molecular excitation state because of the energy losing during the transition process from the donor to the acceptor excited states. This is why we get the CT emission red-shifted. And during this new CT state molecules are much more active and polar than the molecular excitation state. In addition, time-domain THz technology can measure electric field

transients directly in the time-domain with sub-picosecond resolution. We therefore use this technology to probe intramolecular charge transfer events. From these measurements we obtain two important results. First, the polarity of the emitted field determines the direction of charge transfer unambiguously. Second, the shape of the field encodes the dynamics of the charge transfer - a slower transfer rate produces a broader temporal pulse. This is why the CT emission is without vibronic progression.

2.5 Device operation.

2.5.1 Electron injection.

Electron injection is achieved in polymer LEDs through using nontransparent metal electrodes. When charge injection occurs from the electrodes into the HOMO and LUMO of the polymer, there are barriers to prevent this process. These barriers arise primarily due to the difference in work functions of the materials used and the electron affinity and ionization potential of the polymer. A simple scheme explaning this is shown below in Figure 2-18.

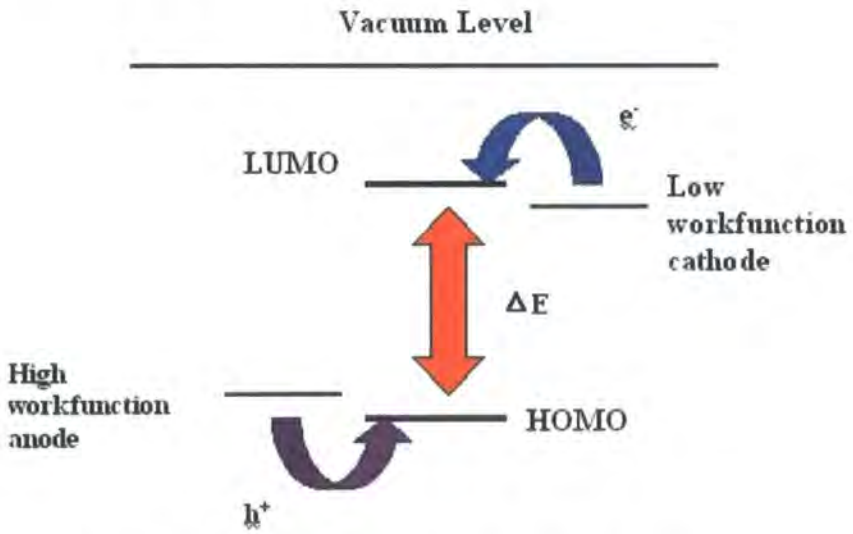

Figure 2-18 Charge injection into polymer LEDs.

Electron injection into PLEDs is usually achieved by using non-transparent metal electrodes[42], such as Al, Ca or Ba. The metal workfunction should be low so that it is easier for electrons to be injected.

However, normally low workfunction metals are very reactive with the air, so every work should be done in a vacuum environment.

2.5.2 Hole injection.

Hole injection is usually achieved in forward bias by using a high workfunction material. And the hole injection electrode should be a transparent or semitransparent one for the light beam to come out. The necessity for transparent electrodes limits the thickness and hence the conductivity of the polymer.

The most commonly used material is ITO (indium tin oxide) glass. And poly(ethylenedioxythiophene) (PEDT) has also been used between the ITO layer and polymer layer to improve the performance of polymer LEDs.

2.5.3 Charge transport.

When charges are injected into polymer HOMO and LUMO levels, they will transport by charge carries in the form of polarons though the polymer LEDs.

Normally hole (positive carrier) mobility is different with electron (negative carrier), so the transport balance is not very perfect. The hole mobility in polymers has been shown to be highly field dependent[43, 44]. The mobility of the positive charge carrier is very important because most organic materials are very good positive charge carriers. Thus most charge carriers in polymer LEDs are positive charge carriers. If the charge transfer balance is not good enough, it will reduce the device efficiency obviously. To solve this problem we often add a hole-transport layer and electron-transport layer into polymer LEDs.

The hole mobility is shown below.

$$\mu_p(E) = \mu_p(0)e^{\gamma\sqrt{E}} = \mu_0 e^{\left(\frac{-\Delta}{KT}\right)} e^{(\gamma\sqrt{E})} \qquad \textbf{(Equation 2-19)}$$

,where E is the applied electric field, $\mu_p(0)$ is the mobility at zero field, Δ is the activation, μ_0 is a prefactor and γ is a material dependent coefficient.

2.5.4 Polaron combination.

Charge carriers (polarons) migrate through the device and then meet with their oppositely charged counterparts. The position where this process happens is mainly decided by the relative mobilities of the two charges in the material which forms the device[45].

When the polarons combine at a certain site, a polaron-exciton is formed, and will become a singlet exciton or triplet exciton described before.

2.5.5 Exciton migration.

Once the polaron-exciton is formed, it will migrate from short conjugation length chain segments with higher energy to longer ones with lower energy. The migration becomes slower with time, as there are fewer energetically available sites the exciton can migrate to.

It is also necessary to point out that sometimes the exciton may also migrate to quenching sites, and hence reduce the efficiency of the polymer LEDs[46]. The migration occurs on a sub picosecond timescale. And the migration of the charge-neutral exciton is not assisted by the field, which implies that the migration will move the exciton only short distances away form the position where it was first formed.

2.5.6 Radiative Decay.

As referred to before, the are two kinds of excitons, which is singlet exciton and triplet exciton. The electron and hole in the singlet exciton can then recombine and emit light, which is called the fluorescence or luminescence. The triplet exciton's recombine and the emission of phosphorescence can also be achieved by more and more new techniques such as spin-orbit coupling effect by adding a heavy metal atom in the polymer system. Light emission is suppressed near the metal/polymer interface, and the presence of the interface seems to have an effect up to about 60 nm into the polymer film[45, 47].

However, not all the light can come out from the polymer after it is generated. Some is waveguided due to the internal and total reflection of the film. The amount of light that actually escapes in the forward direction is believed to be a factor $2n^2$ lower, where n is the refractive index of the polymer, than the amount of light generated inside the film[48].

2.6 References.

1. P. Y. Bruice, Organic Chemistry (Prentice Hall, 2004).
2. W. Locke and the ICSTM Department of Chemistry 1996-97.
3. http://chemed.chem.purdue.edu/genchem/topicreview/bp/ch8/mo.html
4. http://wps.prenhall.com/wps/media/objects/724/741576/chapter_01.html
5. http://wps.prenhall.com/wps/media/objects/724/741576/chapter_01.html
6. http://wps.prenhall.com/wps/media/objects/724/741576/chapter_01.html
7. http://wps.prenhall.com/wps/media/objects/724/741576/chapter_01.html
8. http://wps.prenhall.com/wps/media/objects/724/741576/chapter_01.html
9. http://cwx.prenhall.com/bookbind/pubbooks/hillchem3/medialib/media_portfolio/24.html

10. R. Peierls, More Surprises in Theoretical Physics, 1 ed. (Princeton University Press, Princeton, 1991).
11. http://en.wikipedia.org/wiki/Fermi_golden_rule
12. B. P. Straughan and S. Walker, Spectroscopy (Chapman and Hall, London, 1976).
13. http://www.monos.leidenuniv.nl/smo/index.html?basics/photophysics.htm
14. 1996, 68, 2283 (IUPAC Compendium of Chemical Terminology 2nd Edition 1997).
15. http://en.wikipedia.org/wiki/Stokes_shift
16. O. B. 187, 216 (IUPAC Compendium of Chemical Terminology 2nd Edition 1997).
17. 1996, 68, 2283 (IUPAC Compendium of Chemical Terminology 2nd Edition 1997).
18. R. H. Friend, R. W. Gymer, A. B. Holmes, J. H. Burroughes, R. N. Marks, C. Taliani, D. D. C. Bradley, D. A. Dos Santos, J. L. Bredas, M. Logdlund, and W. R. Salaneck, Nature (London) 397, 121 (1999).
19. S. N. Yaliraki and R. J. Silbey, J. Chem. Phys. 104, 1245 (1996).
20. G. D. Scholes, D. S. Larsen, G. R. Fleming, G. Rumbles, and P. L. Burn, Phys. Rev. B 61, 13670 (2000).
21. S. C. J. Meskers, J. Hubner, M. Oestreich, and H. Bassler, J. Phys. Chem. B 105, 9139 (2001).
22. M. M. L. Grage, P. W. Wood, A. Ruseckas, T. Pullerits, W. Mitchell, P. L. Burn, I. D. W. Samuel, and V. Sundstrom, J. Chem. Phys. 118, 7644 (2003).
23. F. B. Dias, A. L. Macanita, J. S. de Melo, H. D. Burrows, R. Guntner, U. Scherf, and A. P. Monkman, J. Chem. Phys. 118, 7119 (2003).
24. D.L.Dexter, Journal of Chemical Physics, 21, 836 (1953).
25. R. Jakubiak, C. J. Collision, W. C. Wan, et al., Journal of Physical Chemistry A 103, 2394 (1999).
26. http://chemistry.mtu.edu/~pcharles/RESEARCH/thesis/ch01/HomePage.html
27. W. P. Su, J. R. Schrieffer and A. J. Heeger, Phys. Rev. Lett., 42, 25 (1979).
28. http://chemistry.mtu.edu/~pcharles/RESEARCH/thesis/ch01/HomePage.html

29. W. P. Su, J. R. Schrieffer and A. J. Heeger, Phys. Rev. Lett., 42, 25 (1979).

30. W. P. Su, J. R. Schrieffer and A. J. Heeger, Phys. Rev. B, 28, 2 (1983), 1138.

31. W. P. Su, J. R. Schrieffer and A. J. Heeger, Phys. Rev. B, 22, 4 (1980), 2099-2111.

32. A, J, Heeger, S. Kivelson, J.R.Schrieffer and W.P.Su, Reviews of Modem Physics, 60, 3 (1988), 781-850.

33. D. D. C. Bradley, et al., in Photochemistry and Polymeric Systems, 1st ed., edited by M. Kelly, C. B. McArdle and M. J. F. Maunder, p. 120-133 (The Royal Society of Chemistry, Cambridge, 1993).

34. K. Fesser, A. R. Bishop and D. K. Campbell, Phys. Rev. B., 27, 8 (1983).

35. B. Schweitzer and H. Bassler, Synthetic Metals 109, 1 (2000).

36. M. Pope and C. E. Swenberg, Electronic Processes in Organic Crystals and Polymers (Oxford University Press, Oxford, 1999).

37. T.H.Forster, in 10th Spiers Memorial Lecture, (1959), p.7.

38. http://probes.invitrogen.com/handbook/images/g000118.gif

39. Moog, R. S., A. Kuki, M. D. Fayer and S. G. Boxer (1984) Excitation transport and trapping in a synthetic chlorophyllide substituted hemoglobin; Orientation of the chlorophyll S1 transition dipole. Biochemistry (A. C. S.) 23, 1564-1571.

40. D.L.Dexter, Journal of Chemical Physics, 21, 836 (1953).

41. 1996, 68, 2232 (IUPAC Compendium of Chemical Terminology 2nd Edition 1997).

42. D.Braun and A.J.Heeger, Thin Solid Films, 216, 1 (1992), 96-98.

43. H. Bassler, Physica Statu Solidi B-Basic Research, 175,1 (1993), 15-56.

44. P. W. M. Blom, M. J. M. deJong and M. G. vanMunster, Phys. Rev. B., 55, 2 (1997), R656-R659.

45. J. Gruner, M. Remmers and D. Neher, Adv. Mat., 9, 12 (1997), 964.

46. R. F. Mahrt, U. Lemmer, A. Greiner, Y. Wada, H. Bassler, E. O. Gobel, R. Kersting, K. Leo and H. Kurz, Journal of Luminescence, 60&61, (1994), 479-481.

47. V.Choong, Y. Park, Y. Gao, T. Wehrmeister, K. Mullen, B. R. Hsieh and C. W. Tang, Appl. Phys. Lett., 69, 10 (1996), 1492-1494.

48. N. C. Greenham, R. H. Friend and D. D. C. Bradley, Adv. Mat., 6, 6 (1994), 491-494.

Chapter 3 Conjugated Polymers.

3.1 Conjugated polymer chain.

As described in the 2.1 part of Chapter 2, in a long molecular chain which is connected through the σ-bonds, we can see that the remaining p_z orbitals can overlap to form π-bonds through the system. And in addition, the π-bonds can produce a bond order of 1.5 for carbon atoms along the chain. This is called the conjugated polymer. And because the π-bonding states are completely filled, while the π-antibonding states are completely empty, an energy gap now exists between the states as a result of the effect called Peierls distortion. Thus, the whole polymer becomes an organic semiconductor.

A typical conjugated polymer chain segment is shown below.

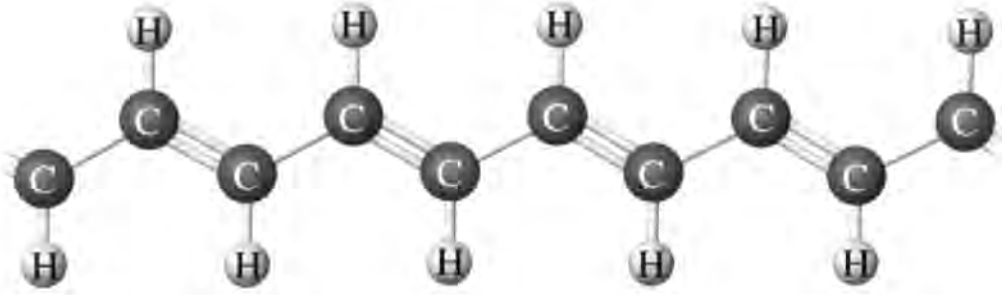

Figure 3-1 The polymer chain of poly(acetylene).

3.2 Copolymers[1].

A copolymer, is a polymer formed when two (or more) different types of monomer are linked in the same polymer chain, as opposed to a homopolymer where only one monomer is used. If exactly three monomers are used, it is called a terpolymer.

The assembly of the monomers in the copolymers can be head-to-tail,

head-to-head, or tail-to-tail.

Since a copolymer consists of at least two types of repeating units (not structural units), copolymers can be classified based on how these units are arranged along the chain. These include:

(1). Random copolymer:

-A-A-B-B-A-A-A-B-A-A-B-B-A-B-A-A-A-B-A-A-A-B-B-

(2). Alternating copolymer:

-A-B-A-B-A-B-A-B-A-B-, or $-(-A-B-)_n-$

(3). Block copolymer:

-A-A-A-A-A-A-A-A-B-B-B-B-B-B-B-B-A-A-A-A-A-A-A-A-B-B-...

(4). Graft copolymer:

-A-A-A-A-A-A-A-A-A-A-A-A-A-A-A-A-A-A-A-A-A-A-A-

|

B-B-B-B-B-B-B-B

(5). Star copolymers

(6). Brush copolymers

Today, the usage of copolymers as the light-emitting layer is a very important and successful way in the field of organic PL and EL, because the added units can normally effectively change the PL and EL peak positions and enhance the efficiencies by energy transfer from the main polymer and direct carrier trapping in devices.

3.3 Polyfluorene and relative copolymers.

Since the EL of conjugated poly(p-phenylenevinylene) (PPV) sandwiched between an anode and a cathode of appropriate work functions was first reported in 1990, knowledge of EL polymers and polymer light emitting diodes have expanded rapidly[2].

Currently, polyfluorene (PFO) with their high solid-state fluorescence quantum

yields, exceptionally high solubility and strong thermal and electrochemical stability, are very promising candidates for blue LEDs. The molecular structure of polyfluorene is shown below in Figure 3-2.

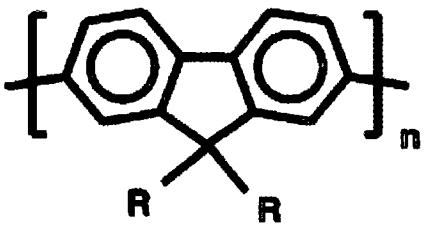

$R = C_8H_{17}$

Figure 3-2 Molecular structure of polyfluorene.

However, PFO exhibit relatively low charge transport ability. PFO have excellent hole mobility, but their mobility and injection of electrons are much lower than holes. So the transport of positive and negative carriers is greatly unbalanced. This will reduce the LED efficiency seriously. In order to overcome this, the common approach is to incorporate electron donor or electron acceptor segments into the side chain or backbone of the conjugated polymers. And after *Ohmori et al* reported the first report of electroluminescence from polyfluorene in 1991[3], more and more based on polyfluorene and its derivatives followed.

Today work on polyfluorene LEDs has focused on achieving emission colors across the entire visible range and improving device stability. Methods of tuning the emission color include adding molecular dopants in polymer systems, attaching emissive moieties and so on.

During these methods, fabricating fluorene-based copolymers is also a very important and effective one. As opposed to making devices with red, green and blue emission, the technique of achieving pure white emission is also a good idea. Copolymers of fluorene based on the theory of charge transfer (CT) states have been used for this idea. That is just the main subject of this thesis.

In addition, by adding rigid moieties, intermolecular interaction between

polymer chains can be prevented and the molecular rigidity of the polymer can be preserved. This leads to high glass transition temperatures and improved thermal and spectral stability. And because excimers formation is prevented, stable emission colors can be achieved. These will be described in more details in Chapter 4 and 5.

3.4 References.

1. http://de.wikipedia.org/wiki/Copolymer.
2. J. H. Burroughes, D. D. C. Bradley, A. R. Brown, et al., Nature 347, 539 (1990).
3. Y. Ohmori, M. Uchida, K. Muro, K. Yoshino, Jpn. J. Appl. Phys., Part 2. 1991, 30, L1941.

Chapter 4 Materials and Experimental Methods.

4.1 Sample Preparation.

4.1.1 Polymer structures.

The polymers for this investigation are two series of polyfluorene (PFO) co-polymers, which are p(F8-28DBTO)s and p(F8-37DBT)s. In the 28 series, dibenzothiophene (DBTO) unit is introduced through the 2,8 position into the PFO backbone, and in the 37 series, the DBT unit is introduced through the 3,7 position into the PF backbone. Each of them contains 5 kinds with different ratios of the co-polymers. The chemical structures of these co-polymers are shown in Figure 4-1 and 4-2 below.

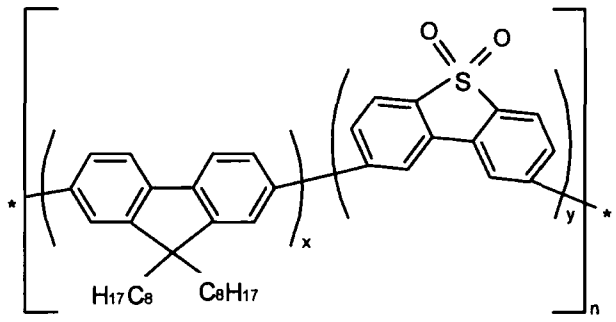

p(F8-co-27DBTO)-2%: x=98%, y= 2%
p(F8-co-27DBTO)-5%: x=95%, y= 5%
p(F8-co-27DBTO)-10%: x=90%, y=10%
p(F8-co-27DBTO)-20%: x=80%, y=20%
p(F8-co-27DBTO)-30%: x=70%, y=30%

Figure 4-1 Chemical structures of p(F8-28DBTO)s.

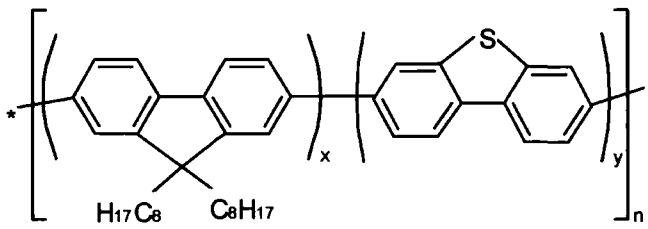

p(F8-co-36DBT)-2%: x=98%, y= 2%
p(F8-co-36DBT)-5%: x=95%, y= 5%
p(F8-co-36DBT)-10%: x=90%, y=10%
p(F8-co-36DBT)-20%: x=80%, y=20%
p(F8-co-36DBT)-30%: x=70%, y=30%

Figure 4-2 Chemical structures of p(F8-37DBT)s.

From these 2 figures, we can see that these two series of copolymers are the compounds of PFO and different concentrations of DBTO, DBT units.

These two series of polyfluorene copolymers were supplied by *Irina I. Perepichka*, *Igor F. Perepichka* and *Maksym* in chemistry department, University of Durham.

4.2 Optical absorption and fluorescence spectroscopy.

4.2.1 Optical absorption spectroscopy.

An absorption spectrum is a measurement of how much light has been absorbed in a wavelength range by a sample such as solution or film. The relative amount of absorption at each wavelength is governed by the relative strength of the optical transition, which follows the *Beer-Lambert* law[1]. See Equation 4-2 below.

$$I_l = I_0 e^{-\alpha C l} \qquad \textbf{(Equation 4-2)}$$

I_l is the incident intensity of the light beam, I_l is the intensity of the light that has transferred from a sample of length l, α is the frequency dependent absorption coefficient, and C is the concentration of the absorbing species.

And the absorbance of the sample can be defined as

$$OD = \lg\left(\frac{I_0}{I_l}\right) = \varepsilon C l \qquad \textbf{(Equation 4-3)}$$

ε is the molar absorption coefficient and is equal to $\frac{\alpha}{\ln(10)}$.

The absorption spectrum is recorded on a Perkin Elmer LambdaII-19

spectrophotometer.

4.2.2 Fluorescence spectroscopy and corrections.

Fluorescence is a measurement of the spectral properties of light that has been emitted from the emitting sample. It is based upon usage of spectrofluorimeters, which allows excitation of the sample at any wavelength in the visible~near UV range. These generally have a UV-VIS excitation source (eg Xenon lamps) which can produce excitation light in the 250-650 nm range with an excitation monchromator. The detection is based upon a collection by the emission through an emission monochromator in combination with a photomultiplier tube.

In addition, we have to correct the fluorescence spectrum after we get it from the Fluoromax-3 spectrofluorimeter, since the detector sensitivity varies as the light wavelength changes. To do this we multiply the spectrum with a correction file that have been generated using a calibrated lamp.

4.2.3 Photoluminescence quantum yield measurements.

Photoluminescence quantum yield (PLQY) is a very important measurement for investigating the sample's optical properties as it measure the light emitting efficiency of the sample material. It is defined as the ratio of the number of photons emitted by the sample to the number of photons absorbed by the sample. It is represented by the following equation.

$$\Phi_{PL} = \frac{n_{emi}}{n_{abs}} \qquad \textbf{(Equation 4-1)}$$

Although the PLQY is defined like this, in fact, we need a more practical approach for measurements of the PLQY. This will be described below.

4.2.4 Solution samples.

For measurements of the PLQY for solutions, a comparative methos muct be used. In this approach we meaure the PLQY of our unknown sample and compare it against a known standard. The solution samples were prepared by the following steps. Add each kind of copolymer powder into one bottle of solvent (I used toluene). The concentration is 1% by weight for all of them.

1. Put a magnetic stirrer into each bottle of solution, and then leave those on a hotplate & stirrer till the copolymer powder absolutely dissolved. The temperature for heating solutions is about 50 °C.
2. Use a 1cm×1cm quartz cuvette to dilute each solution, until the maximum absorbance of the absorption spectrum's peak is about 0.2.

When the above steps are finished, we can begin to measure the absorption and photoluminescence. And after we get the spectra, we can begin to measure the solution's PLQY.

The PLQY of solution is measured by subsequently comparing the integrated emission spectrum of the solution with that of a standard (reference) solution of known PLQY. For this investigation, I used 9,10-Dimethylanthracene as the standard (reference) solution.

The equation for measuring the solution's PLQY is shown below.

$$\Phi_s = \Phi_{ref} \frac{1-10^{-Aref}}{1-10^{-As}} \left(\frac{n_s}{n_{ref}}\right)^2 \frac{\int F_s(\lambda)d\lambda}{\int F_{ref}(\lambda)d\lambda} \qquad \textbf{(Equation 4-4)}$$

Φ_s is the PLQY of the solution sample, Φ_{ref} is the PLQY of the reference solution, $\left(1-10^{-Aref}\right)$ and $\left(1-10^{-As}\right)$ are the peak data of the (1-T) absorption spectrum of the reference solution and solution sample, n_s and n_{ref} are the refractive indexes of the sample and reference solution, $\int F_s(\lambda)d\lambda$ and $\int F_{ref}(\lambda)d\lambda$

are the integrations of the photoluminescence spectrum of the sample and reference solution.

4.2.5 Film samples.

The comparative method can not be used for film samples as there fluorescence may not isotropic. Films may exhibit extensive wave guiding and to overcome this, an integrating sphere is used[2]. The film samples were prepared by the following steps.

1. Put a blank quartz film on the spin-coating substrate, and set the spin speed as 2500 rpm (rounds per minute) and time as 60 seconds.
2. Drop small amounts of the dissolved solution onto the surface of the blank quartz film, and make sure the solution covers the surface smoothly. Then start spin-coating.

The PLQY can then be obtained as outlined by Pålsson and Monkman. A simplified equation for calculating the film's PLQY is shown below.

$$\Phi_f = \frac{N_E}{N_A} = \frac{\int F(\lambda)d\lambda}{\int P_s(\lambda)d\lambda - \int P_c(\lambda)d\lambda} \qquad \textbf{(Equation 4-5)}$$

Φ_f is the PLQY of the film sample, N_E is the number of photons emitted from the film sample, and N_A is the one of photons absorbed by the film. $\int F(\lambda)d\lambda$ is the integration of the PL spectrum of the film sample. $P_s(\lambda)d\lambda$ is the integration of the pump light intensity with the sample on the film, while $\int P_c(\lambda)d\lambda$ is the one with a clean film (without sample on it). This equation does not take into account secondary excitation effects but we have found that these are small (~1-5%) so the approximation is valid.

After we get the fluorescence spectrum of film, we also need to correct it because the responsibility of the integrating sphere varies as the wavelength of the fluorescence spectra changes. So we need to correct the fluorescence intensity at

every wavelength by multiply it with the correction data of the integrating sphere at the same wavelength to get the actual intensity.

4.2.6 Experimental set-up.

The absorption spectra of solution and film were measured using a commercial Perkin-Elmer Lambda 19 absorption spectrometer, which allows absorption, transmission, specular reflectivity and low temperature spectra (down to 10 K using cryostats) to be measured in the spectral range of 185 to 3250 nm.

Figure 4-3 Perkin-Elmer Lambda 19 absorption spectrometer[3].

While the emission spectra of solution and film were measured using a Jobin Yvon FluoroMax-3 spectrometer.

Figure 4-4 FluoroMax-3 spectrometer[4].

And the integrating sphere for calculating the PLQY of film samples is shown in Figure 4-5.

Figure 4-5 Integrating sphere[5].

4.3 Electroluminescence characterisation.

4.3.1 Device structure.

All the OLEDs have the same structure of five layers, which are ITO glass, PEDT (poly(ethylenedioxythiophene)), Light emitting layer (LEL), Ba (5nm) and Al (50nm). See Figure 4-6.

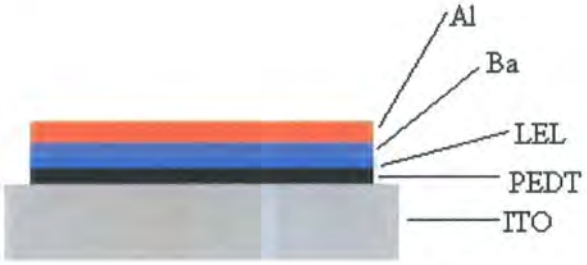

Figure 4-6 OLEDs structure.

ITO (Indium-tin-oxide) glass is one of the most frequently used materials as the anode of an electroluminescent device. It has high surface conductivity and high optical transmission.

On the ITO layer we usually spin a PEDT (poly(ethylenedioxythiophene)) layer.

This layer has a strong ability of transferring holes, which have been injected from the ITO anode.

Above the PEDT layer it is the light-emitting layer, or in other words, it is the polyfluorene copolymer layer.

The final layer is the cathode layer. It is made up of 5nm Ba and then 50nm Al during all my works in this thesis.

The electroluminescence light-emitting diodes (LEDs) were fabricated by the following steps.

1. ITO preparation.

(1). Cut big ITO glass (about $0.5m^2$) into small pieces with the size of 1.5cm 1.0cm.

(2). Clean them use DECON then acetone then Isopropanol to wash them for 5 minutes each in order to remove any glass shards and grease etc.

(3). Set the spin coater to

Stage 1: 280rpm for 10s, this is the smoothing stage.

Stage 2: 2200rpm for 30s, this is the solvent evaporation stage.

Then spin coat the photo resist (S1813) directly from the bottle using a disposable pipette.

(4). Remove the remaining solvent by soft baking the samples for about 3 minutes at $95^{o}C$ using the digital hotplate.

And the hotplate is shown below in Figure 4-7.

Figure 4-7 Hotplate & stirrer[6].

(5). Cover the sample with the mask and expose to the UV lamp for 30 seconds.

(6). Prepare the developer solution using 2 parts DI water and 1 part 351. By suing a pair of tweezers, hold the substrates into the developer until the red colour begins to take off. Then wash them in DI water twice.

(7). Hard bake the substrates at 124°C for 10~15 minutes using the digital hotplate.

(8). Prepare the etch solution by mixing the concentrated HCL: concentrated HNO_3: DI water at the ratio of 20:1:20. Heat this solution to 50°C using the non-digital hotplate. Use the thermo couple with a second DI water containing glass in order to check the temperature. Do not use the thermo couple directly with the acid. Etch the samples for 150 seconds using the alarm clock.

(9). Immediately, remove the acid with acetone by washing them in acetone twice.

And the final etched ITO glass is shown below.

Figure 4-8 One piece of etched ITO glass.

(4). Put the etched ITO glasses face up in the UVO-Cleaner for about 4 minutes to oxidize their ITO surfaces. The reaction functions are shown below.

$$O_2 \overset{UV}{\Rightarrow} O_1 + O_1$$

$$O_2 + O_1 \Rightarrow O_3 \qquad \textbf{(Equation 4-6)}$$

And the UVO-Cleaner (Jelight Company Model 42) is shown below in Figure 4-9.

Figure 4-9 UVO-Cleaner[7].

2. PEDT (poly(ethylenedioxythiophene)).

(1). Put the ITO glasses on the spin-coating substrate, set the speed as 2500rpm and time as 60 seconds, and then start spin PEDT.
(2). Put the ITO glasses with PEDT layer on a hotplate and bake them under the temperature of about 50 degree for about 10 minutes. This is also necessary because the PEDT is provided in an aqueous solution, and the water will reduce the device's efficiency if it is not evaporated.
(3). Take the glasses away form the hotplate and cool them to room temperature.

3. Polymer layer.

(1). Put the cooled glasses on the spin-coating substrate, set the speed and time. Then put 2 drops of well-dissolved polymer solution on it and start spin.
(2). Put them in a sample box, and note that the polymer layer surface should face down. Then send them into the glove box.

4. Metal evaporate.

(1). Put the sample glasses and Ba, Al in position in the glove box.
(2). Start vacuum pumping until the inside pressure goes down to about 10^{-6} Mbar.
(3). Start evaporating, first 5nm Ba and then 50nm Al.
(4). Stop pumping and take the samples out.

3.3.2 Thickness measurements.

For the thickness measurement we use a HAMAMATSU L7893 light source and F20-UV thin-film analyser. The HAMAMATSU L7893 light source and F20-UV thin-film analyser are shown below in Figure 4-10 and 4-11.

Figure 4-10 HAMAMATSU L7893 light source[8].

Figure 4-11 F20-UV thin-film analyser[9].

4.3.3 OLEDs test.

In contrast to the photoluminescence (PL) characterization, the electroluminescence (EL) mainly contains two parts, which are the spectral measurement and the intensity measurements.

From measuring the spectral output for a range of current/voltage values we can subsequently interpolate a device's efficiency, stability and spectral emission profile.

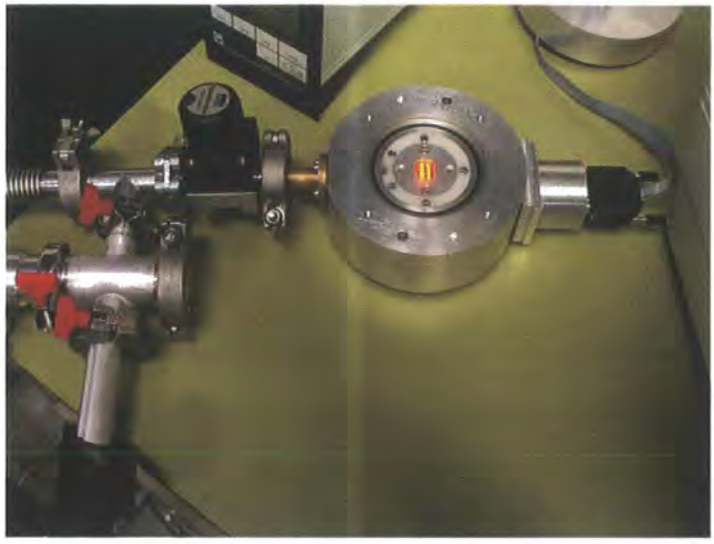

Figure 4-12 The LEDs test rig[10].

The intensity of a select pixel is measured by using a Keithley 2000 Multimeter, and the current-voltage behavior is measured by using a Keithley 2400 Source-Measure unit.

The characterization process is largely automated, with a homewritten NI Labview software designed to run the Keithley 2400 through a range of biases whilst the 2000 records the signal from a large area photodiode used to collect the visible output of a pixel.

The Keithley 2000 Multimeter and Keithley 2400 Source-Measure unit are shown below.

Figure 4-13 Keithley 2000 Multimeter[11].

Figure 4-14 Keithley 2400 Source-Measure unit[12].

The spectral output is measured by using a spectrograph attached to a CCD camera while a selected pixel is held at a constant voltage.

4.3.4 OLEDs efficiency analysis.

The OLEDs efficiency analysis mainly includes 3 parts during the whole investigation, which is the current-voltage property, voltage-luminance property and the external quantum yields.

First, by using the Keithley 2400 Source-Measure unit we can get a current-voltage result in the form of a comma delimited ASCII form. Then we can construct a graph of the I-V curves of the tested electroluminescent devices using Origin 7.0.

By using the Keithley 2000 Multimeter we can get a intensity-voltage result in a similar fashion.

Finally, we incorporate the two data sets into an Excel micro program called QEandBRIGHTNESS (home written) to calculate the external quantum efficiency and brightness of the device.

The external quantum efficiency is defined as the ratio of the number of photons emitted in the forward direction to the number of injected charges. See Equation 4-7.

$$E_{ext} = \frac{N_{photons}}{N_{charges}} \qquad \textbf{(Equation 4-7)}$$

And the number of injected charges is given by

$$N_{charges} = \frac{I_p}{e} \qquad \textbf{(Equation 4-8)}$$

I_p is the current injected into light emitting diodes, and e is the magnitude of the electronic charge on one electron.

4.3.5 Chromaticity co-ordinates.

Wyszecki and Stiles provided the important method of measuring the color property, which is called the chromaticity co-ordinates. The chromaticity co-ordinates of a color are the ratios of each tristimulous value of the color to their sum[13].

The most common system of chromaticity co-ordinates is the 1931 CIE- (X,Y,Z) system of color specification. It has three color matching functions, x_λ, y_λ and z_λ. See Figure 4-15.

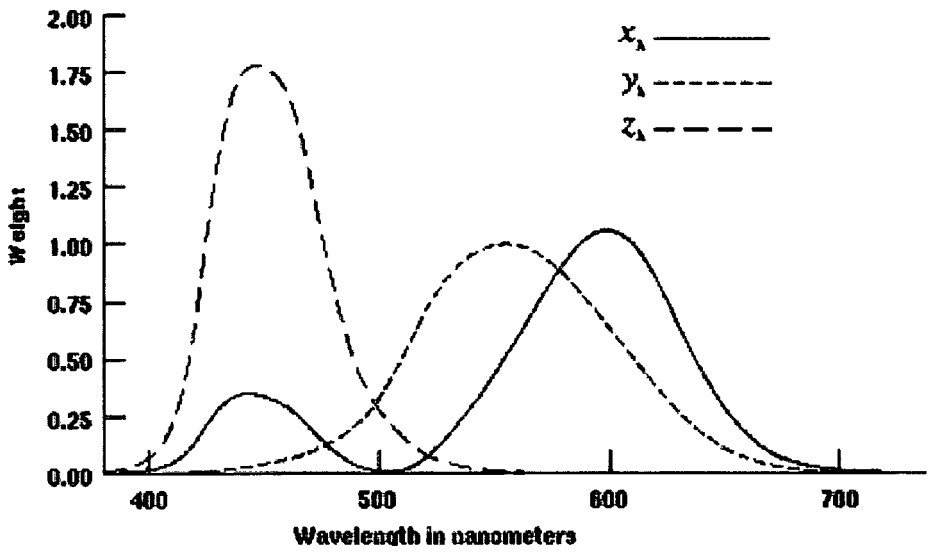

Figure 4-15 CIE color matching functions[14].

And the 2-dimensional x, y color space is shown in Figure 4-16.

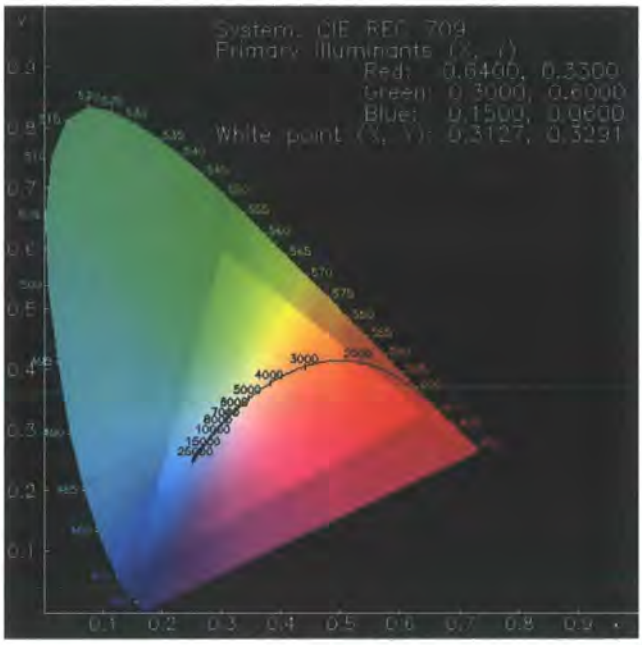

Figure 4-16 2-dimensional representation of x, y color space.

After we get the EL spectrum of the OLEDs, we use another home-written Excel micro program to calculate the CIE- (X, Y, Z) data.

4.4 References.

1. J. R. Lakowicz, Principals of Fluorescence Spectroscopy (Kluwer Academic, New York, 1999).
2. L.O. Pålsson and A.P.Monkman, Advanced Materials 14 (10), 757 (2002).
3. http://www.polymtl.ca/larfis/Labo/Spectro.htm
4. http://www.jobinyvon.com/pressreleases/0101fluoromax3.htm
5. http://www.fishlarvae.com/photos.asp?AID=8&GID=51&PID=375
6. http://www.nelabgear.co.uk/stirrers.html
7. http://www.ncnr.nist.gov/userlab/e132_frams.html
8. http://www.alldatasheet.com/datasheet.pdf/pdf/HAMAMATSU/L7893.html
9. http://www.filmetrics.com/f20.html

10. http://www.dur.ac.uk/oem.group/Research/VirtualTour.htm
11. http://www.used-line.com/c5035116s371-Keithley_2000.htm
12. http://www.giannigiorgetti.com/pcr/index.php?redir=control
13. G. Wyszecki and W. S. Stiles, Color Science, 1 ed. (John Wiley & Sons, Inc., 1967).
14. http://www.fourmilab.ch/documents/specrend/

Chapter 5 Photo and Electro luminescece of 28 Series.

5.1 Absorption and Photo luminescence in solutions.

The solutions for all the five copolymers are prepared with the concentration of 1% powder in toluene [w/w]. The solutions were also stirred for about 2 hours to make sure they are well dissolved before investigations. The solutions were subsequently diluted to absorption of ~0.2.

5.1.1 Absorption spectra.

The absorption spectra of 28 series in solution are shown in Figure 5-1 below. These spectra were measured in the room temperature.

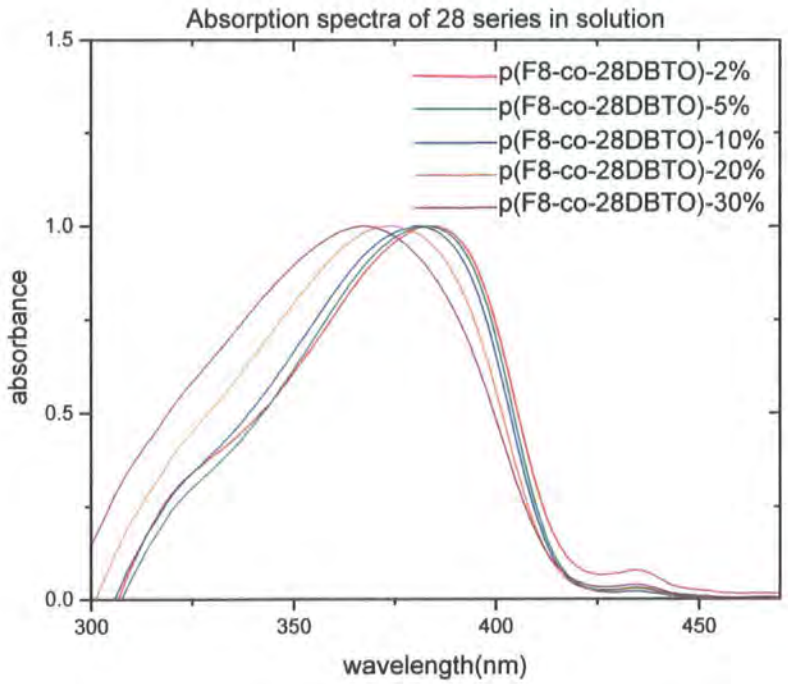

Figure 5-1 Absorption spectra of 28 series in solution.

From this figure we can see that all of the five absorption spectra have a similar shape, which shows a full width at half maximum (FWHM) of about 50nm. The absorbance maxima are around 360nm to 390nm for all copolymers. In addition to the strongest absorption peak, they all have a second weak peak around 435nm as well, with a varying degree of strength.

5.1.2 β-phase.

PFO adopts a particular type of conformation in dilute solutions of the poor solvent below 273 K, which is revealed by the appearance of a red-shifted absorption peak around 435nm[1]. When PFO is dissolved in toluene which is a poor solvent, some ordered segments, termed β-conformations, coexist with less ordered domains in the same PFO chain. This is called the β-phase phenomena of PFO in dilute solution. The transition between the disordered and the ordered PFO conformations is adequately described by a mechanism that involves two steps: a first, essentially intramolecular, one from a relatively disordered (β) to an ordered conformation (β), followed by aggregation of chains containing β-conformation domains[2].

As we have seen in Figure 4-1, we still get the β-phase phenomena in our five PF copolymer solutions, which results in the new second absorption peak around 435nm.

Another effect we can see in Figure 4-1 is that as the DBTO's ratio increases, the new peak will become slightly weaker. This is due to the addition of more DBTO unit in the PFO backbone, the formation of ordered segments (β-conformation) will be more difficult because of the interaction effect with the new side chain-DBTO.

Returning to the strong absorption peaks around 360nm to 390nm, the important observation is that, the position of this peak is blue-shifted when the DBTO ratio increases in solution, from about 385nm to 365nm. This is because when we increase the concentration of this new side chain-DBTO, the energy gap between the HOMO and LUMO levels of the copolymer chain will be larger. That leads to the blue-shifted in the solution absorption spectra.

5.1.3 Photoluminescence spectra.

Figure 5-2 shows the photoluminescence (PL) spectra of these five copolymers in solution, which is excited at their maximum absorption peak separately.

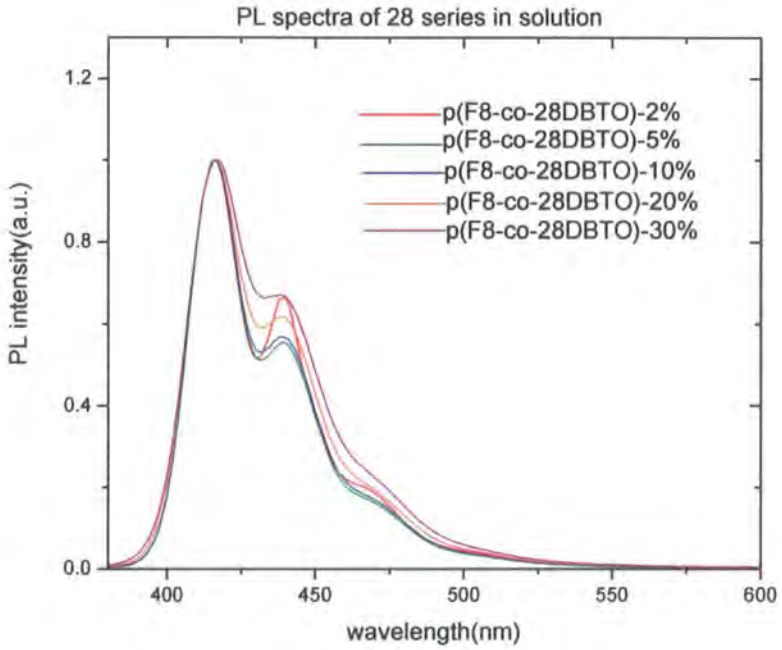

Figure 5-2 PL spectra of 28 series in solution.

The PLQYs are shown in the table below.

Sample	28-2%	28-5%	28-10%	28-20%	28-30%
PLQY	80%	87%	89%	93%	94%

As in normal PF solutions, we can still observe typical PL spectra with clear vibronic structure in the 28 series PF copolymers. From Figure 5-2 we see that they both show a 0-0' peak around 416nm, a 0-1' peak around 440nm, a 0-2' peak around 470nm, and even a weak 0-3' peak around 500nm.

The positions of these vibronic peaks are not changed when the DBTO's ratio

increases from 2% to 30%. The observation is instead that, as the DBTO's ratio increases, the second, third and fourth PL peaks will become weaker and weaker. Especially in p(F8-co-28DBTO)-30% solution, the three other peaks besides the 0-0' peak have almost totally disappeared in its PL spectrum. This must be due to the new side chain-DBTO. So another conclusion we can draw is that the DBTO unit will also reduce the vibronic coupling in PF in solution.

We also observe that with the decreasing the vibronic structure of the PL in solution, the PLQY shows an opposite trend. There is an increase of the PLQY as the DBTO's ratio increases from 80% to 94% which shows another important effect of the new side chain.

Another important aspect is that, although we observe the β-phase phenomena in the absorption spectra, we do not observe it in the PL spectra. When the ordered domains (β) are present they act as efficient energy traps and the fluorescence from the disordered regions is quenched. But quenching of their PL spectra is not observed.

It is also interesting to see the relationship between the absorption and PL spectra of these copolymers solution. These are shown in Figure 5-3 to 5-7 below.

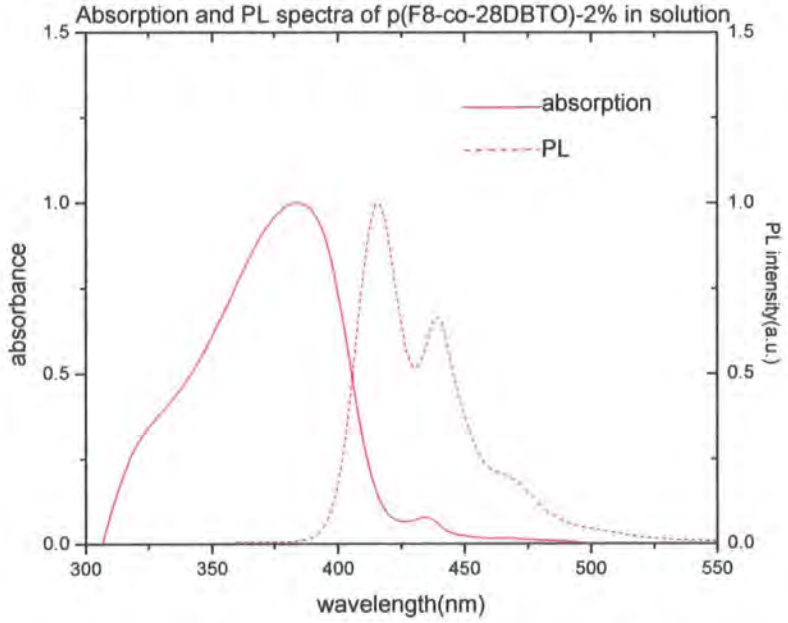

Figure 5-3 Absorption and PL spectra of 28-2% in solution.

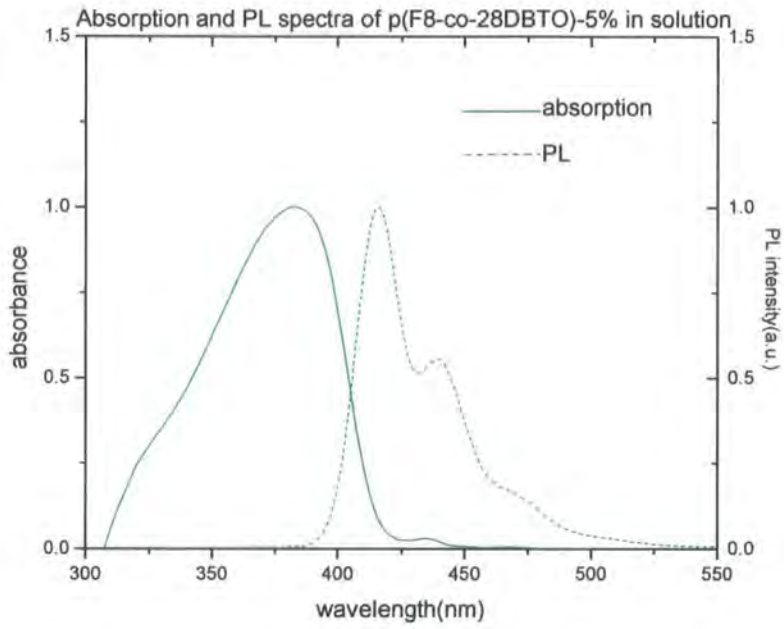

Figure 5-4 Absorption and PL spectra of 28-5% in solution.

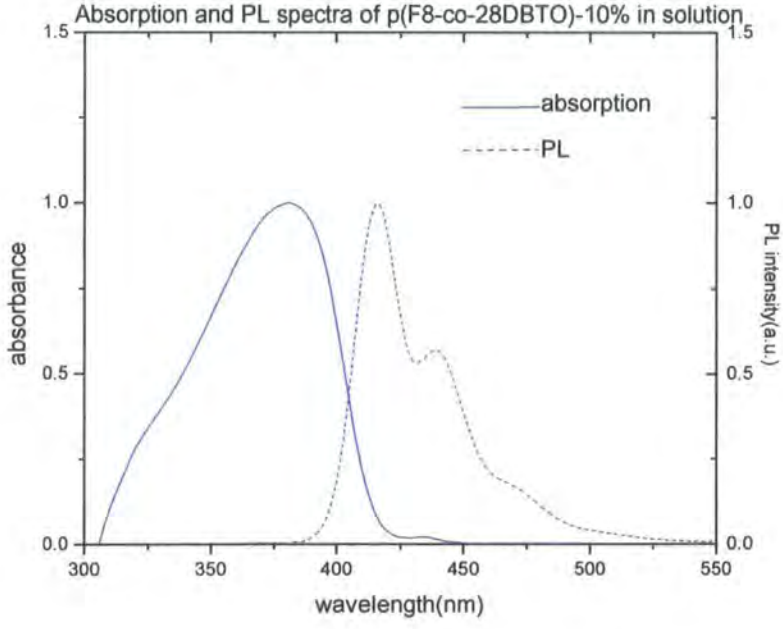

Figure 5-5 Absorption and PL spectra of 28-10% in solution.

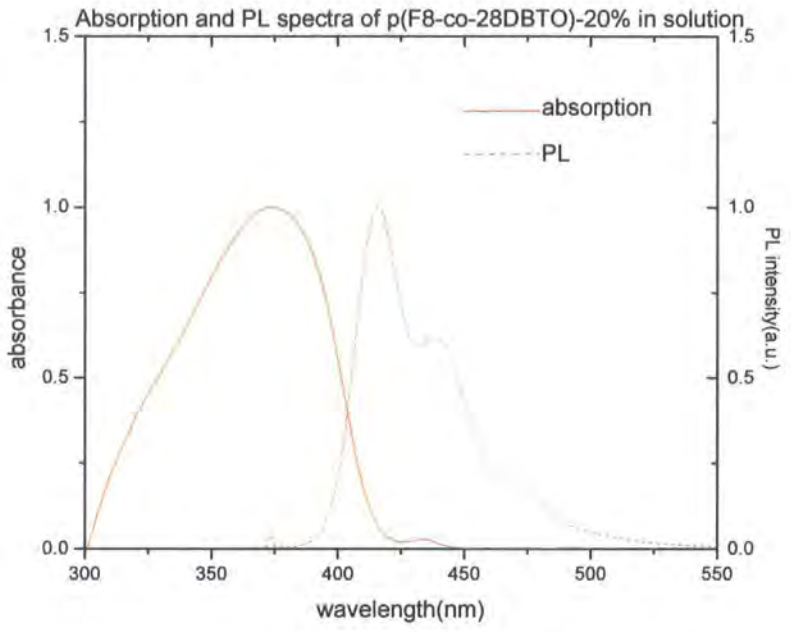

Figure 5-6 Absorption and PL spectra of 28-20% in solution.

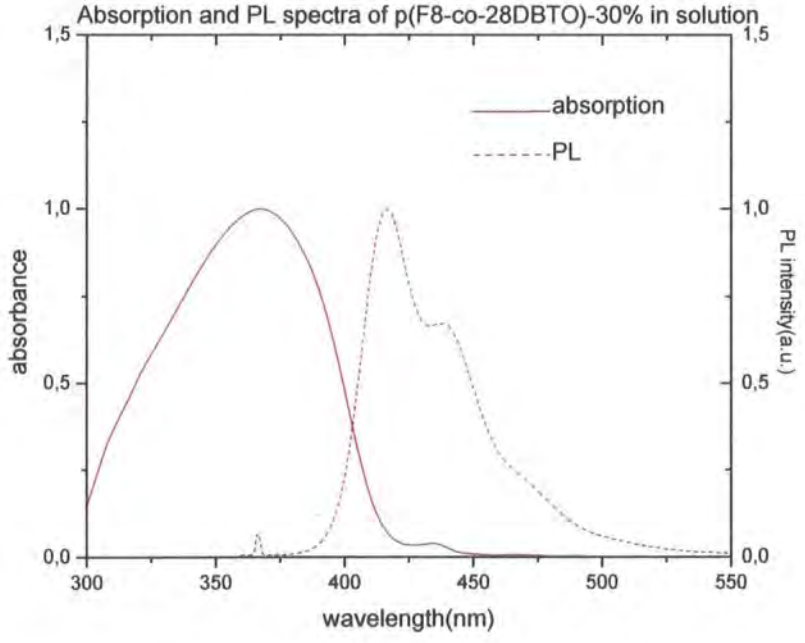

Figure 5-7 Absorption and PL spectra of 28-30% in solution.

From these 5 figures we see that for all of the five copolymers, the absorption

and PL spectra present a *Stoke's* shift, and the shift increases from about 30nm to 50nm as the DBTO unit's ratio increases from 2% to 30%.

5.1.4 CIE coordinates.

Finally, let's consider the CIE coordinates of the PL spectra of them. See the table and Figure 5-8 below.

Sample	28-2%	28-5%	28-10%	28-20%	28-30%
CIE	(0.156,0.062)	(0.157,0.059)	(0.157,0.061)	(0.156,0.064)	(0.155,0.069)

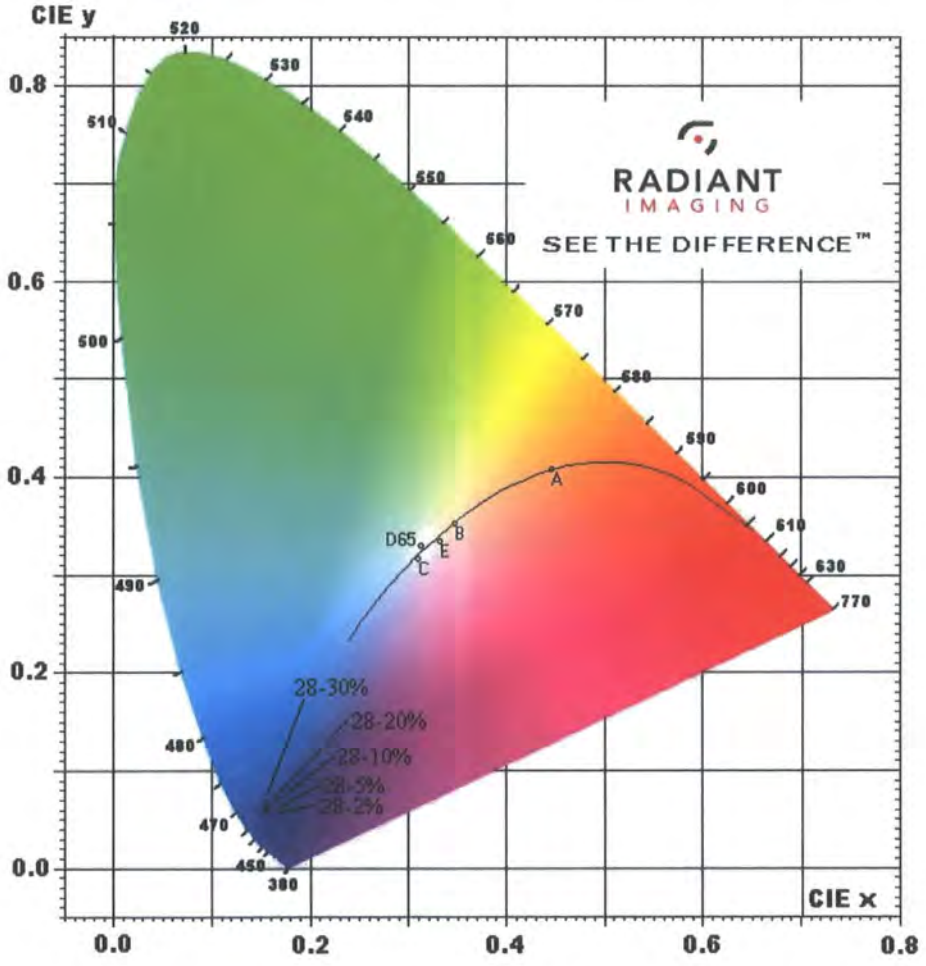

Figure 5-8 CIE co-ordinates of PL spectra of 28 series in solution.

From this figure we see that the PL emission wavelength of these copolymers is almost all the same in their solution state and with a small cyan-shift, which indicates that the DBTO unit has little impact on the emission wavelength in solution.

5.1.4 Conclusion.

In solution state of 28 series, the new unit-DBTO can cause the absorption spectra to be blue-shifted, decreases the β-phase phenomena in the absorption spectra. There will also be an impact on the PL vibronic structure which becomes less pronounced. The PLQY increases for all systems due to the new side chain.

5.2 Absorption and Photoluminescence in films.

5.2.1 Absorption spectra.

The absorption spectra of 28 series in film are shown in Figure 5-9 below. These spectra were measured in the room temperature.

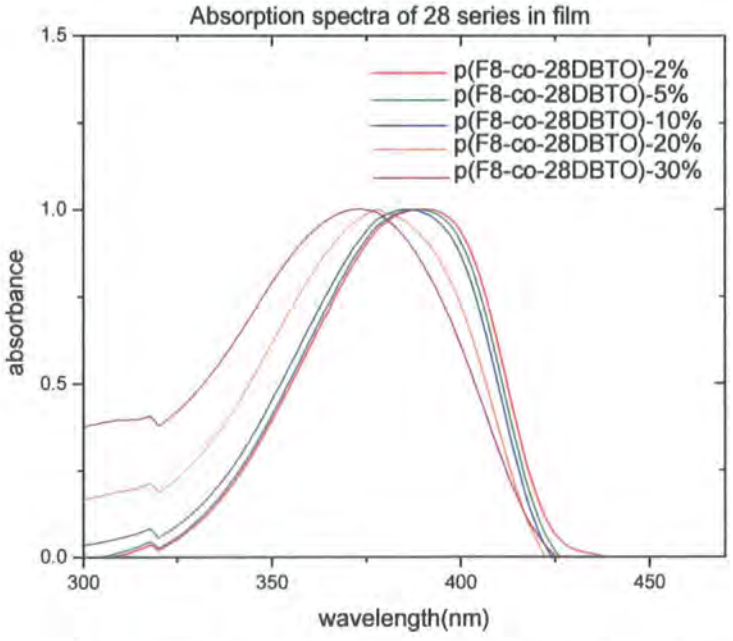

Figure 5-9 Absorption spectra of 28 series in film.

We can see that all of the five absorption spectra of the different co-polymer systems spectra still exhibit a similar absorption shape, which shows a full width at half maximum (FWHM) of about 50nm. However, each sample now only shows one single peak from 370nm to 390 nm. In contrast to the solution, we do not see the second absorption peak of the β-phase peak in the film absorption spectra. This is because in the solid film state, the distance between polymer chains is much closer than solution state, so the side chain interaction is much stronger than solution. As a result, the formation of ordered segments (β-conformation) has been effectively reduced by the new side unit-DBTO.

And again we see that the peak position has a little blue-shift from about 390nm to 370nm as the DBTO's ratio increases from 2% to 30% in solid state. The reason for this is the same with solution-the DBTO side chain has increased the gap between HOMO and LUMO level of the copolymer chain, which in turn has an impact on the excitation energy from LUMO to HOMO and results in a blueshift of the absorption.

5.2.2 Photoluminescence spectra.

Figure 5-10 shows the PL spectra of these five copolymers in film, which is excited at their maximum absorption peak separately.

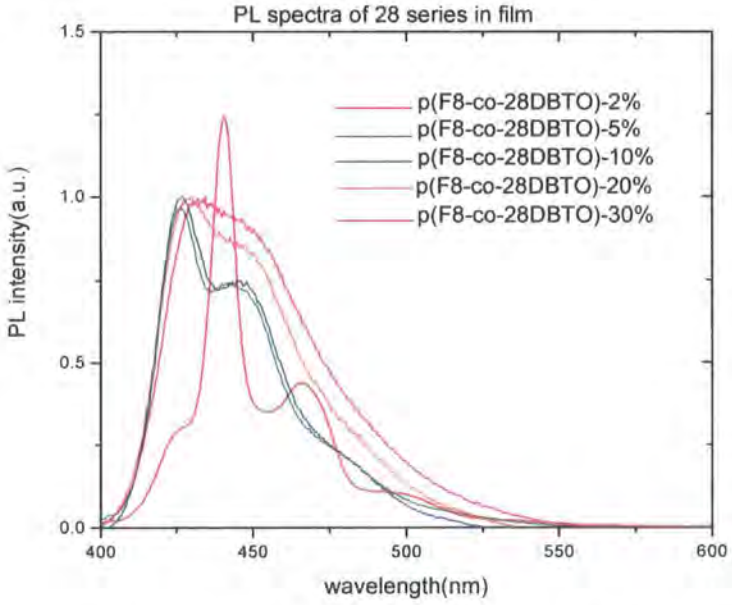

Figure 5-10 PL spectra of 28 series in film.

And the PLQYs are shown below.

Sample	28-2%	28-5%	28-10%	28-20%	28-30%
PLQY	39%	36%	35%	28%	28%

As we see, in the PL spectra of film, the vibronic structure of PF has been reduced much considerably compared to the solution state. When the DBTO's ratio increases to 20% and 30%, the original well resolved vibronic structure of the PL spectrum has change into a new broad structure with nearly only one maximum. This effect originates from the DBTO chain's interaction as described in the former previous section 4.2.3 of solutions. In films, the PLQY is in the range 39% to 28% with increasing the DBTO's concentration. But the results are still very high compared with other PF copolymer systems[3].

In the PL spectra of films another new phenomena is also observed: this is a slight red-shift of the PL peak. This originates from the DBTO unit and it is important because it demonstrates the possibility to change the emission towards white light by the addition of new side chain into PF polymer backbone in solid state. But more experiments are needed to confirm this hypothesis and the exact origin of the effect.

The final important phenomena in the PL spectra is that the strong β-phase peak in p(F8-co-28DBTO)-2% film, has most completely disappeared in 28-5%, 10%, 20% and 30% films PL spectra. This result has definitely proved at least two facts, first is that the β-phase actually exits in PF solid state emission spectra, and the second one is that the DBTO side chain's interaction can indeed effectively reduced the β-phase conformation in PF polymer system.

Let us return to the relationship between the absorption and PL spectra of these copolymers film. These are shown in Figure 5-11 to 5-15 below.

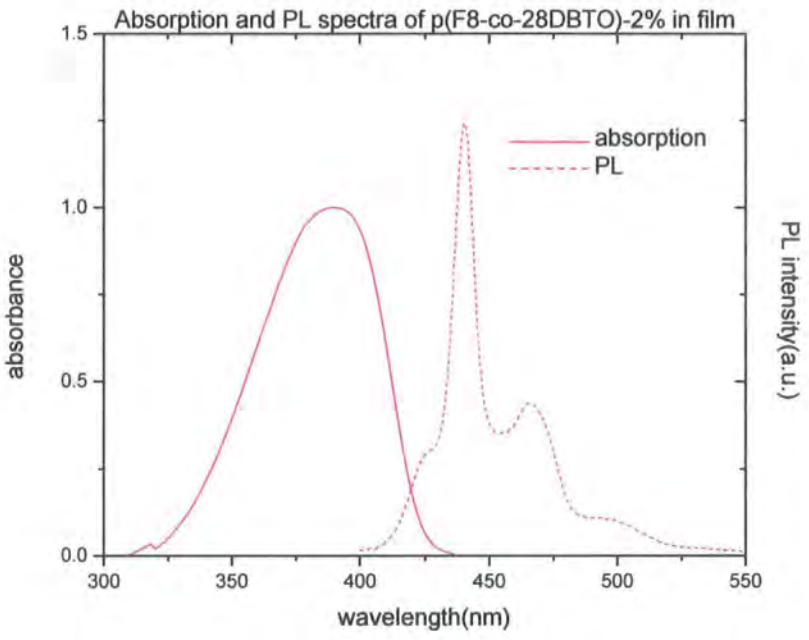

Figure 5-11 Absorption and PL spectra of 28-2% in film.

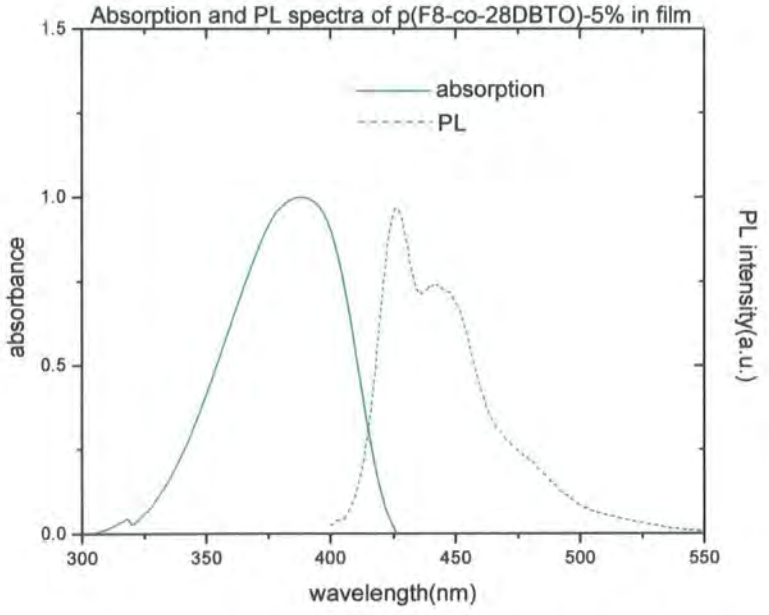

Figure 5-12 Absorption and PL spectra of 28-5% in film.

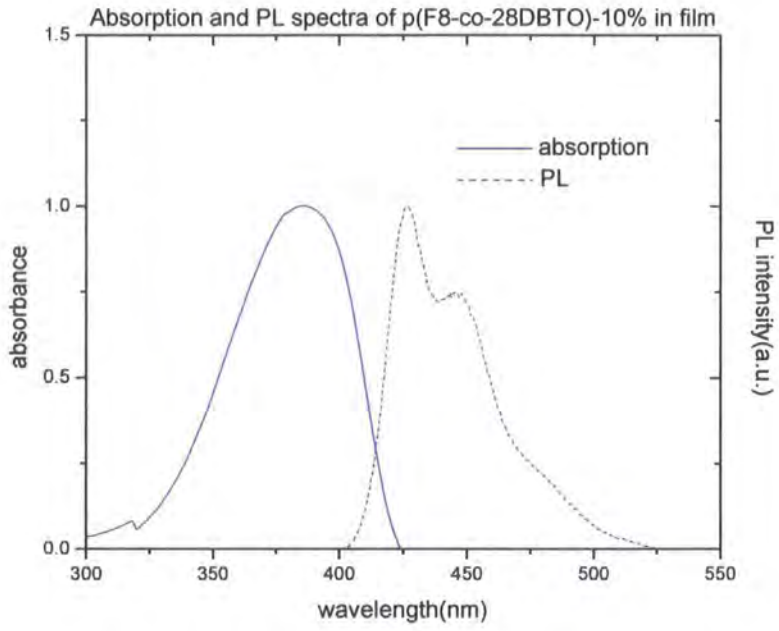

Figure 5-13 Absorption and PL spectra of 28-10% in film.

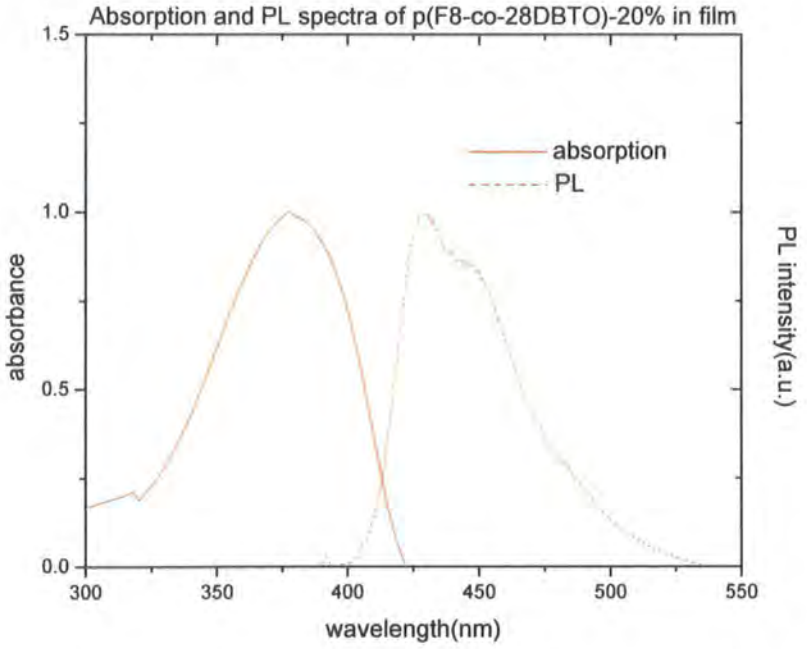

Figure 5-14 Absorption and PL spectra of 28-20% in film.

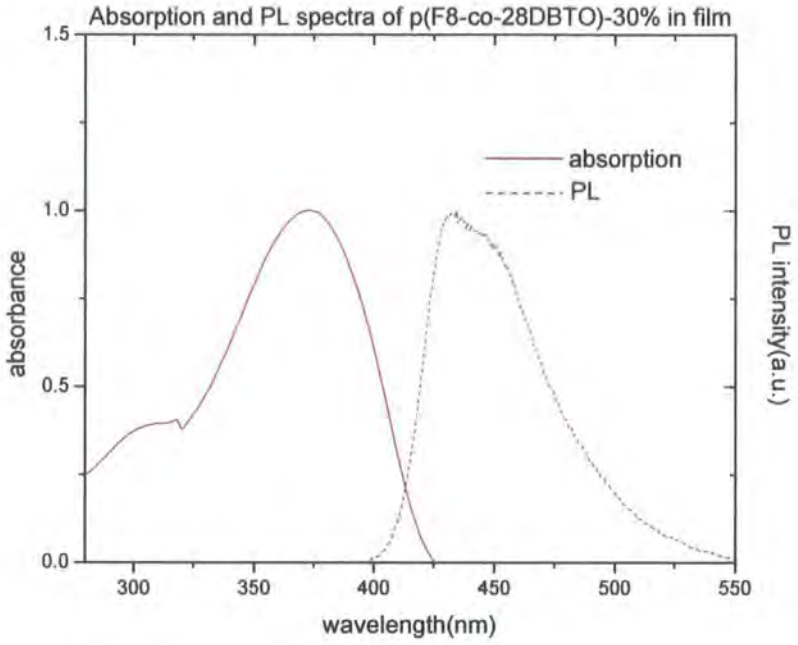

Figure 5-15 Absorption and PL spectra of 28-30% in film.

Again we get a Stokes shift in each co-polymer system, and the shift increases from about 35nm to 60nm as the DBTO unit's ratio increases from 2% to 30%.

5.2.3 CIE coordinates.

The CIE coordinates of these PL spectra are shown below.

Sample	28-2%	28-5%	28-10%	28-20%	28-30%
CIE	(0.143,0.127)	(0.153,0.127)	(0.155,0.142)	(0.158,0.178)	(0.148,0.172)

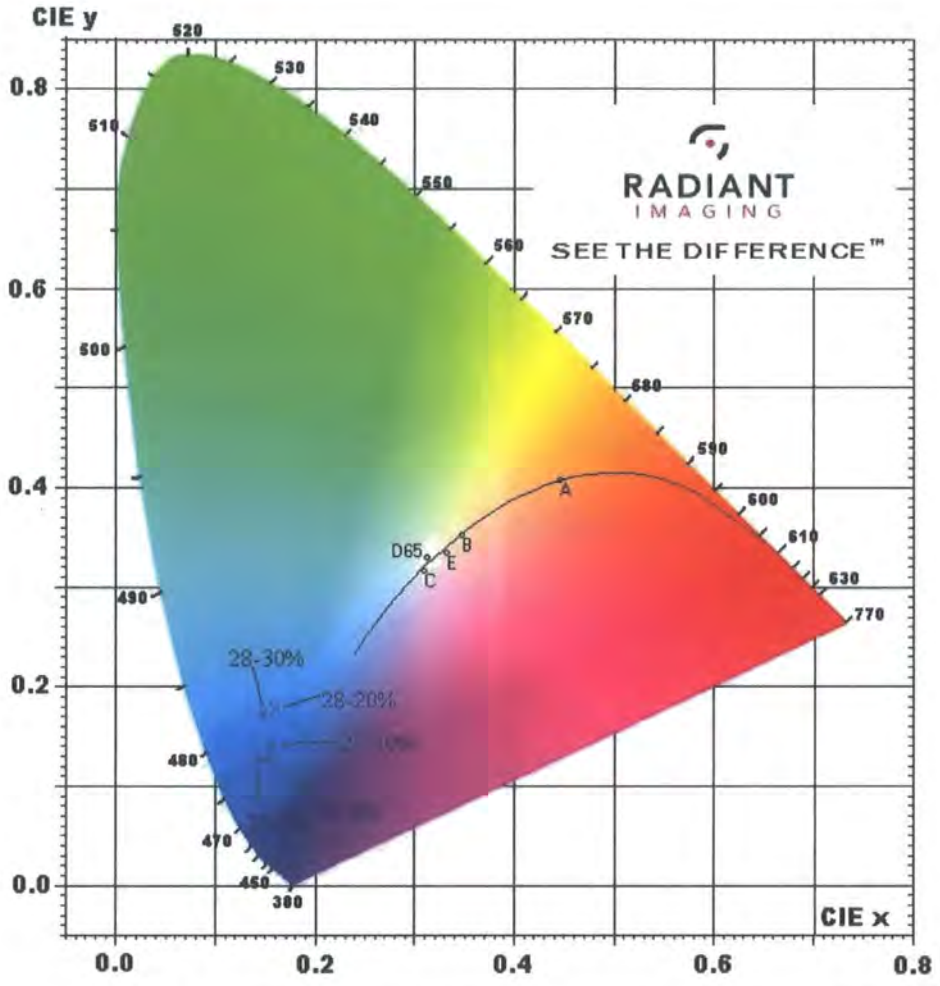

Figure 5-16 CIE co-ordinates of PL spectra of 28 series in film.

In this CIE graph we can see that the PL wavelength in the film has shifted from deep blue to redder wavelengths than in solution. This means the DBTO unit can change PF polymer's PL colour from dark blue to light blue in the solid state.

5.2.4 Conclusion.

In film state of 28 series, the new unit-DBTO can also cause the absorption spectra to blue-shift, and significantly reduce the β-phase phenomena in their PL spectra when the concentration of side chains is larger than 5%. This will also make the PL vibronic structure less pronounced and collapse into a single broad peak, cause the PL peak to red-shift slightly, and decrease the PLQY. In addition, the PL emission colour has been changed from dark blue to light blue as the DBTO unit's ratio

increases from 2% to 30%.

5.3 Electro luminescence properties.

5.3.1 Electro luminescence spectra and external quantum efficiency (EQE).

5.3.1.1 Electro luminescence of devices at 6V.

The first group of devices has the structure with the light-emitting layer (LEL) spin coated with the speed of 2500rpm for 60s, which is normally used in device fabricating. However, the thicknesses of their LEL are not still absolutely the same because of the different DBTO concentrations in the copolymer. Their thicknesses are shown below.

Sample	28-2%	28-5%	28-10%	28-20%	28-30%
LEL thickness	25.41nm	25.30nm	24.50nm	24.28nm	23.62nm

The bias voltage for this group of devices is set as 6V in the beginning. The EL spectra of them are shown in Figure 5-17.

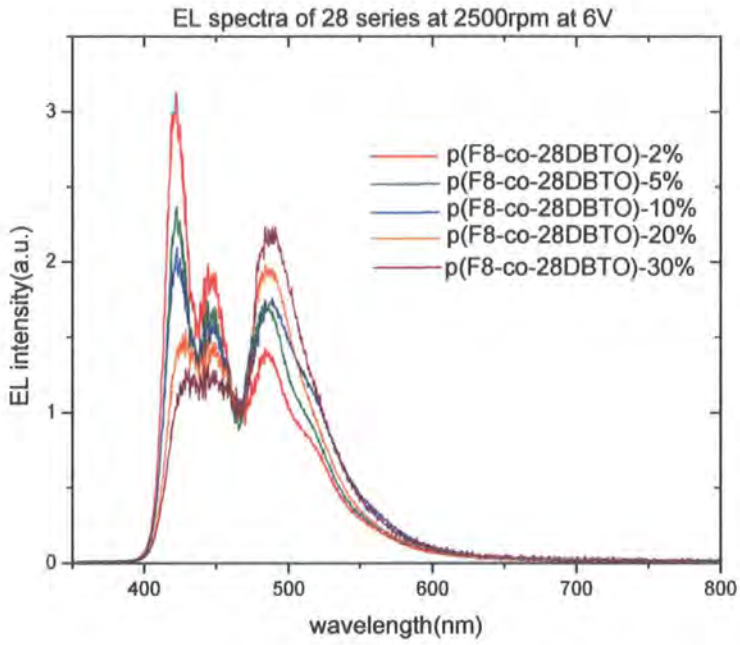

Figure 5-17 EL spectra of 28 series at 2500rpm at 6V normalized by the EL intensity at around 465nm.

From this figure, we can see that in contrast to the PL spectra of these five copolymer samples in solution and films, a new strong and broad peak appear in the EL spectra located around 485nm. The relative intensity of this new peak will increase as the DBTO unit's ratio increases, but the position will not change. But this new peak still may be the result of the keto defect[4].

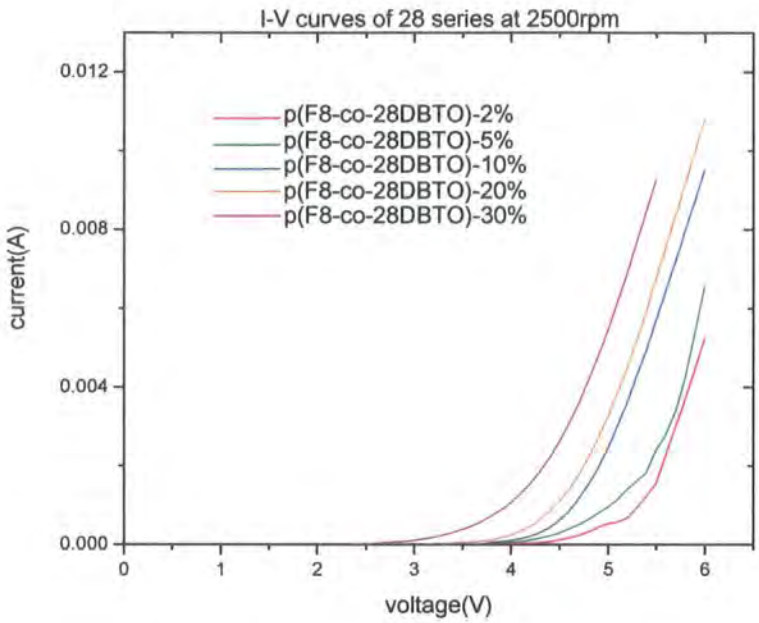

Figure 5-18 I-V curves of 28 series at 2500rpm.

In this figure of I-V curves we can see that the starting voltage decreases from about 4.3V to 2.7V as the DBTO unit's ratio increases. This is favourable because the working voltage is of course the better the lower it is in the OLED displays.

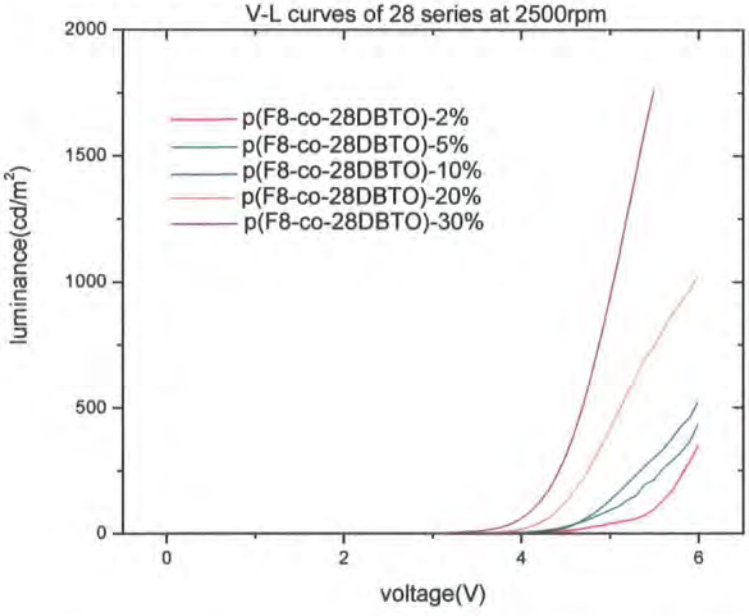

Figure 5-19 V-Luminance curves of 28 series at 2500rpm.

In this figure of V-L curves we can find that as the DBTO unit's ratio increases, the luminance will also increase very quickly from about 350cd/m^2 to 1760cd/m^2.

And finally the Luminance-External quantum efficiency curves.

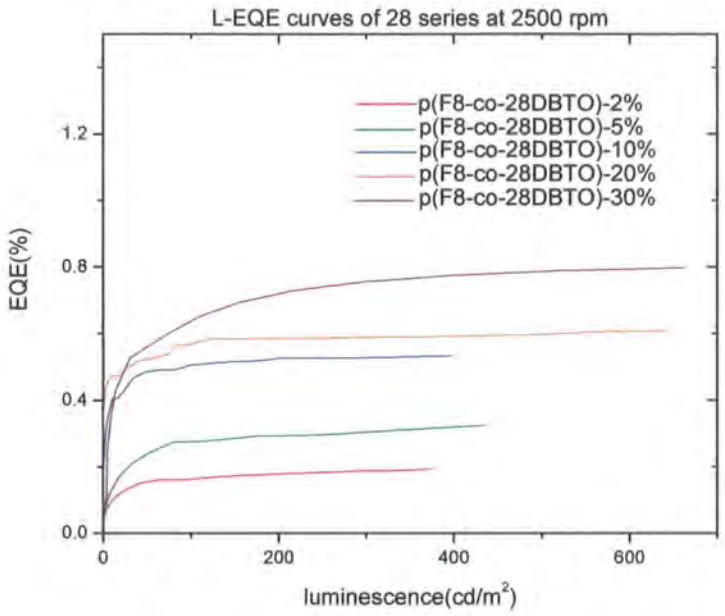

Figure 5-20 L-EQE curves of 28 series at 2500rpm.

One of the most important properties of the OLEDs is its external quantum efficiency (EQE). It will present the device's value directly. From this figure we can see that the EQE goes up quickly as the DBTO's ratio becomes larger from about 0.2%, which is very low for PF copolymers, to 0.8%.

Figures 5-18 to 5-20 have shown the tendency that as the DBTO unit's concentration increases, the EQE and luminance will both be enhanced largely. That means the new peak appeared in the former EL spectra is not because of keto defect but another important reason-the charge transfer (CT) state in these new copolymers chain system. This is also the reason why the new red-shifted peak around 495nm appears and the EQE and luminance is strongly enhanced as the DBTO's ratios increases.

In addition, another reason for the increased EQE and luminance is that the structure of DBTO unit. This new side chain is an electron acceptor, hence adding this electron acceptor structure into the PF backbone increases the charge transfer rate.

5.3.1.2 Electro luminescence of devices at 10V.

To find the best bias voltage, we tried another voltage at 10V. The figure below therefore shows the EL spectra of the group of devices at 10V.

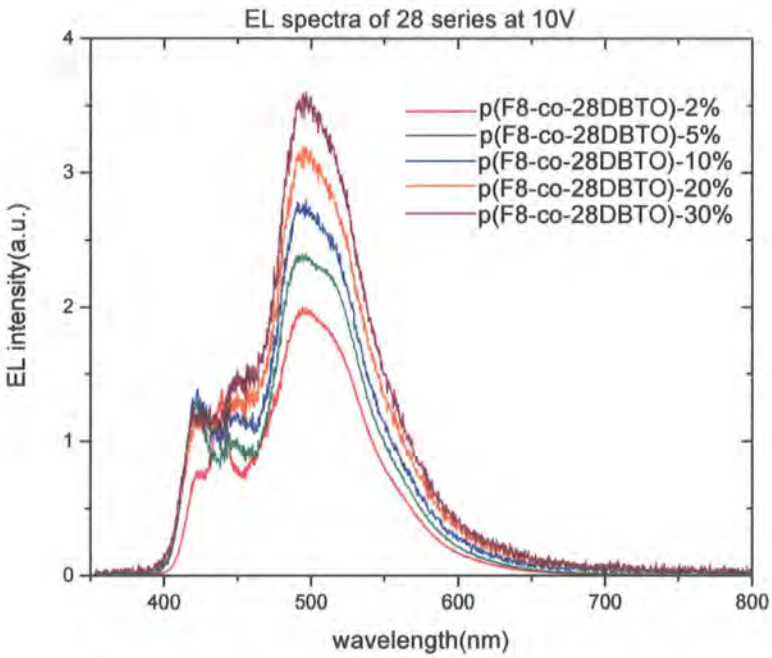

Figure 5-21 EL spectra of 28 series at 2500rpm at 10V normalized by the EL intensity at around 440nm.

In comparison, these two figures show that although the second figure, which is the EL spectra at 10V, gives a much stronger new red-shifted peak around 495nm as compared to the 6V spectra, the electroluminescence during the test is very unstable and the light will disappear after some time. So the first bias voltage 6V is much more suitable for these samples.

5.3.1.3 Properties of devices spun at 2000rpm for 60s at 6V.

Although the EQE and luminance is clearly enhanced by adding the new electron-acceptor unit DBTO into the PFO backbone to form a new electron state

called CT state, the EQE of 0.8% is still not very high. So there is a need to change the LEL thickness to find the best structure, and thus try to optimise the device performance.

For this reason, different thicknesses have been tested. First is the group of devices with the ELE of 2000rpm for 60s. Their LEL thicknesses are shown below.

Sample	28-2%	28-5%	28-10%	28-20%	28-30%
LEL thickness	36.37nm	35.60nm	33.53nm	32.48nm	30.62nm

The figure below shows the EL spectra of them.

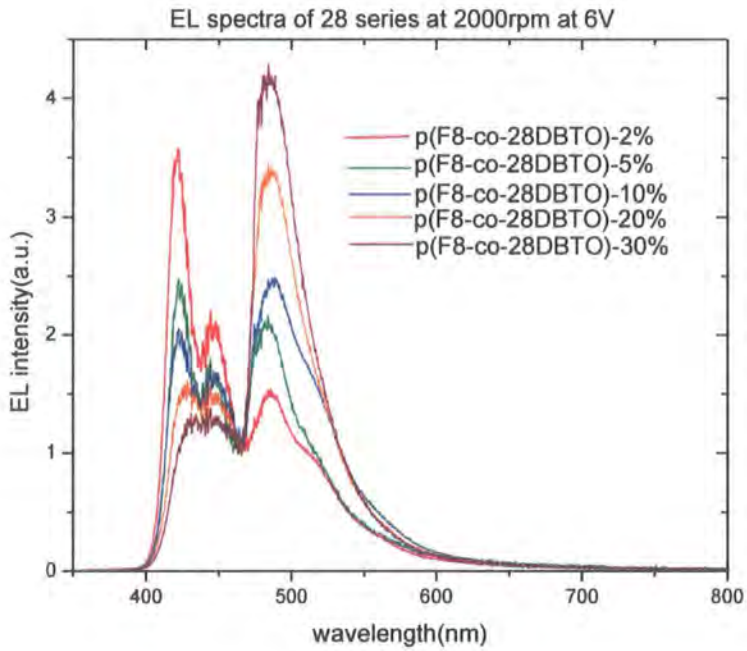

Figure 5-22 EL spectra of 28 series at 2000rpm at 6V normalized by the EL intensity at around 465nm.

From this figure we see that in contrast to the first group of EL spectra at 2500rpm, the only one difference between them is that the new red-shifted peak's relative intensity is much stronger in the EL spectra at 2000rpm. This indicates that

the device spun at 2000rpm gives a more efficient charge transfer speed and form a stronger CT state in the copolymer system. But we still need to prove this by calculating their EQE and luminance. Figures below show their I-V, V-L and L-EQE curves.

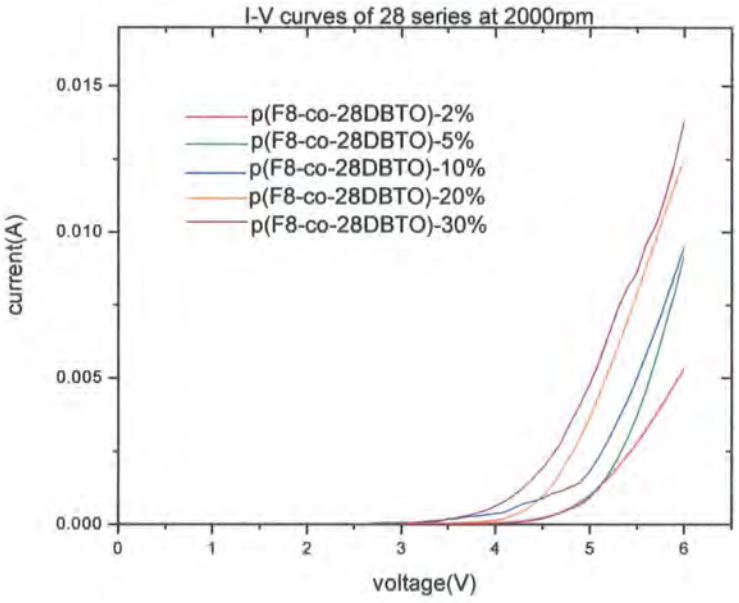

Figure 5-23 I-V curves of 28 series at 2000rpm.

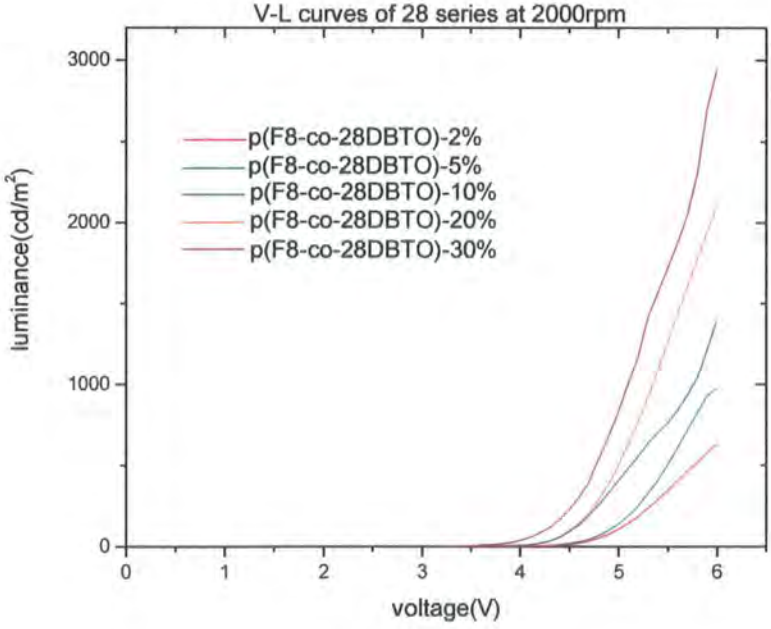

Figure 5-24 V-Luminance curves of 28 series at 2000rpm.

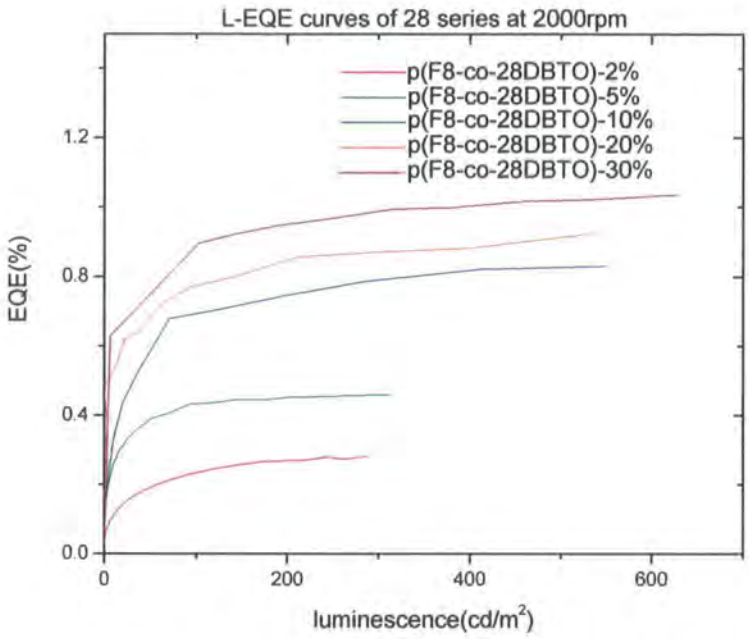

Figure 5-25 L-EQE curves of 28 series at 2000rpm.

From these figures we see that both the EQE and luminance are enhanced compared with those devices whose LEL is spinned at 2500rpm. This has proved that the thicker LEL layer can provide better EL properties in these five PF copolymers LEDs.

5.3.1.4 Properties of devices spun at 1500rpm for 60s at 6V.

To find the best thickness, we tested a third thickness, which is 1500rpm. Their LEL thicknesses are shown below.

Sample	28-2%	28-5%	28-10%	28-20%	28-30%
LEL thickness	48.67nm	45.29nm	43.52nm	39.58nm	37.50nm

Figures below shows their EL spectra, I-V, V-L and L-EQE curves.

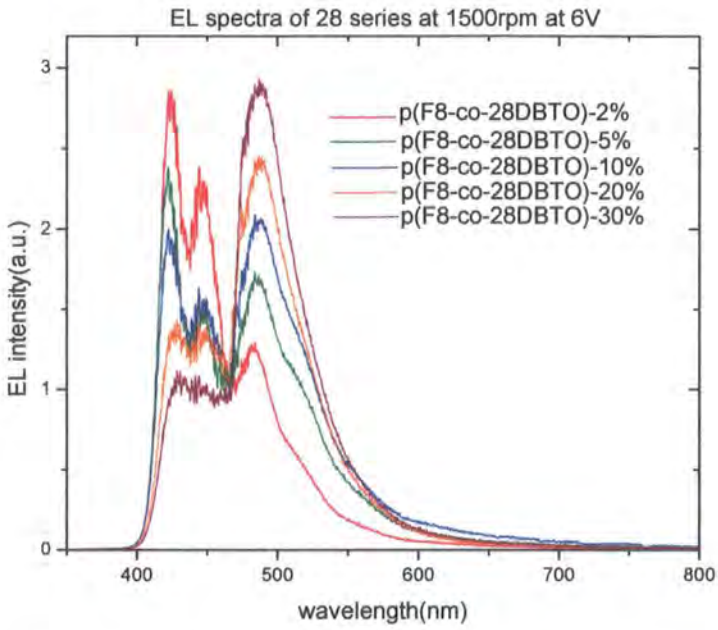

Figure 5-26 EL spectra of 28 series at 1500rpm at 6V normalized by the EL intensity at around 465nm.

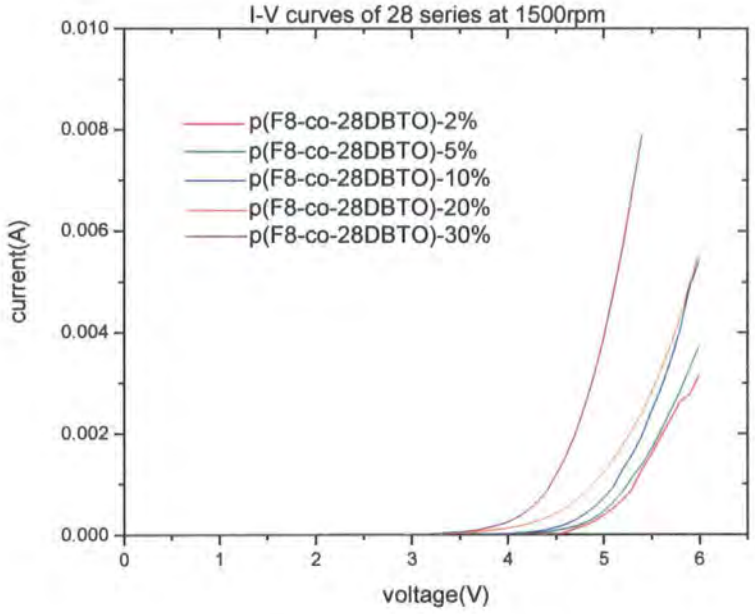

Figure 5-27 I-V curves of 28 series at 1500rpm.

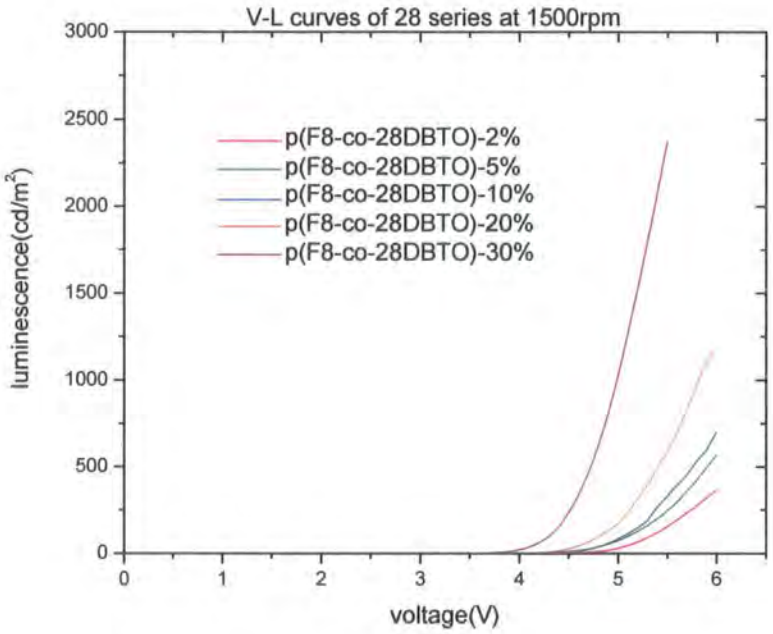

Figure 5-28 V-Luminance curves of 28 series at 1500rpm.

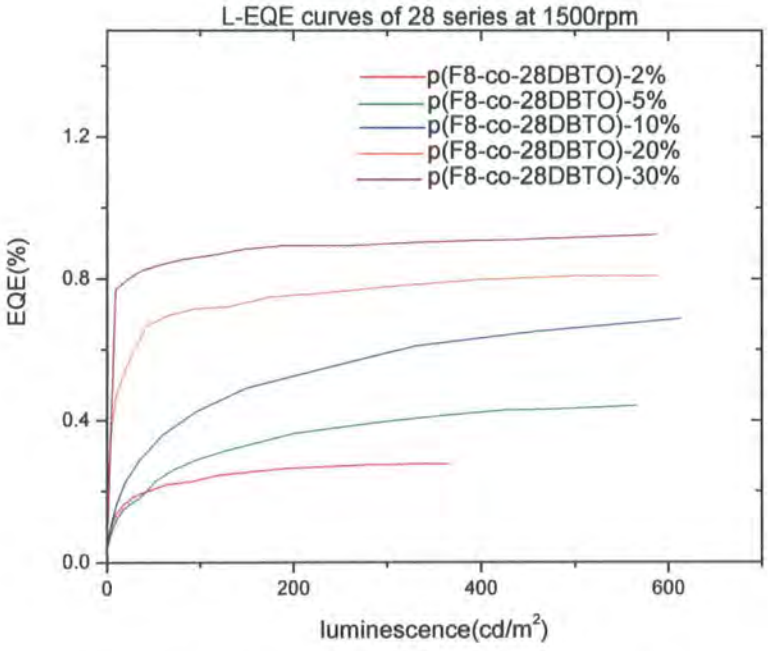

Figure 5-29 L-EQE curves of 28 series at 1500rpm.

From these we can see that the EQE and luminance of the group of device at 1500 has decreased again.

The following table shows the summary of the EL EQE of all these three groups of devices with different LEL thicknesses.

Sample	28-2%	28-5%	28-10%	28-20%	28-30%
2500rpm	0.194%	0.326%	0.535%	0.609%	0.798%
2000rpm	0.280%	0.458%	0.830%	0.924%	1.036%
1500rpm	0.277%	0.442%	0.688%	0.809%	0.926%

From this table we see that the second group of devices with the LEL of 2000rpm for 60s is the best set.

5.3.1.5 Material and thickness dependence of the cathode.

Although the light-emitting properties and thickness of the conjugated polymer (or the LEL) is very important during the operation of the polymer LEDs, the material choice and thickness of the cathode also play a rather important role in the devices' EL properties. The choice of the cathode material and the thickness of it will effect the EQE and device operating lifetime.

For example, in the MDMO-PPV devices, the initial performance is strongly dependent on the thickness of the Ba layer; EQE increases as the Ba thickness is decreased below 1000Å. For Ba thickness less than 45Å, even down to only 5Å of Ba, EQE is constant within experimental error[5].

Experiments also show that if we compared the half life for otherwise identical devices (prepared from sae batch of MDMO-PPV and deposited under the same conditions) except with different thickness of Ca and Ba cathodes, we obtain the maximum operating life for a cathode thickness of approximately 30Å for both Ca and Ba; for devices with cathode thicknesses between 30 and 200Å, the half life decreases as the cathode thickness increases; for cathode thickness larger than 200Å, the half life becomes nearly constant. For thin cathode layers equal to or less than 10Å,

the stress life is significantly decreased. A similar thickness dependence for the half life was observed for devices fabricated with strontium as cathode. The half life for Sr-cathode devices is larger than for Ca-cathode devices but less than for Ba-cathode devices with the same thickness. In other words, we find a definite dependence of the half life on the mass of the cathode metal atom-the heavier metal atom yields the longer half life[4].

Thus we can conclude that for these devices of 28 series, which have the Ba layer of about 5nm as the cathode, the EQE and operating lifetime can even be enhanced by fabricating a cathode of thinner layer, or by using another kind of appropriate metal atom that has a heavier mass than Ba as the cathode material.

5.3.1.6 CIE coordinates of the best group of devices.

As described in the PL section (5.2 and 5.3), apart from enhancing the EQE and luminance, another important aspect for the new DBTO unit is the colour-changing from blue to white. And as described above (5.4.1.1 to 5.4.1.4), the best group of devices are the ones with LEL of 2000rpm for 60s at the bias voltage of 6V. The following table and figure shows the EL spectra CIE coordinates of this best group of devices.

Sample	28-2%	28-5%	28-10%	28-20%	28-30%
CIE	(0.160,0.249)	(0.157,0.297)	(0.156,0.360)	(0.138,0.384)	(0.126,0.409)

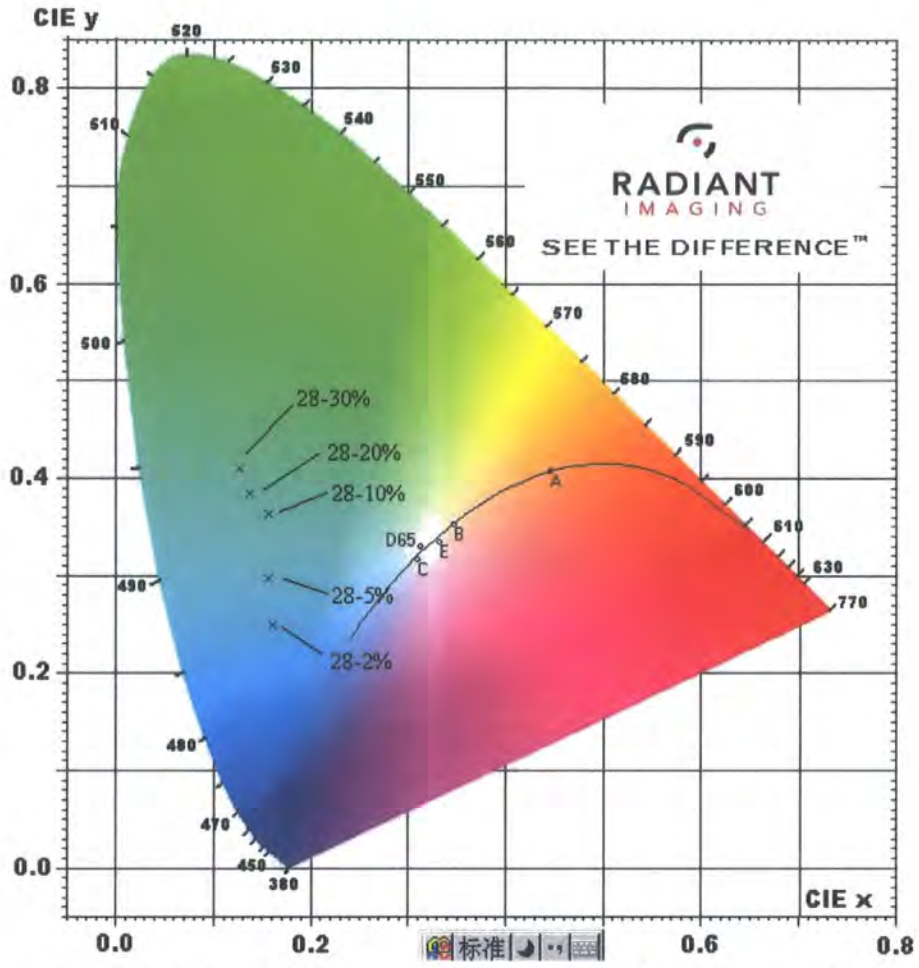

Figure 5-30 CIE co-ordinates of EL spectra of 28 series at 2000rpm.

From this CIE figure, we can see that the EL colour has been clearly changed from blue to blue-green, but not towards white.

5.3.2 Conclusion

In the 28 series of PF copolymer LEDs, the new electron acceptor unit DBTO forms a strong charge transfer (CT) state and gives off a new strong red-shifted EL peak around 495nm. The relative intensity of this peak will increase as the DBTO unit's ratio goes up, while the position of it will not change. The EL colour has shifted from blue to blue-green as the DBTO's ratio increases. And because of the electron acceptor structure of DBTO, charge transfer speed is enhanced obviously during these devices, which gives the result of enhanced EQE and luminance. In addition, the EQE

and luminance will also be strongly enhanced by changing the LEL thickness from 2500rpm to 2000rpm.

5.4 References.

1. Fernando B. Dias, Jorge Morgado, António L. Maçanita, Fernando P. da Costa, Hugh D. Burrows, Andrew P. Monkman, Kinetics and Thermodynamics of Poly(9,9-dioctylfluorene) β-phase Formation in Dilute Solution
2. E.J.W. List, R. Guentner, P. Scanducci de Freitas, U. Scherf, Advanced Materials 14 (5), 374-378 (2002).
3. O. Inganas, T. Granlund, M. Theander, M. Berggren, M. R. Andersson, A. Ruseckas, V. Sundstrom, Opt. Mater. NY 9 (1998) 104.
4. S. I. Hintschich, C. Rothe, S. Sinha, A. P. Monkman, P. Scandiucci de Freitas and U. Scherf, The Journal of Chemical Physics -- December 8, 2003 -- Volume 119, Issue 22, pp. 12017-12022.
5. Yong Cao, Gang Yu, lan D. Parker, and Alan J. Heeger, Journal of Applied Physics, Volume 88, No. 6, 15 Sep. 2002.

Chapter 6 Photo and electroluminescence of 37 Series.

6.1 Absorption and Photoluminescence in solutions.

The solutions for all the five copolymers are also in this case prepared with the concentration of 1% powder in toluene [w/w]. The solution was also stirred for about 2 hours to make sure they are well dissolved before the investigations. The solutions were subsequently diluted to an absorption of ~0.2 for the following investigation.

6.1.1 Absorption spectra.

The absorption spectra of 37 series in solution are shown in Figure 6-2 below. These spectra were measured in the room pressure and temperature.

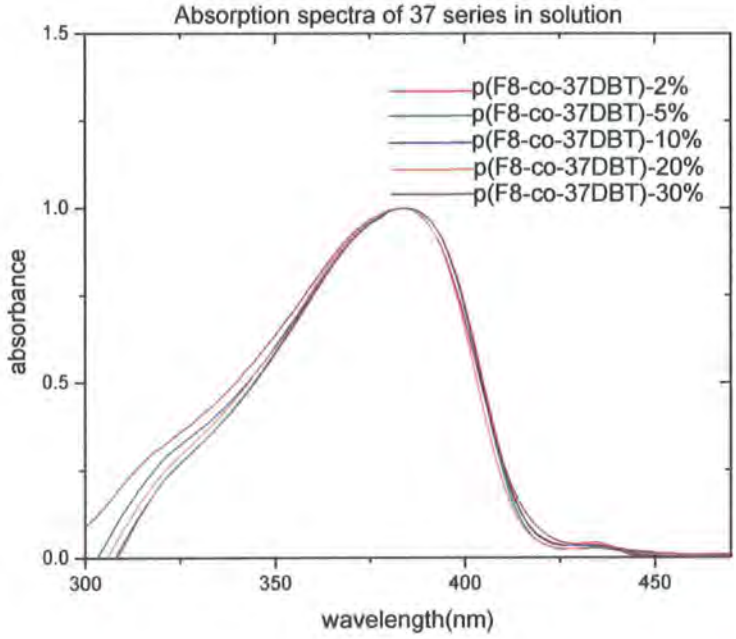

Figure 6-1 Absorption spectra of 37 series in solution.

From this figure we can see that all of the five absorption spectra have a similar shape, which shows a full width at half maximum (FWHM) of about 50nm. The absorbance maxima are around 385nm for all copolymers. Again, we find a second weak peak around 435nm in their absorption spectra, which shows that the β-phase phenomena also exist in the solution state of 37 series of PFO copolymers. But this second weak peak does not become weaker as the DBT's concentration increases. This is due to the fact that the new added DBT unit can not reduce the formation of the ordered segments (β-conformation) in the PFO system very well.

The other difference with the 28 series is that as the DBT unit's percentage increases, the position of the strongest peak doesn't blue-shift. This means that the DBT unit can't change the HOMO and LUMO energy gap like the former DBTO unit in 28 series.

6.1.2 Photoluminescence spectra.

Figure 6-3 shows the photoluminescence (PL) spectra of these five copolymers in solution, which is excited at their maximum absorption peak separately.

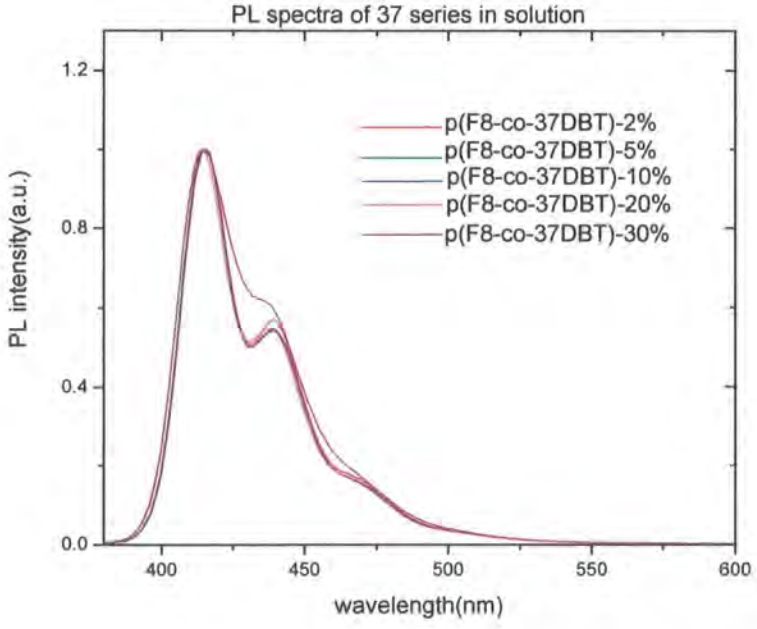

Figure 6-2 PL spectra of 37 series in solution.

And the PLQYs are shown in the table below.

Sample	37-2%	37-5%	37-10%	37-20%	37-30%
PLQY	81%	81%	76%	81%	77%

As in normal PFO solutions, we can still observe typical PL spectra with clear vibronic structure in the 37 series PF copolymers. From Figure 6-2 we see that they both show a 0-0' peak around 415nm, a 0-1' peak around 440nm, a 0-2' peak around 470nm, and even a weak 0-3' peak around 500nm.

As the DBT's ratio increases, the second, third and fourth PL peaks will again become weaker and weaker. Especially in p(F8-co-37DBT)-30% solution, the three other peaks besides the 0-0' peak have almost totally disappeared in its PL spectrum. So we can draw the similar conclusion with the DBTO that the DBT unit also can reduce the vibronic coupling in PL in solution.

As the DBT unit's percentage increases, we observe that the PLQY doesn't change obviously but keeps the same around 80%. And similar with the 28 series, we don't observe the β-phase phenomena in the PL spectra of the 37 series in solution, either.

Again let's see the relationship between the absorption and PL spectra of these copolymers solution. These are shown in Figure 6-3 to 6-7 below.

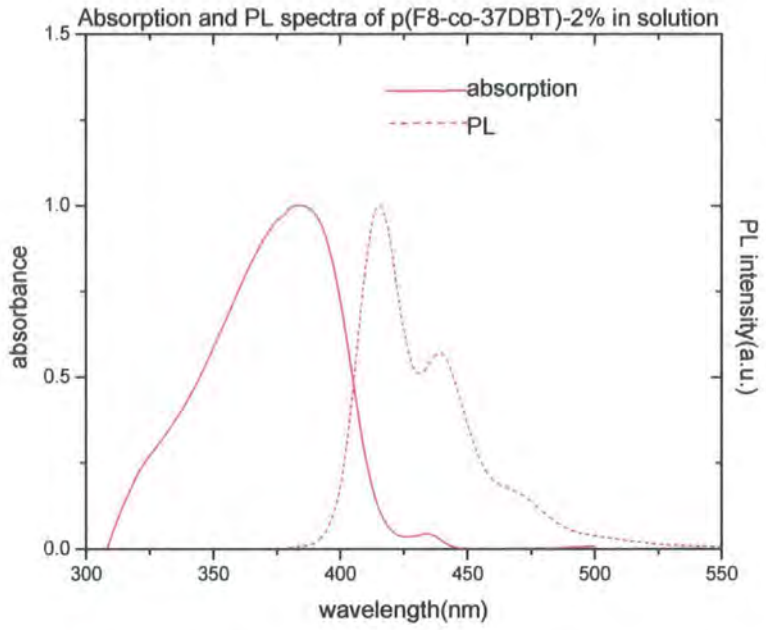

Figure 6-3 Absorption and PL spectra of 37-2% in solution.

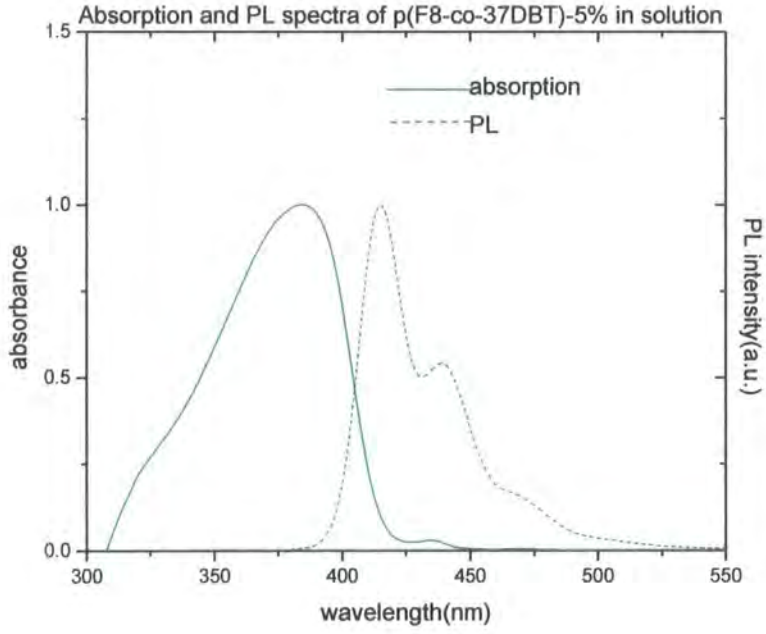

Figure 6-4 Absorption and PL spectra of 37-5% in solution.

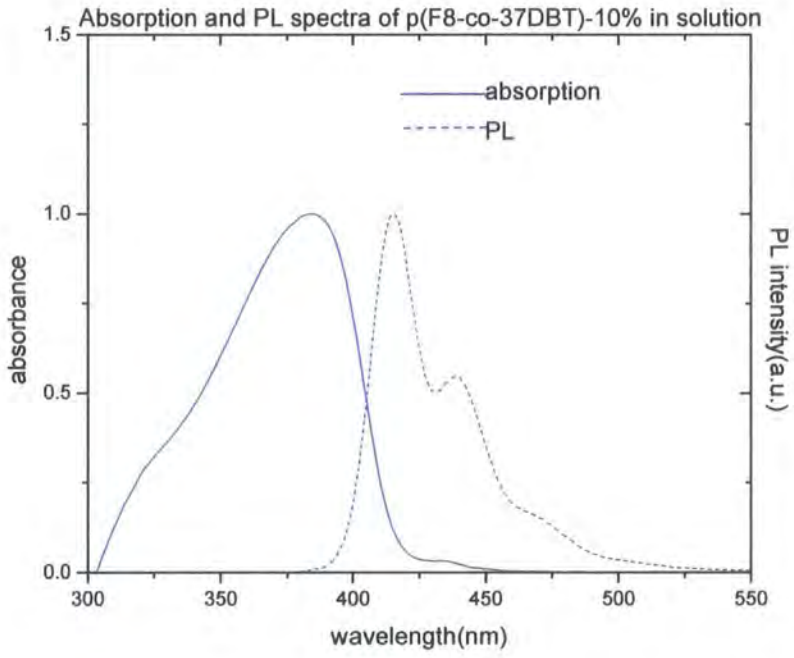

Figure 6-5 Absorption and PL spectra of 37-10% in solution.

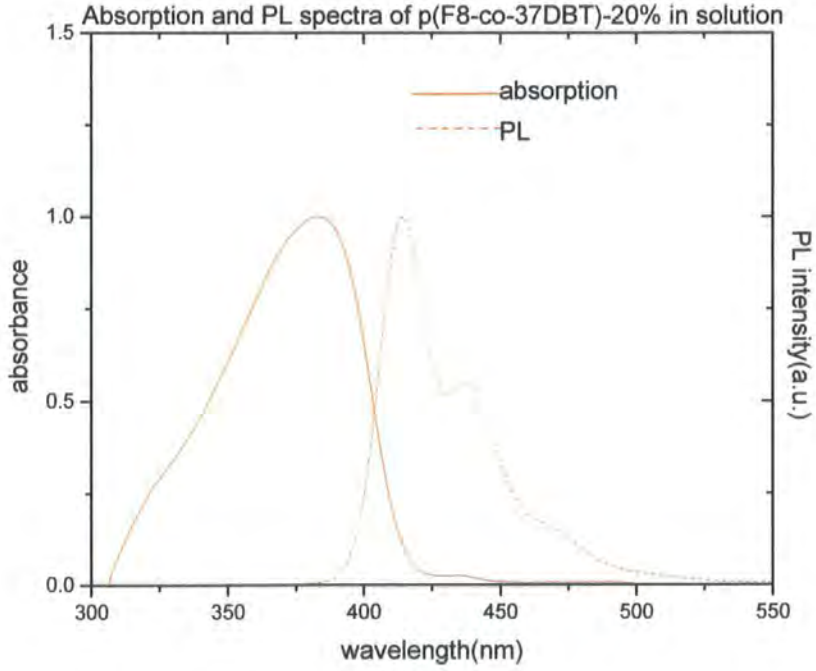

Figure 6-6 Absorption and PL spectra of 37-20% in solution.

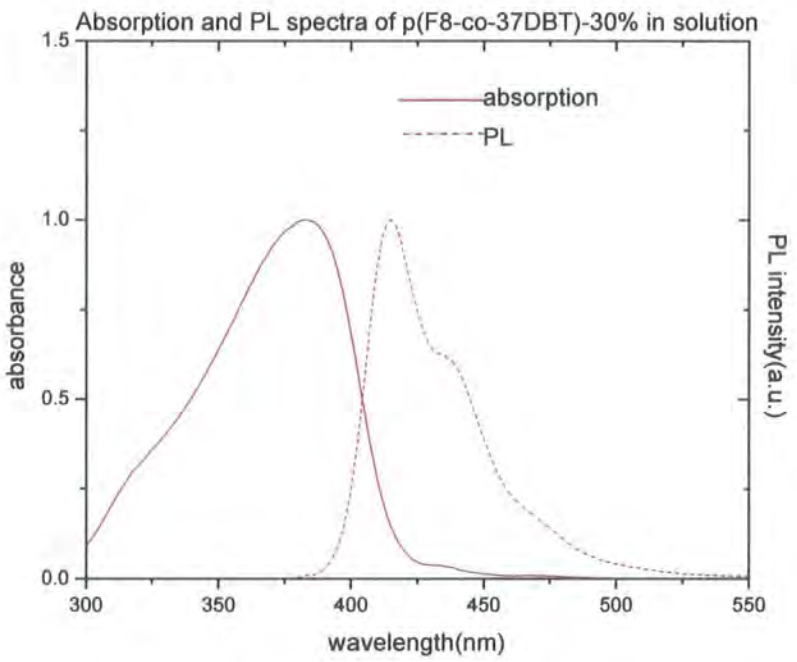

Figure 6-7 Absorption and PL spectra of 37-20% in solution.

From all these 5 figures we see a *Stoke's* shift between the absorption and PL spectra of about 30nm, which doesn't change as the DBT, unit's ratio goes up.

6.1.3 CIE coordinates.

Finally, let's have a look at the CIE coordinates of the PL spectra of them. See the table and Figure 6-8 below.

Sample	37-2%	37-5%	37-10%	37-20%	37-30%
CIE	(0.159,0.060)	(0.159,0.058)	(0.159,0.058)	(0.160,0.056)	(0.159,0.058)

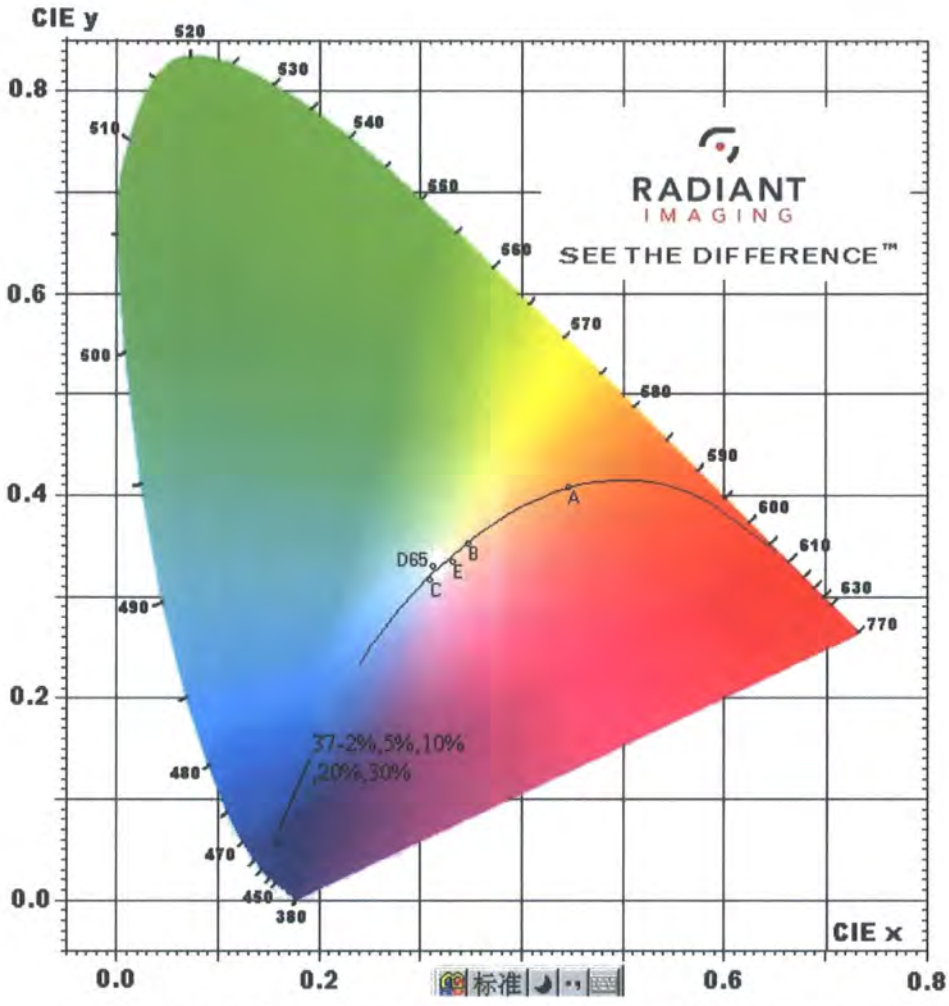

Figure 6-8 CIE co-ordinates of PL spectra of 37 series in solution.

From this figure we see that the PL wavelength of these copolymers are almost the same in their solution state.

6.1.3 Conclusion.

In solution state of 37 series, the new unit-DBT can't decreases the β-phase phenomena in the absorption spectra, and can't cause the absorption peak to be blue-shifted, either. There will only be an impact on the PL vibronic structure which becomes less pronounced. The PLQY keeps the same for all systems of around 80%.

6.2 Absorption and photoluminescence in films.

6.2.1 Absorption spectra.

The absorption spectra of 37 series in film are shown in Figure 6-9 below. These spectra were measured in the room temperature.

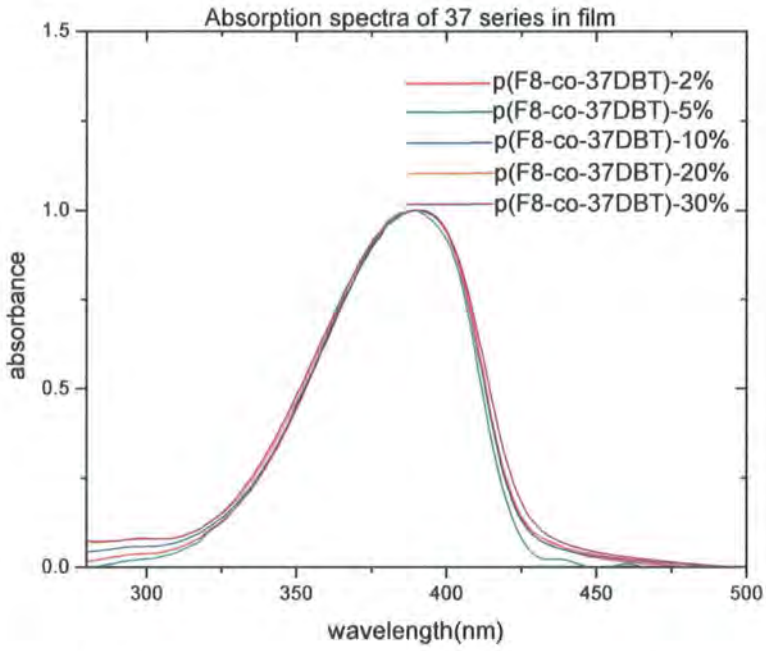

Figure 6-9 Absorption spectra of 37 series in film.

We can see that all of the five absorption spectra of the different co-polymer systems still exhibit a similar absorption shape, which shows a full width at half maximum (FWHM) of about 50nm. However, each sample now only shows one single peak around 390 nm. In contrast to the solution, we do not see the second absorption peak-the β -phase peak in the film absorption spectra. This is because in the solid film state, the distance between polymer chains is much closer than solution state, so the side chain interaction is much stronger than solution. As a result, the formation of ordered segments (β -conformation) has been effectively reduced by the new side unit-DBT. This is the same with the former 28 series copolymers in film.

In contrast to the 28 series, the maximum absorption peak's position doesn't shift in the 37 series in film, which is the same result as in solution. And this means that the DBT unit can't change the HOMO and LUMO energy gap like the former DBTO unit in 28 series in solid state, either.

6.2.2 Photoluminescence spectra.

Figure 6-10 shows the PL spectra of these five copolymers in film, which is excited at their maximum absorption peak separately.

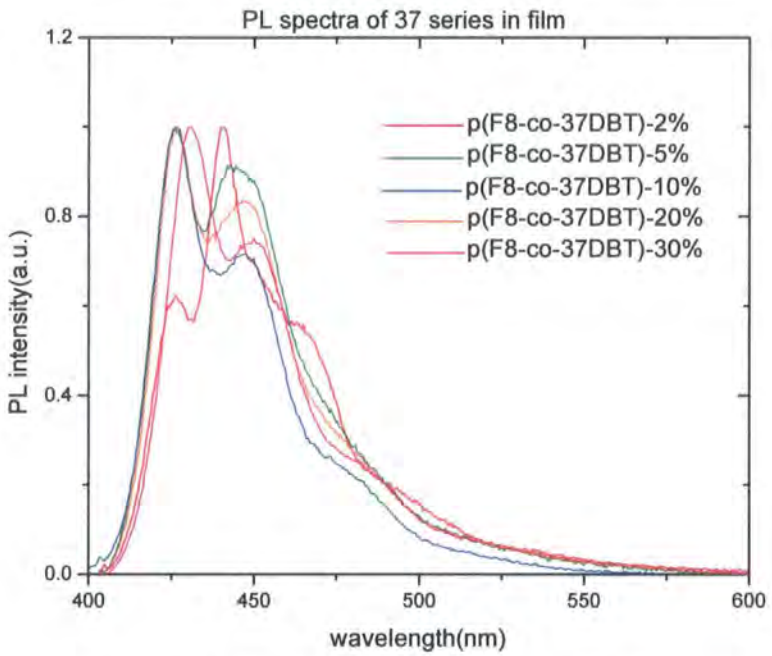

Figure 6-10 PL spectra of 37 series in film.

And the PLQYs are shown below.

Sample	37-2%	37-5%	37-10%	37-20%	37-30%
PLQY	16%	21%	23%	28%	29%

In contrast to the 28 series, as the DBT unit's ratio goes up, the reduction of the PF's vibronic structure is not so obvious. Even in the PL spectra of

p(F8-co-37DBT)-30%, we can still see the 0-0' peak around 430nm, a 0-1' peak around 450nm, and a 0-2' peak around 480nm. The observation is that as the DBT's percentage increases, the second peak, which is the 0-1' peak will become a little smaller. But the change is still not very clear. And different with the solution, the PLQY of the 37 series in film has increased a little from 16% of p(F8-co-37DBT)-2% to 29% of p(F8-co-37DBT)-30%.

Similar with the 28 series, the slight red-shift phenomenon is observed again. And in the 37 series, the red-shift gap seems to be a little wider. But more experiments are still needed to confirm this hypothesis and the exact origin of the effect.

And another observation is that the strong β -phase peak in p(F8-co-37DBT)-2% film has almost completely disappeared in 37-5%, 10%, 20% and 30% films PL spectra. This proved the important hypothesis that similar with the 28 series: the DBT side chain in the 37 series can also effectively reduced the β -phase conformation in PFO polymer system.

Let us return to the relationship between the absorption and PL spectra of these copolymers film. These are shown in Figure 6-11 to 6-15 below.

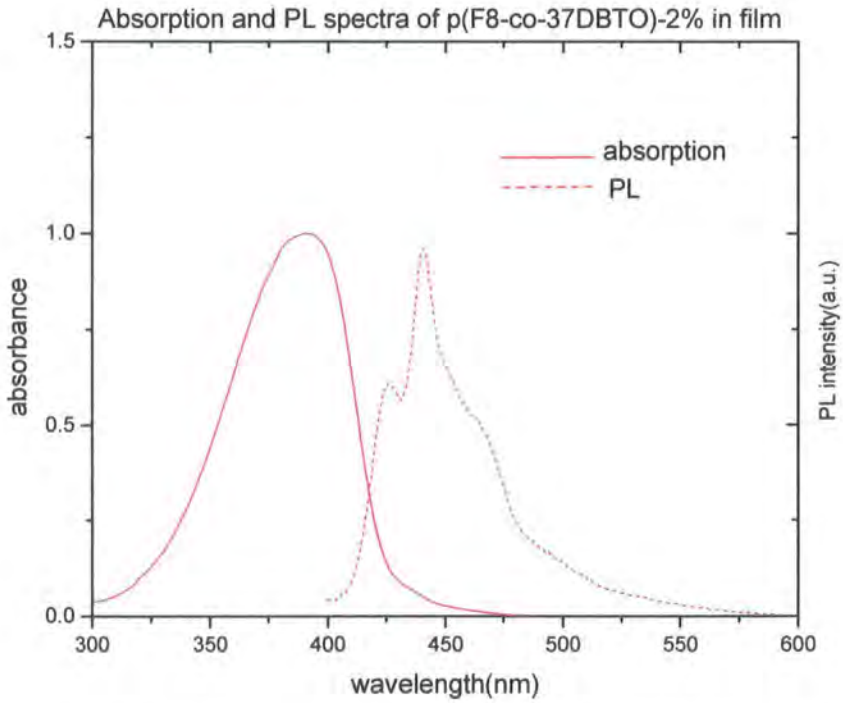

Figure 6-11 Absorption and PL spectra of 37-2% in film.

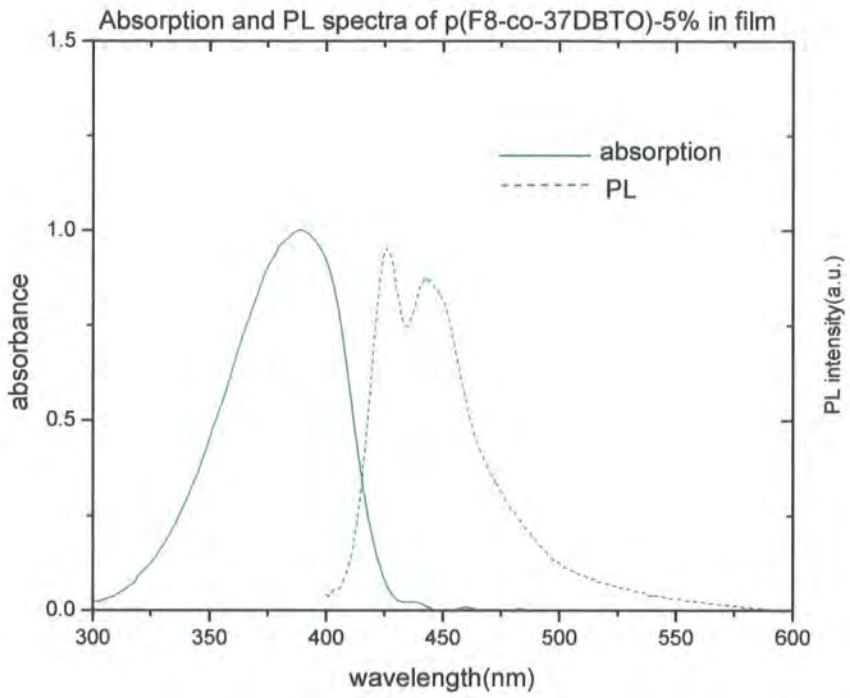

Figure 6-12 Absorption and PL spectra of 37-5% in film.

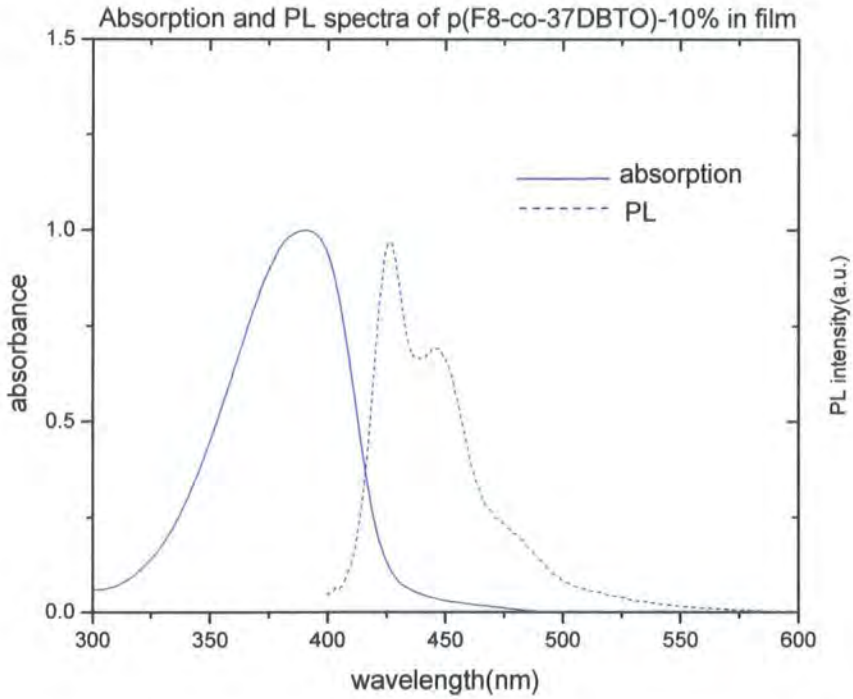

Figure 6-13 Absorption and PL spectra of 37-10% in film.

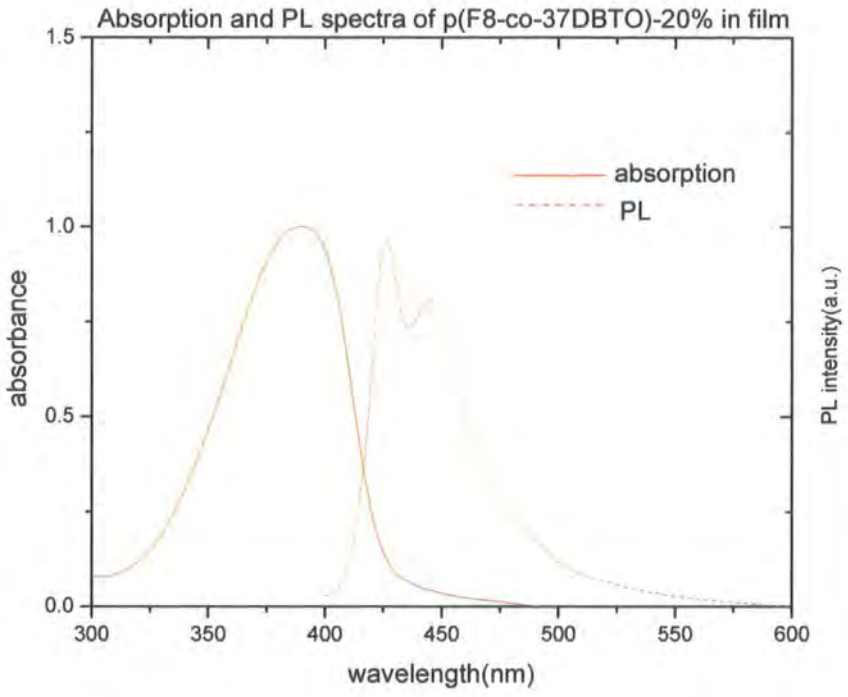

Figure 6-14 Absorption and PL spectra of 37-20% in film.

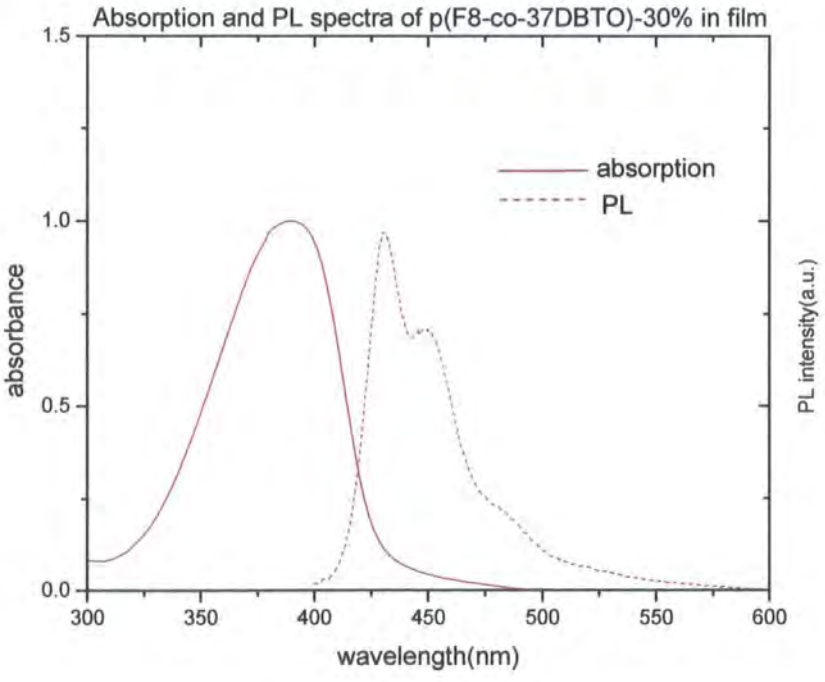

Figure 6-15 Absorption and PL spectra of 37-30% in film.

Again we get a Stokes shift in each copolymer system, but in contrast to the solution state, we can see the shift increases from about 35nm to 40nm as the DBT unit's ratio increases from 2% to 30%. This is because the red-shift in the PL spectra of film.

6.2.3 CIE coordinates.

The CIE coordinates of these PL spectra are shown below.

Sample	37-2%	37-5%	37-10%	37-20%	37-30%
CIE	(0.141,0.145)	(0.146,0.131)	(0.138,0.079)	(0.147,0.135)	(0.149,0.145)

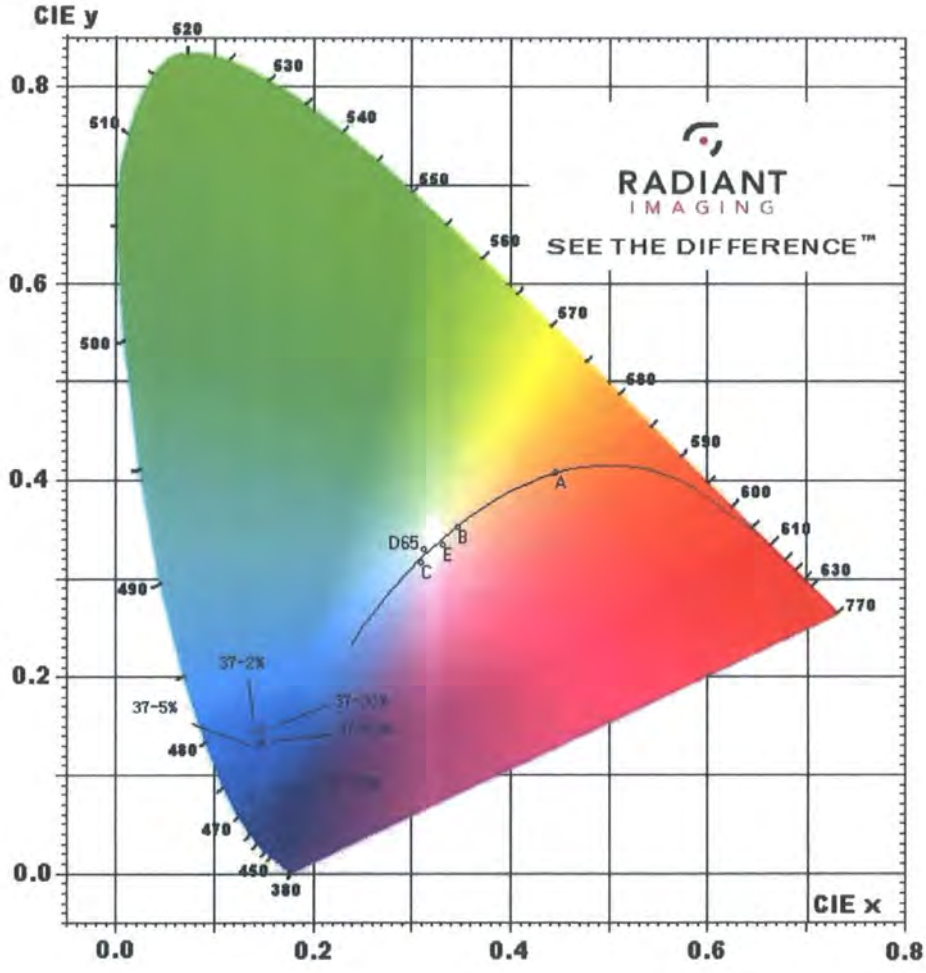

Figure 6-16 CIE co-ordinates of PL spectra of 37 series in film.

In this CIE figure we can see that the PL wavelength in film still does not shift very significantly. And the interest observation is that the colour of p(F8-co-37DBT)-10% suddenly jumps into deep blue, while the other four still stay in the light blue area.

6.2.4 Conclusion.

In film state of 37 series, the new unit-DBT becomes to decrease the β -phase phenomena in their absorption spectra, but still can't cause the absorption peak blue-shifted. It can make the PL vibronic structure just a little less significant, and make the PL peak a little red-shifted. Different with the 28 series, the PLQY of them will increase from 16% of p(F8-co-37DBT)-2% to 29% of p(F8-co-37DBT)-30%. In addition, the shift of the colour from deep blue to light blue is not so obvious as the former film state of the 28 series.

6.3 Electroluminescence properties.

6.3.1 Electro luminescence spectra and external quantum efficiency (EQE).

6.3.1.1 Properties of devices spun at 2500rpm for 60s at 6V.

The first group of devices has the structure with a LEL spun with the speed of 2500rpm for 60s. Still, the thicknesses of their LEL are not absolutely the same because of the different DBT concentrations in the copolymer. Their thicknesses are shown below.

Sample	37-2%	37-5%	37-10%	37-20%	37-30%
LEL thickness	24.55nm	24.32nm	23.41nm	23.37nm	23.03nm

And to find the best bias voltage, two different voltages of 6V and 10V for this group was used. The EL spectra of them are shown in Figure 6-17.

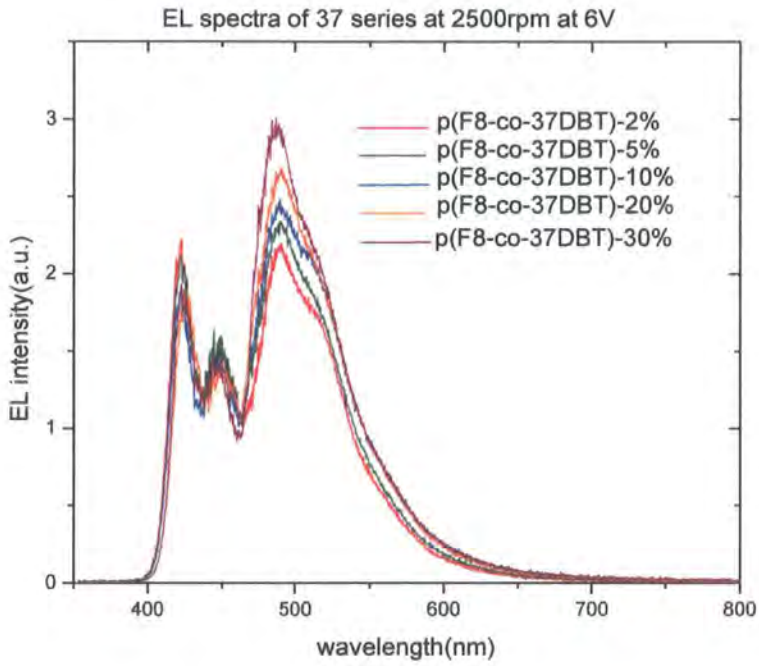

Figure 6-17 EL spectra of 37 series at 2500rpm at 6V normalized by the EL intensity at around 465nm.

Just as with the 28 series, we can find that in contrast to the PL spectra of these five copolymer samples in solution and films, a new strong and broad peak appear in the EL spectra located around 485nm. The relative intensity of this new peak will increase as the DBTO unit's ratio increases, and the position almost does not change. The only difference with the 28 series is that the reduction of the small peak is not so obvious in the 37 series EL spectra.

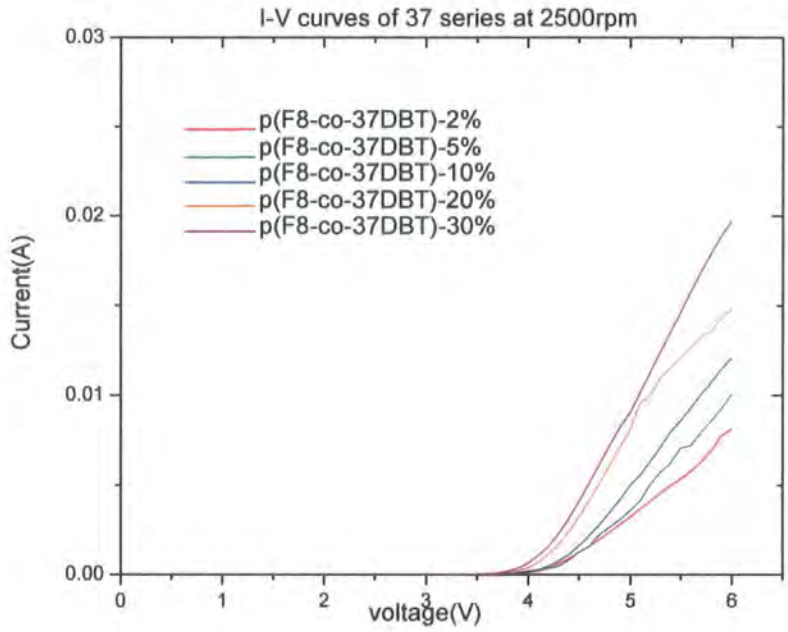

Figure 6-18 I-V curves of 37 series at 2500rpm.

In this figure of I-V curves we can see that the starting voltage do not change as the DBT unit's ratio increases. This is in contrast to the 28 series.

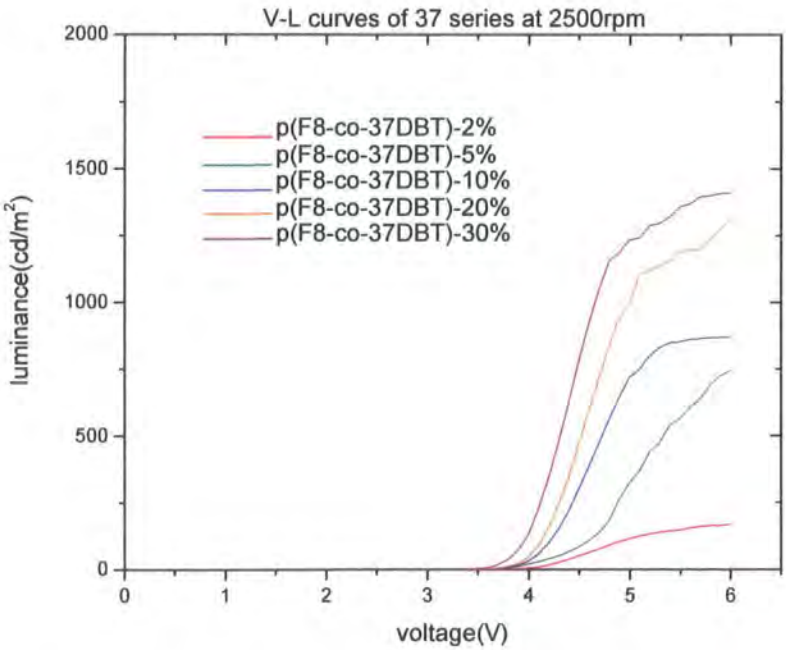

Figure 6-19 V-Luminance curves of 37 series at 2500rpm.

In this figure of V-L curves we can find that as the DBT unit's ratio increases, the luminance will also increases quickly from about 170cd/m^2 to 1400cd/m^2. However, this increase is not as obvious as in the former 28 series.

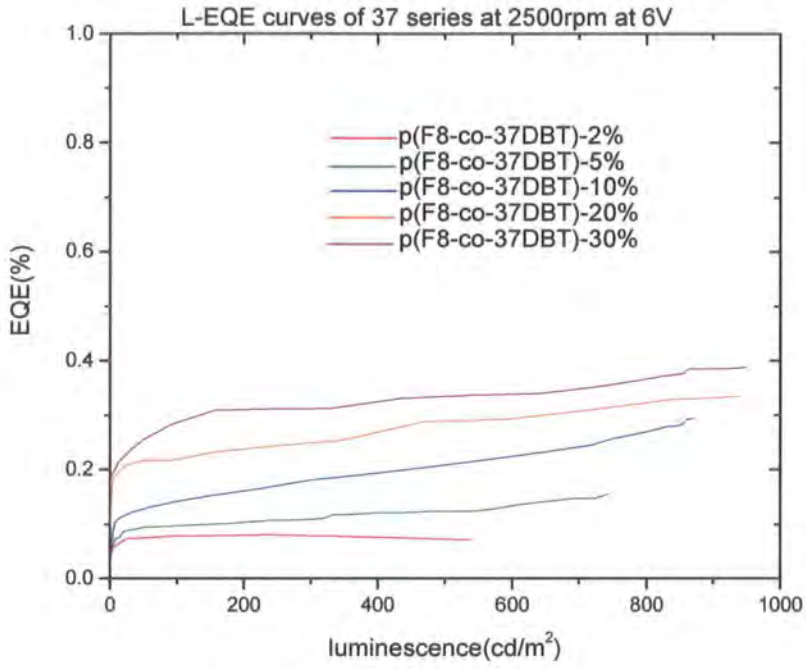

Figure 6-20 L-EQE curves of 37 series at 2500rpm.

From this figure we can see that the EQE goes up quickly as the DBT's ratio increases, from about 0.07%, which is rather low for PF copolymers, to 0.38%. This EQE is also lower than the 28 series. But it is still enhanced a lot by adding the DBT unit into the PF backbone. That means the new peak appeared in the former EL spectra is not due to a keto defect but the charge transfer (CT) state in these new copolymers chain system, which is just the same with the 28 series. In addition, the EQE is not enhanced as quickly as the former 28 series, this is due to that the DBT unit is not an electron acceptor structure, so the charge transfer rate can not been increased.

6.3.1.2 Properties of devices spun at 2500rpm for 60s at 10V.

To find the best bias voltage, we tried another voltage at 10V. The figure below shows the EL spectra of the group of devices at 10V.

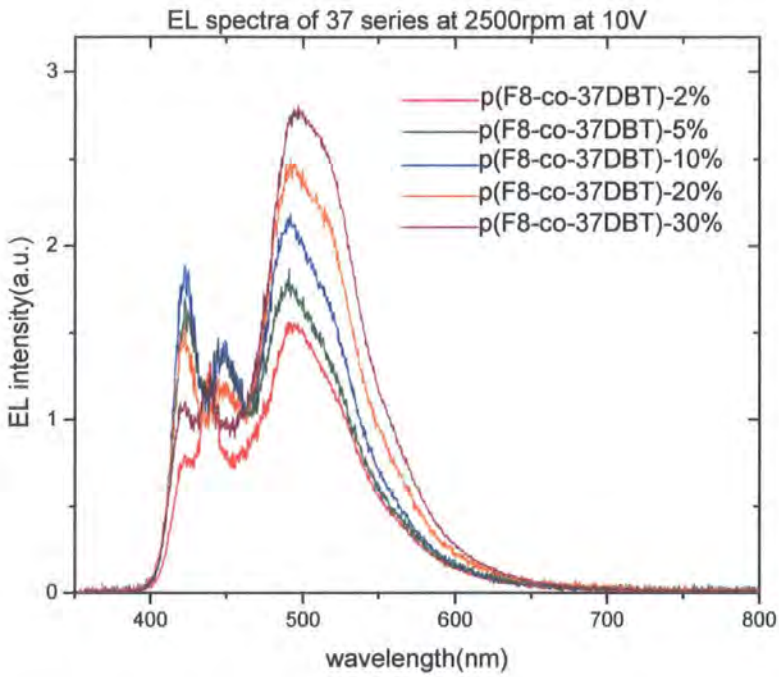

Figure 6-21 EL spectra of 37 series at 2500rpm at 10V normalized by the EL intensity at around 440nm.

In comparison, although the second figure, which is the EL spectra at 10V, gives a much stronger new red-shifted peak around 495nm than 6V, the EL during the test is very unstable and the light will disappear after some time. So the bias voltage of 6V is much more suitable for these samples.

6.3.1.3 Propertiesof devices spun at 2000rpm for 60s at 6V.

The group of devices with the LEL of 2000rpm for 60s still needs to be tested. Their LEL thicknesses are shown below.

Sample	37-2%	37-5%	37-10%	37-20%	37-30%
LEL thickness	35.66nm	35.10nm	33.28nm	31.18nm	30.02nm

The figure below shows the EL spectra of them.

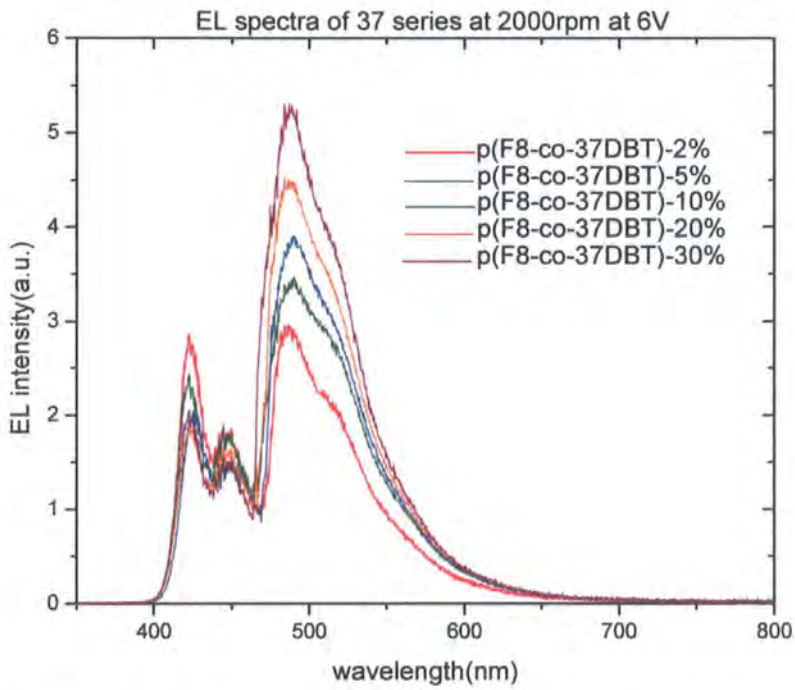

Figure 6-22 EL spectra of 37 series at 2000rpm at 6V normalized by the EL intensity at around 465nm.

From this figure we see that in contrast to the first group of EL spectra at 2500rpm, the only one difference between them is that the new red-shifted peak's relative intensity is stronger in the EL spectra at 2000rpm. This indicates that the device spun at 2000rpm gives a more efficient charge transfer balance and form a stronger CT state in the copolymer system. Figures below show their I-V, V-L and L-EQE curves.

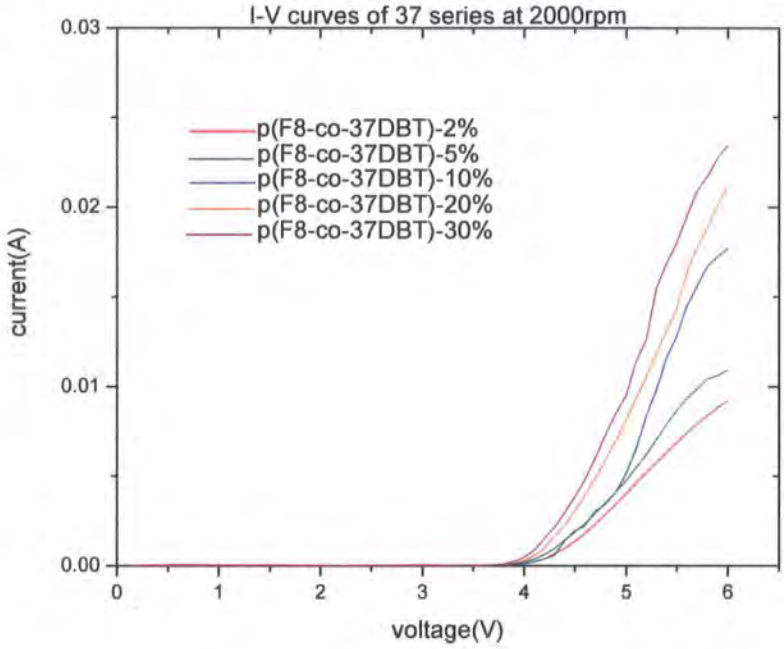

Figure 6-23 I-V curves of 37 series at 2000rpm.

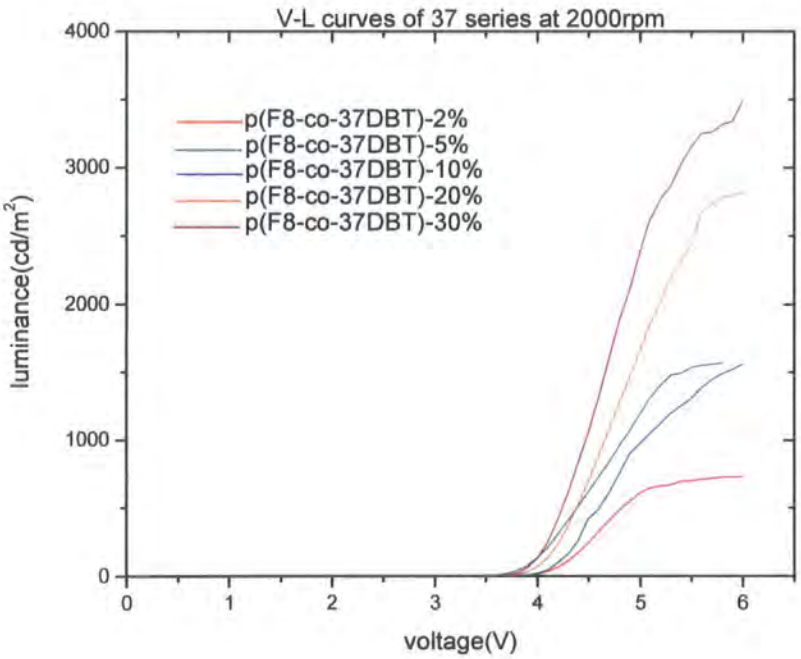

Figure 6-24 V-Luminance curves of 37 series at 2000rpm.

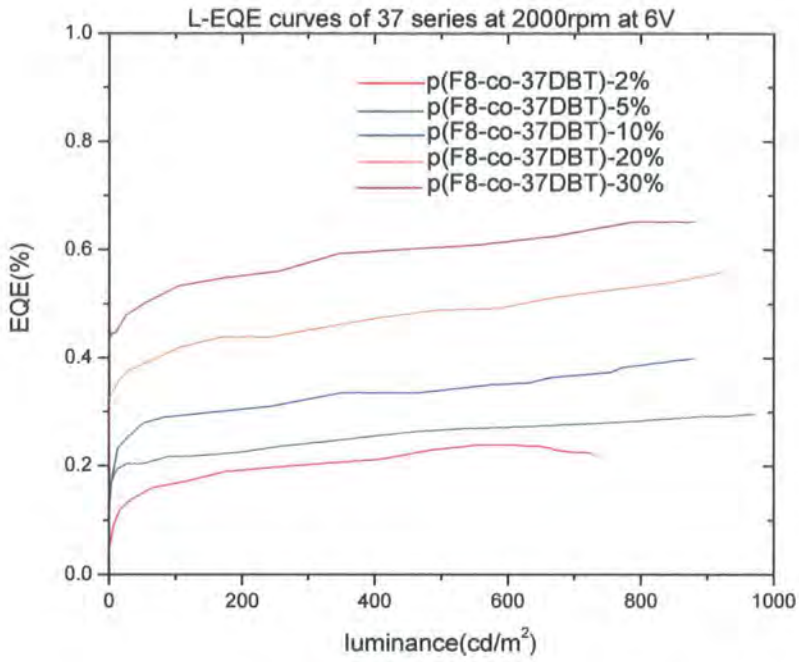

Figure 6-25 L-EQE curves of 37 series at 2000rpm.

From these figures we see that both the EQE and luminance are enhanced compared with those devices whose LEL is spinned at 2500rpm. This has proved that the LEL layer thickness of 2000rpm can provide better EL properties for the 38 series devices.

6.3.1.4 Properties of devices spun at 1500rpm for 60s at 6V.

To find the best thickness, we still need to test a third thickness, which is 1500rpm. Their LEL thicknesses are shown below.

Sample	37-2%	37-5%	37-10%	37-20%	37-30%
LEL thickness	46.22nm	44.10nm	42.51nm	38.98nm	37.04nm

Figures below shows their EL spectra, I-V, V-L and L-EQE curves.

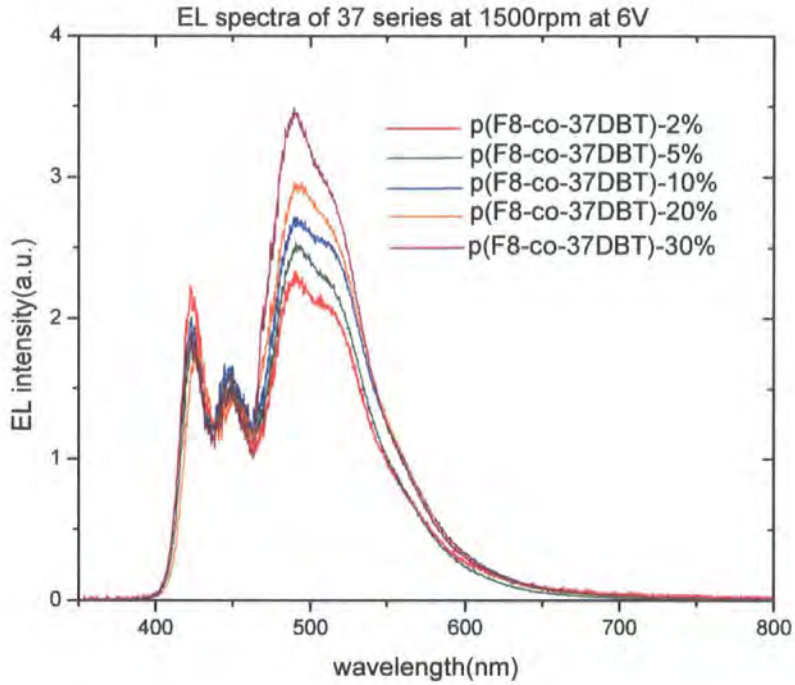

Figure 6-26 EL spectra of 37 series at 1500rpm at 6V normalized by the EL intensity at around 465nm.

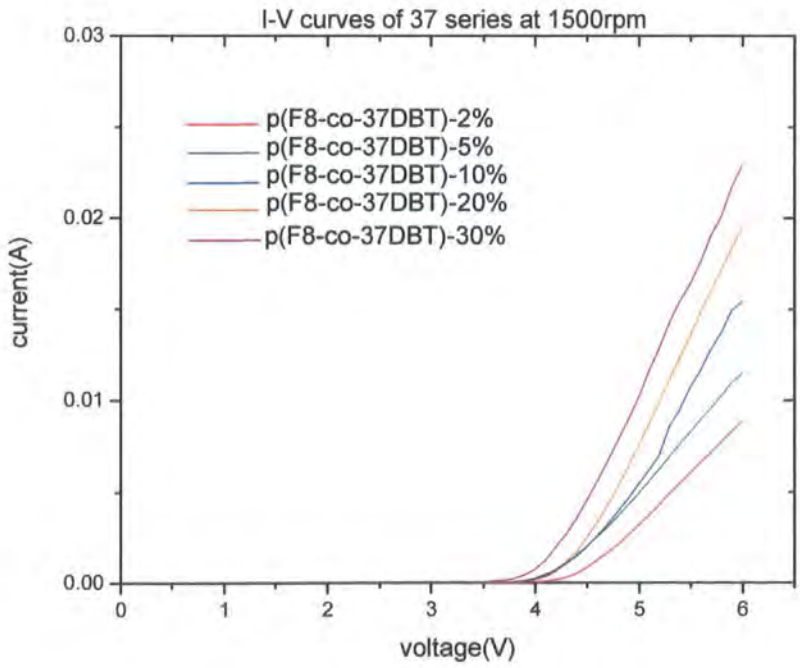

Figure 6-27 I-V curves of 37 series at 1500rpm.

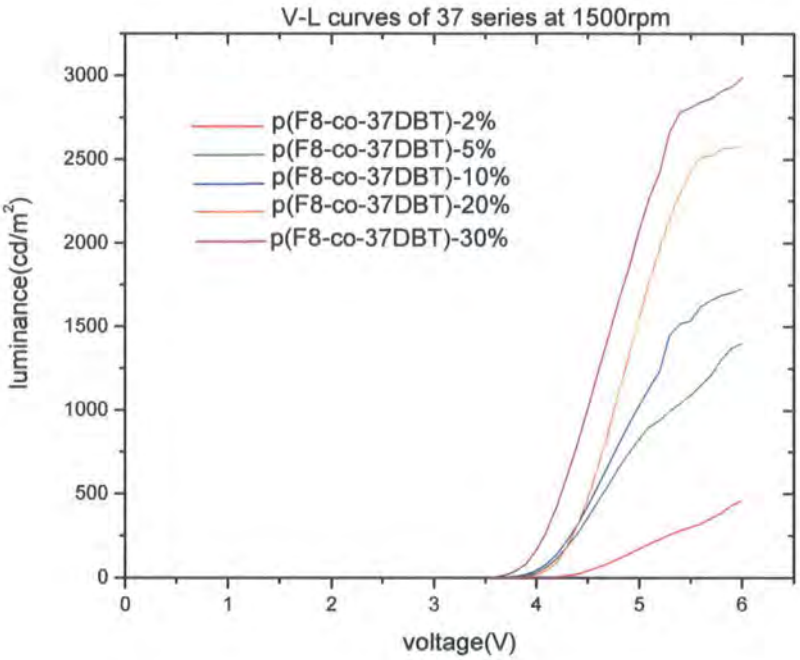

Figure 6-28 V-Luminance curves of 37 series at 1500rpm.

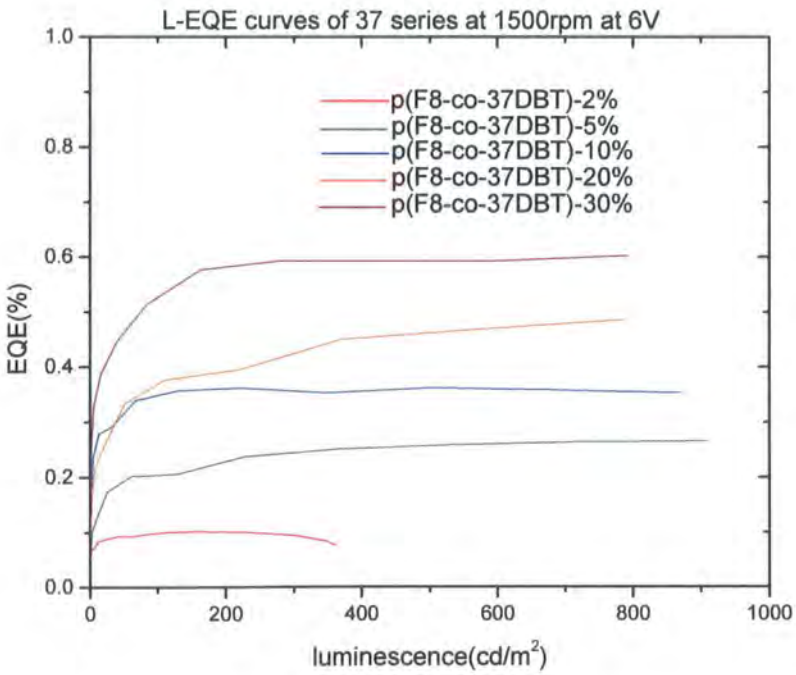

Figure 6-29 L-EQE curves of 37 series at 1500rpm.

From these we can see that the EQE and luminance of the group of device at 1500 has decreased again.

The following table shows the summary of the EL EQE of all these three groups of devices with different LEL thicknesses.

Sample	37-2%	37-5%	37-10%	37-20%	37-30%
2500rpm	0.072%	0.157%	0.293%	0.335%	0.389%
2000rpm	0.238%	0.296%	0.398%	0.557%	0.651%
1500rpm	0.101%	0.266%	0.353%	0.486%	0.603%

From this table we see that the second group of devices with the LEL of 2000rpm for 60s are the best set.

6.3.1.5 CIE coordinates of the best group of devices.

The following table and figure shows the EL spectra CIE coordinates of the group of devices whose ELE layer is spin coated at 2000rpm.

Sample	37-2%	37-5%	37-10%	37-20%	37-30%
CIE	(0.183,0.401)	(0.172,0.421)	(0.184,0.428)	(0.178,0.439)	(0.170,0.441)

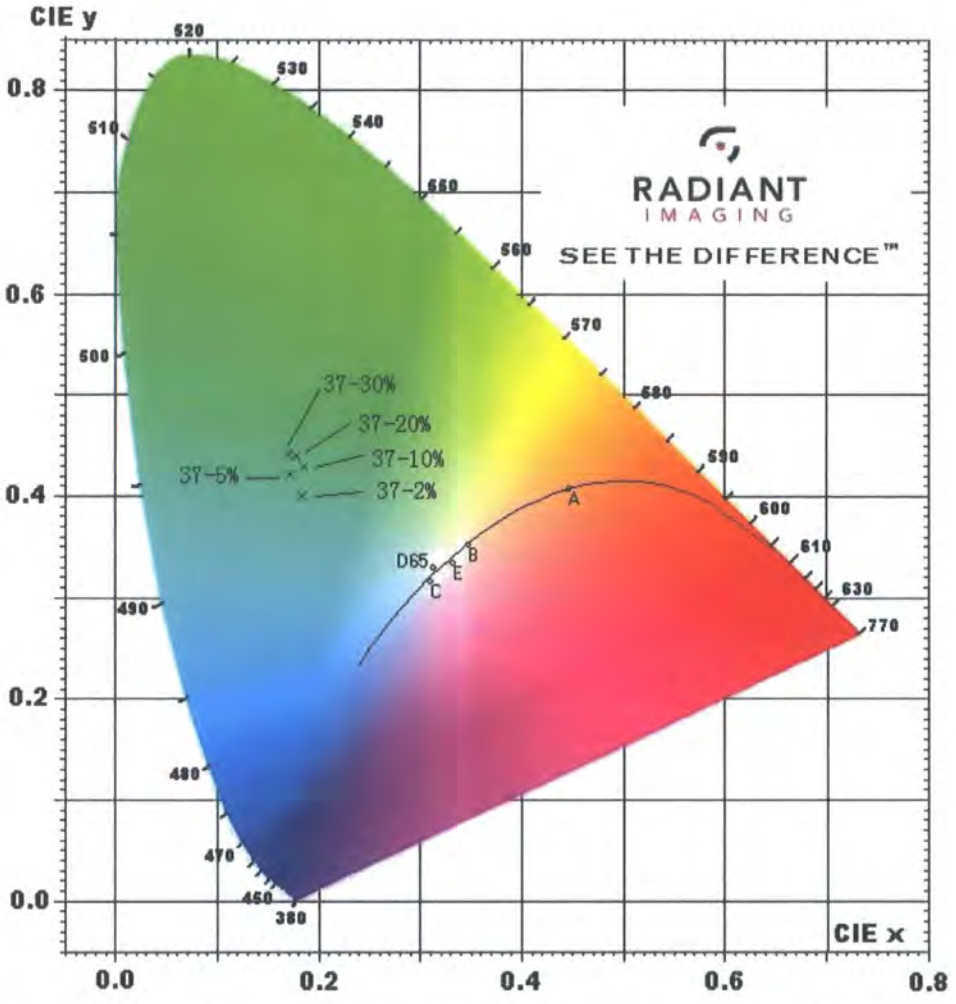

Figure 6-30 CIE co-ordinates of EL spectra of 37 series at 2000rpm.

From this CIE figure, we can see that the EL colour has been changed from blue to blue-green, but not towards white. And what's more, the change in this 37 series is not so obvious as that in the former 28 series.

6.3.2 Conclusion.

In the 37 series of PF copolymer OLEDs, the unit DBT also forms a strong charge transfer (CT) state and gives off a new strong red-shifted EL peak around 495nm. The relative intensity of this peak will increase as the DBTO unit's ratio goes up, while the position of it will not change. But the difference with the former 28 series with the DBTO unit is that the relative intensity of the new red-shift peak is not so strong as the former one. The EL colour can also shift from blue to blue-green as

the DBT's ratio increases. But the shift tendency is also not so obvious. The main reason for these is that the DBT unit is not an electron-acceptor unit, so neither the enhancement in EQE nor the colour shift is so obvious as the DBTO unit. However, because the DBT can still form a strong CT state, the EQE and luminance are still enhanced a lot as the percentage goes up. In addition, the EQE and luminance will also be strongly enhanced by changing the LEL thickness from 2500rpm to 2000rpm, which is the same with the 28 series.

Chapter 7 Conclusions.

As mentioned in the former chapters, polyfluorene (PFO) is a particularly promising electroluminescent polymer for light-emitting diodes because of the thermal and chemical stability, good solubility in common organic solvents and high fluorescent quantum yields in the solid state. However, PFO still have some defects, such as the low electrons transport ability which reduces the LED efficiency, the β -phase which causes the unstable light-emitting, the narrow electroluminescence spectrum which reduces the light-emitting color.

Today, work on PFO LEDs has focused on achieving emission colors across the entire visible range and improving device stability. Methods of tuning the emission color include adding molecular dopants in polymer systems, attaching emissive moieties and so on. In implementing these methods, desingning fluorene-based copolymers is a very important and effective approach. The dibenzothiophene (DBTO) is one of these moieties, which has been reported to be a prospective copolymer unit.

In this work, two new series of PFO copolymers have been investigated, which is the p(F8-co-28DBTO)s and the p(F8-co-37DBT)s. In the 28 series, dibenzothiophene (DBTO) unit is introduced through the 2,8 position into the poly(2,7-(9,9-dioctyl)fluorene backbone, and in the 37 series, DBT unit is introduced through the 3,7 position into the PF backbone. Both the PL properties and EL properties of these two co-polymer systems have been investigated through experiments and subsequent analysis. And a series of observations interesting and promising observations have been made.

Firstly, in the solution state of 28 series, the new unit-DBTO can cause the absorption spectra to be blue-shift, decreases the β-phase phenomena in the absorption spectra, cause the PL vibronic structure to be less significant, and increase the PLQY of the optical system. While the result was obtained that the emission wavelength changed towards white light for solid state EL, this is not observed in solution state PL.

In film state of 28 series, the new unit-DBTO can also cause the absorption spectra blue-shifted, significantly reduce the β-phase phenomena in their PL spectra as the DBTO's concentration is more than 5%, make the PL vibronic structure less significant to a single broad peak, make the PL peak a little red-shifted, and decrease the PLQY of them. In addition, the PL emission colour has been change from dark blue to light blue as the DBTO unit's ratio increases from 2% to 30%.

And the most important conclusions are in the copolymer light-emitting diodes (LEDs). The new electron acceptor unit DBTO forms a strong charge transfer (CT) state and gives off a new strong red-shifted EL peak around 495nm. The relative intensity of this peak will increase as the DBTO unit's ratio goes up, while the position of it will not change. The EL colour has shifted from blue to blue-green as the DBTO's ratio increases. And because of the electron acceptor structure of DBTO, charge transfer speed is enhanced obviously during these devices, which gives the result of enhanced EQE and luminance. In addition, the EQE and luminance will also be strongly enhanced by changing the LEL thickness from 2500rpm to 2000rpm.

Secondly, in solution state of 37 series, the new unit-DBT can't decreases the β -phase phenomena in the absorption spectra, and can't cause result in the absorption peak to be blue-shifted, either. These 2 observations are opposite to the 28 series. It can only make the PL vibronic structure less significant, which is similar with the 28 series, and keep the PLQY of them the same at around 80%. And the phenomenon that the emission wavelength to be changed towards white is still not observed in the solution state like the 28 series.

In film state of 37 series, the new unit-DBT becomes to decrease the β -phase phenomena in their absorption spectra, but still can't cause the absorption peak blue-shifted. It can make the PL vibronic structure just a little less significant, and make the PL peak a little red-shifted. Different with the 28 series, the PLQY of them will increase from 16% of p(F8-co-37DBT)-2% to 29% of p(F8-co-37DBT)-30%. In addition, the shift of the colour from deep blue to light blue is not so obvious as the former film state of the 28 series.

Finally, in the 37 series of PF copolymer OLEDs, the unit DBT also forms a

strong charge transfer (CT) state and gives off a new strong red-shifted EL peak around 495nm. The relative intensity of this peak will increase as the DBTO unit's ratio goes up, while the position of it will not change. But the difference with the former 28 series with the DBTO unit is that the relative intensity of the new red-shift peak is not so strong as the former one. The EL colour can also shift from blue to blue-green as the DBT's ratio increases. But the shift tendency is also not so obvious.

The main reason for these is that the DBT unit is not an electron-acceptor unit, so neither the enhancement in EQE nor the colour shift is so obvious as the DBTO unit. However, because the DBT can still form a strong CT state, the EQE and luminance are still enhanced a lot as the percentage goes up. In addition, the EQE and luminance will also be strongly enhanced by changing the LEL thickness from 2500rpm to 2000rpm, which is the same with the 28 series.

From all the discussions above, we can get the conclusion that both the 28 series (DBTO copolymers) and the 37 series (DBT copolymers) can reduce the β -phase phenomena of PFO both in solution and film, can enhance the EQE and luminance of the PFO devices a lot, expend the EL spectra and change the EL spectra colours from blue to blue-green. And we can also improve the LEDs properties by changing the LEL thickness of them. In one word, as we hoped in the beginning, these 2 series of PFO copolymers are promising organic electroluminescence materials during the LEDs technology.